（a） The point-by-point response to the reviews

- Referee #2

(1) Explain the abbreviations ICS, NCS and PCS in the abstract.

Sorry for my carelessness.

In abstract: “In general, the accuracy of the retrieval temperature of ICS is improved. Especially, from 100 hPa to 0.01 hPa, the accuracy of ICS can be improved by more than 11 %; (3) Statistical inversion comparison experiments in four typical regions indicate that ICS in this paper is significantly better than NCS and PCS in different regions and shows latitudinal variations.” (L 31-L 37)

This has been modified to “In general, the accuracy of the retrieval temperature of ICS (Improved Channel Selection) is improved; (3) Statistical inversion comparison experiments in four typical regions indicate that ICS in this paper is significantly better than NCS (NWP Channel Selection) and PCS (Primary Channel Selection) in different regions and shows latitudinal variations, which shows potential for future applications.” (L 30-L 36)

Thanks.

(2) p. 21, L. 429: Include the following citation: Saunders, R., Hocking, J., Turner, E., Rayer, P., Rundle, D., Brunel, P., Vidot, J., Roquet, P., Matricardi, M., Geer, A., Bormann, N., and Lupu, C.: An update on the

RTTOV fast radiative transfer model (currently at version 12), Geosci. Model Dev., 11, 2717–2737, https://doi.org/10.5194/gmd-11-2717-2018, 2018.

Yes, you are right.

This has been added. "…RTTOV can now simulate around 90 different satellite sensors measuring in the MW (microwave), IR (infrared) and VIS (visible) regions of the spectrum (Saunders et al., 2018)" (L 420-L 423)

"Saunders, R., Hocking, J., Turner, E., Rayer, P., Rundle, D., Brunel, P., Vidot, J., Roquet, P., Matricardi, M., Geer, A., Bormann, N., and Lupu, C.: An update on the RTTOV fast radiative transfer model (currently at version 12), Geosci. Model Dev., 11, 2717-2737, https://doi.org/10.5194/gmd-11-2717-2018, 2018." (L 1000-L 1004)

Thanks.

(3) p. 21, L. 429-430: The sentence "RTTOV is an evaluation of RTTOV v11, adding and upgrading many features" should be removed because explained is only the common procedure.

Yes, you are right.

The sentence "RTTOV is an evaluation of RTTOV v11, adding and upgrading many features" has been removed. (L 419-L 420)

Thanks.

(4) Table 1 and table 2 should be removed or shifted to the appendix.

Yes, we agree with you.

The two tables have been shifted to the Appendix A. (L 846-L 854)

Thanks.

(5) p. 44, L. 747-748: Description of figure is too universal. Please specify the behavior in more detail.

Sorry about this. We explain this as follows.

"In order to further compare the regional differences of inversion accuracy, the temperature standard deviations of ICS in four typical regions are compared in Sect. 5.2." (L 722-L 724)

Thanks.

(6) p. 3, L. 65: Atmospheric Infrared Sounder -> Atmospheric InfraRed Sounder.

Yes, we agree with you. This has been modified. (L 64)

Thanks.

(7) p. 14, L. 302: bright-> brightness.

Yes, you are right. This has been modified. (L 296; L 321; L 503; L 512)

Thanks.

(8) p. 16, L. 327: bright->brightness.

Yes, you are right. This has been modified. (L 296; L 321; L 503; L 512)

Thanks.

(9) p 26, L. 495: add last access date.

Yes, we agree with you.

“The error covariance matrix of the background, Sa, is calculated using 5000 samples of the IFS-137 data provided by the ECMWF dataset. The last access date is April 26th, 2019 (download address: https://www.nwpsaf.eu/site/update-137-level-nwp-profile-dataset/, 2019).” has been added to “The error covariance matrix of the background, S_a, is calculated using 5000 samples of the IFS-137 data provided by the ECMWF dataset (The detailed information will be introduced in Sect. 4). The last access date is April 26th, 2019 (download address: https://www.nwpsaf.eu/site/update-137-level-nwp-profile-dataset/, 2019).” (L 477-L 482)

Thanks.

(10) p. 39, L. 656: Do not write and so on. Either specify the variables or stop the sentence after cloud information.

Yes, you are right.

“Moreover, the IFS-91 database also supports the mode with input parameters, such as detection angle, 2 m temperature, cloud information, and so on.” has been modified to “The coverage of the IFS-137 data set is more homogeneous than the IFS-91 data set. Moreover, the IFS-137 database supports the mode with input parameters, such as detection angle, 2 m temperature, and cloud information.” (L 629-L 632)

Thanks.

(11) p. 39, L. 664: add last access date.

Yes, we agree with you.

"Red parts represent precipitation. (from https://www.nwpsaf.eu/site/update-137-level-nwp-profile-dataset/ , 2019)." has been added to "Red parts represent precipitation. The last access date is April 26th, 2019. (from https://www.nwpsaf.eu/site/update-137-level-nwp-profile-dataset/ , 2019)." (L 638-L 641)

Thanks.

(12) p. 40, L. 674: Do not write etc. Either specify the variables or stop the sentence after wind speed.

Yes, you are right.

"5000 profiles and their corresponding surface factors, including surface air pressure, surface temperature, 2 m temperature, 2 m specific humidity, 10 m wind speed, etc." has been modified to "5000 profiles and their corresponding surface factors, including surface air pressure, surface temperature, 2 m temperature, 2 m specific humidity, 10 m wind speed." (L 650)

Thanks.

(13) p. 51, l. 872: at 4.3 µm.

Yes, you are right.

"…and 4.3 µm for the CO_2 absorption bands;" has been modified to "…and at 4.3 µm for the CO_2 absorption bands;" (L 833)

Thanks again for your careful review.

- Referee #4

(1) L1-3: I would like to suggest to streamline the title a bit, e.g., "A channel selection method for hyperspectral atmospheric infrared sounders based on layering". Perhaps the reference to the AIRS instrument can be neglected in the title as the method will be applicable to other instruments, too?

Yes, we agree with you.

The method will be applicable to other instruments. Your suggested title "A channel selection method for hyperspectral atmospheric infrared sounders based on layering" is more proper.

This has been modified. (L 1-L 3)

Thanks.

(2) L22-24: The statement "The distribution of the temperature weight function is more continuous, more closely approximating that of the actual atmosphere" is unclear to me. Do you mean the coverage or sensitivity of the weighting functions is more evenly distributed over height with this method?

Sorry about this.

The statement has been rewritten. "The coverage of the weighting functions is more evenly distributed over height with this method and closer to the actual atmosphere” (L 22-L 24)

Thanks.

(3) L28: The term "near space layer" is not commonly used, I think. I would suggest to rephrase it by "stratosphere and mesosphere" here and in other places of the manuscript, for clarity.

Yes, you are right.

“In the near space layer especially” has been modified to “In the stratosphere and mesosphere especially”. (L 28)

“Near space (20–100 km)” has been modified to “Stratosphere and mesosphere”. (L 542; L 696-L 697)

“(the near space layer)” has been modified to “(the stratosphere and mesosphere)”. (L 751-L752; L 825- L 826)

“The reason is that near space (20–100 km) is less affected by the ground surface…”has been modified to “The reason is that stratosphere and mesosphere are less affected by the ground surface…” (L 830-L 832)

Thanks.

(4) L31-35: The acronyms ICS, NCS, and PCS need to be introduced in the abstract

Sorry for my carelessness.

In abstract: “In general, the accuracy of the retrieval temperature of ICS is improved. Especially, from 100 hPa to 0.01 hPa, the accuracy of ICS can be improved by more than 11 %; (3) Statistical inversion comparison experiments in four typical regions indicate that ICS in this paper is significantly better than NCS and PCS in different regions and shows latitudinal variations." (L 31-L 37)

This has been modified to "In general, the accuracy of the retrieval temperature of ICS (Improved Channel Selection) is improved; (3) Statistical inversion comparison experiments in four typical regions indicate that ICS in this paper is significantly better than NCS (NWP Channel Selection) and PCS (Primary Channel Selection) in different regions and shows latitudinal variations" (L 31-L 36)

Thanks.

(5) L 50-55: The word "detection" is frequently used in the manuscript, but considering that you are referring to temperature, I would recommend to change this to "sounding", "observation", or "measurement" in most instances.

Yes, you are right. This has been modified as follows.

"…satellite detection technology has developed rapidly" has been modified to "…satellite observation technology has developed rapidly" (L 40-L 41)

"From the perspective of vertical atmospheric detection, satellite instruments are developing rapidly. In their infancy, the traditional infrared detection instruments for detecting atmospheric temperature and moisture profiles …” has been modified to “From the perspective of vertical atmospheric observation, satellite instruments are developing rapidly. In their infancy, the traditional infrared measurement instruments for detecting atmospheric temperature and moisture profiles …” (L 47-L 50)

“… in terms of detection accuracy … filter-based spectroscopic detection instrument, therefore, …To meet this challenge, …for the creation of high-spectral resolution atmospheric detection instruments …” has been modified to “… in terms of observation accuracy … filter-based spectroscopic measurement instrument, therefore, …To meet this challenge,… for the creation of high-spectral resolution atmospheric measurement instruments…” (L 55-L 61)

“… such advanced detection technologies. … techniques of hyperspectral resolution atmospheric detection.” has been modified to “… such advanced sounding technologies. … techniques of hyperspectral resolution atmospheric observations.” (L 72-L 75)

“detection data” has been modified to “observation data” (L 80)

“…the general satellite detection instrument” has been modified to “…the typical satellite instruments” (L 85)

“With the development of detection technology…”has been modified to “With the development of measurement technology…” (L 88-L 89)

“temperature detection” has been modified to “temperature observation”

(L 391; L 530; L 547; L 701-L 702; L 777-L 778; L 835)

Thanks.

(6) L 61-62: Can you add a more recent reference regarding "today's needs" of NWP? Eyre et al. (1993) is more than 20 years old.

Sorry for my carelessness.

Two recent references have been added to "(Eyre et al., 1993; Prunet et al., 2010; Menzel et al., 2018)" (L 59)

"Menzel, W. P., Schmit, T. J., Zhang, P. and Li, J.: Satellite-based atmospheric infrared sounder development and applications, Bull. Amer. Meteor. Soc., 99, 583–603, https://doi.org/10.1175/BAMS-D-16-0293.1, 2018." (L 974- L 977)

"Prunet, P., Thépaut J. N., and Cass, V.: The information content of clear sky IASI radiances and their potential for numerical weather prediction, Q. J. Roy. Meteor. Soc., 124, 211-241, https://doi.org/10.1002/qj.49712454510, 2010." (L 978- L 981)

Thanks.

(7) L 70-72: IASI became operational in 2007 and not in 2010.

Yes, you are right.

This has been modified to "The United States and Europe, in 2010 and in 2007, also installed the CRIS (Cross-track Infrared Sounder) and the IASI (Inter-Attractive Atmospheric Sounding Interferometer) on polar-orbiting satellites". (L 68-L 71)

Thanks.

(8) L129-130 and L140-142: Which instruments are you referring to here? AIRS has more than 2000 channels.

Yes, you are right. AIRS has more than 2000 channels. We are sorry for the confusion. This has been modified as follows.

"Kuai et al. (2010) analyzed both the Shannon information content and degrees of freedom in channel selection when retrieving CO2 concentrations using thermal infrared remote sensing and indicated that 40 channels could contain 75% of the information from the total of 1016 channels." has been modified to "Kuai et al. (2010) analyzed both the Shannon information content and degrees of freedom in channel selection when retrieving CO2 concentrations using thermal infrared remote sensing and indicated that 40 channels could contain 75% of the information from the total channels." (L 125-L 129)

"Richardson et al. (2018) selected 75 from 853 channels using information content analysis to retrieve the cloud optical depth, cloud properties, and position." has been modified to "Richardson et al. (2018) selected 75 from 853 channels based on the high spectral-resolution oxygen A-band instrument on NASA's Orbiting Carbon Observatory-2 (OCO-2), using information content analysis to retrieve the cloud optical depth, cloud properties, and position." (L 138-L 142)

Thanks.

(9) L147: I would suggest to rephrase "weight function" by "weighting function" here and throughout the manuscript.

Yes, we agree with you.

“weight function” has been modified to “weighting function” throughout the manuscript.

Thanks.

(10) L 147-148: The statement "... use only the weight function to study appropriate numerical methods, the use of which allows sensitive channels to be selected." is unclear to me. Please rephrase.

Sorry for this.

“Today’s main methods for channel selection (such as the data precision matrix method (Menke, 1984), singular value decomposition method (Prunet et al., 2010; Zhang et al., 2011; Wang et al., 2014), and the Jacobi method (Aires et al., 1999; Rabier et al., 2010) use only the weight function to study appropriate numerical methods, the use of which allows sensitive channels to be selected.” has been modified to “Today’s main methods for channel selection use only the weighting function to study appropriate numerical methods, such as the data precision matrix method (Menke, 1984), singular value decomposition method (Prunet et al., 2010; Zhang et al., 2011; Wang et al., 2014), and the Jacobi method (Aires et al., 1999; Rabier et al., 2010). The use of the methods allows sensitive channels to be selected.” (L 143-L 149)

Thanks.

(11) L 155-161: The concept of information content itself does consider all the height dependencies of the kernel matrix K (Rodgers, 2000 or Eq. (1) in the present manuscript). Earlier work may have neglected the height dependencies of K for simplicity and to ease the calculations. These sentences should be rephrased so that they do not give the wrong impression that the information content ignores the height dependencies of the weighting functions in general.

Yes, you are right.

"Currently, information content is often employed in channel selection. During retrieval, this method delivers the largest amount of information for the selected channel combination (Rodgers, 1996; Du et al., 2008; He et al., 2012; Richardson et al., 2018). Although this method has made great breakthroughs in both theory and practice, however, it does not take the sensitivity of different channels at different heights into consideration." has been modified to "Currently, information content is often employed in channel selection. During retrieval, this method delivers the largest amount of information for the selected channel combination (Rodgers, 1996; Du et al., 2008; He et al., 2012; Richardson et al., 2018). This method has made great breakthroughs in both theory and practice, and the concept of information content itself does consider all the height dependencies of the kernel matrix K (Rodgers, 2000). However, earlier works have neglected the height dependencies of K for simplicity." (L 155-L 163)

Thanks.

(12) L 195-195: This is redundant and can be deleted.

. Yes, you are right.

The sentence "where S_a is the error covariance matrix of the background or the estimated value of the atmospheric profile, and $\hat{S}$ represents the observation error covariance matrix of each hyperspectral detector channel."has been deleted. (L 195)

Thanks.

(13) L 216-219: This sentence is unclear and should be rephrased.

Yes, you are right.

"Furthermore, under the maximum one p-value, the corresponding channel combination is used as the optimum channel combination; therefore, the entire atmosphere must be calculated $M \cdot C_N^n$ times." has been modified to "Furthermore, there are M layers in the vertical direction of the atmosphere. Therefore, the entire atmosphere must be calculated $M \cdot C_N^n$ times." (L 212-L 214)

Thanks.

(14) L 221-227: The "sequential absorption method" has been described elsewhere before, e.g., (Dudhia et al., 2002):

Dudhia, A., Jay, V. L., & Rodgers, C. D. (2002). Microwindow selection for high-spectral-resolution sounders. Applied Optics, 41(18), 3665-3673.

Yes, you are right. The corresponding references have been cited.

It has been modified to “Therefore, it is necessary to design an effective calculation scheme, and such a scheme, i.e., a channel selection method, using iteration is proposed, called the “sequential absorption method” (Dudhia et al., 2002; Du et al., 2008).” (L 216-L 219)

“Dudhia, A., Jay, V. L., and Rodgers, C. D.: Microwindow selection for high-spectral-resolution sounders, Appl. Opt. 41, 3665-3673, https://doi.org/10.1364/AO.41.003665, 2002.” (L 916-L 918)

Thanks.

(15) L 231: The expression "\partial^2\Omega / \partial\nu^2" has not been explained and the derivative looks wrong, maybe skip it here?

Yes, you are right.

The expression " $s_\varepsilon \frac{\partial^2 \Omega}{\partial v^2}$ " has not been explained, which is an unimportant item and can be skipped.

The sentence “A diagonal element, $s_\varepsilon \frac{\partial^2 \Omega}{\partial v^2}$, in the S_ε matrix is the error variance in the channel.” has been deleted. (L 227)

Thanks.

(16) L 262-263: The sentence "According to S_a, S_\epsilon...can be calculated" is unclear and should be rephrased.

Sorry about this.

“According to S_a, S_ε , K and Eq. (6), R, which is r corresponding to all the selected channels, can be calculated." has been modified to "According to S_a, S_ε , K and Eq. (6), R can be calculated." (L 258)

Thanks.

(17) L 271-275: I would suggest to remove the phrase "... but it still satisfies the optimum value in a certain sense". The method cannot find the global optimum as it applies only a sequential search strategy. It is good to point out this limitation, no need to oversell the results.

Yes, you are right.

The sentence "Of course, the combination selected by this method is not completely equivalent to the channel combination corresponding to the optimum value of C_N^n p, but it still satisfies the optimum value in a certain sense." has been removed. (L 265)

Thanks.

(18) L 283-285: I did not understand how you are actually making use of the different channel selections for the different heights in the retrieval process. Does this mean the different channel sets are used to evaluate only certain heights in the retrieved profile?

Yes, you are right.

This has been explained "In this way, different channel sets can be used to evaluate corresponding height in the retrieved profiles." (L 276-L 278)

Thanks.

(19) L 330 and 344: I got confused about the notation, what is "\hat T'"

referring to?

Sorry for my carelessness.

"where $\overline{\mathrm{T}}$ and $\overline{\mathrm{T_b}}$ are the corresponding average values of the elements, respectively. T' and $\mathrm{T_b}'$ represent the corresponding anomalies of the elements, respectively." has been modified to "where $\hat{\mathrm{T}}$ stands for the retrieval atmospheric temperature. $\overline{\mathrm{T}}$ and $\overline{\mathrm{T_b}}$ are the corresponding average values of the elements, respectively. $\hat{\mathrm{T}}'$ and $\mathrm{T_b}'$ represent the corresponding anomalies of the elements, respectively." (L 326-L 329)

Thanks.

(20) L 379-380: "after retrieval of observations has been complete several times" is unclear to me.

Sorry for the confusion.

"It should be noted that the least squares solution obtained here aims to minimize the sum of the error variance for each element in the atmospheric state vector after retrieval of observations has been completed several times." has been modified to "It should be noted that the least squares solution obtained here aims to minimize the sum of the error variance for each element in the atmospheric state vector after retrieval for several times." (L 372-L 374)

Thanks.

(21) L 380-383: How do you deal with non-linearity inherent atmospheric radiactive transfer? Isn't that a major problem for multiple

regression?

Yes, you are right. We have explained this as follows.

"Because the statistical inversion method does not directly solve the radiation transfer equation, it has the advantages of fast calculation speed. In addition, the solution is stable, which makes it one of the highest precision methods (Chedin et al., 1985)." (L 288-L 290)

This study is aimed to examine the effectiveness of a channel selection method for hyperspectral atmospheric infrared sounders based on layering. The most particular aspect of this work is that it takes the height dependencies of the kernel functions into account. Thus, considering the calculation speed, the statistical inversion method is used for our channel selection experiment.

Thanks.

(22) L 387: Add a reference for the AIRS instrument, e.g. (Aumann et al., 2003).

Sorry for my carelessness. The references have been added.

"…(Aumann et al., 2003; Hoffmann and Alexander, 2009)" (L 383-L 384)

Thanks.

(23) L 395: The AIRS footprint size 13.5 km at nadir, please check.

Yes, you are right. The AIRS footprint size 13.5 km at nadir.

"The spatial footprint of the infrared channels is 1.1° in diameter, which corresponds to about 15×15 km at the nadir." has been modified to "The footprint size 13.5 km at nadir (Susskind et al., 2003)." (L 389)

"Susskind, J., Barnet, C. D. and Blaisdell, J. M.: Retrieval of atmospheric and surface parameters from AIRS/AMSU/HSB data in the presence of clouds, IEEE Trans. Geosci. Remote Sensing, 41, 390-409, https://doi.org/10.1109/TGRS.2002.808236, 2003." (L 1005- L 1008)

Thanks.

(24) L 396-398: 4.3 and 15 micron are used simultaneously for both, temperature and carbon dioxide retrievals, I think.

Yes, you are right.

"The spectral range includes 4.2 μm for important temperature observation, 15 μm for CO2, 6.3 μm for water vapor, and 9.6 μm for ozone absorption bands." has been modified to "The spectral range includes 4.3 μm and 15.5 μm for important temperature observation and CO2, 6.3 μm for water vapor, and 9.6 μm for ozone absorption bands (Menzel et al., 2018)." (L 389-L 392)

Thanks.

(25) L398: When you refer to "absolute accuracy", does this include noise as well? Noise should not be included as it counts as "precision".

Yes, you are right.

"The absolute accuracy of the measured radiation is better than 0.2 K ." has been modified to "The root mean square error (RMSE) of the measured radiation is better than 0.2 K (Susskind et al., 2003)”. (L 392-L 394)

Thanks.

(26) L 399-401: "the four imaging channels of visible/near infrared are always filled" is unclear, please explain or remove.

Yes, you are right. The sentence has been removed. (L 394-L 395)

Thanks.

(27) L406-411: This paragraph can be deleted. Everything was already said in the introduction.

Yes, you are right. This paragraph has been deleted. (L 400)

Thanks.

(28) L412: Does the "root-mean square error" include both, accuracy and prediction, in this study?

Root mean square error (RMSE) in this study can be described as accuracy in this study.

Thanks.

(29) L 416-417: Delete the sentence "Moreover, not all channels possess the same measurement error." This is obvious from the figure.

Yes, you are right. The sentence "Moreover, not all channels possess the same measurement error." has been deleted. (L 404)

Thanks.

(30) L 415: Please provide a reference or a web link for the RMS errors

shown here.

Yes, you are right.

"There are a few with extremely large measurement errors, which reduce the accuracy of prediction to some extent." has been modified to "There are a few channels with extremely large measurement errors, which reduce the accuracy of prediction to some extent. Among them, some extremely large measurement errors reduce the accuracy of prediction to some extent. (Susskind et al., 2003)" (L 402-L 406)

Thanks.

(31) L 429: Introduce acronym and provide reference for RTTOV.

Yes, you are right.

"For the radiative transfer model and its weight function matrix, K, the RTTOV v12 fast radiative transfer model is used. RTTOV is an evolution of RTTOV v11, adding and upgrading many features." has been modified to "For the radiative transfer model and its weighting function matrix, K, the RTTOV (Radiative Transfer for TOVS) v12 fast radiative transfer model is used. Although initially developed for the TOVS (TIROS Operational Vertical Sounder) radiometers, RTTOV can now simulate around 90 different satellite sensors measuring in the MW (microwave), IR (infrared) and VIS (visible) regions of the spectrum (Saunders et al., 2018)." (L 417-L 423)

Thanks.

(32) L 429-430: Delete sentence saying "RTTOV is an evolution of..." as this does not provide really useful information.

Yes, you are right. The sentence has been deleted. (L 423)

Thanks.

(33) L 431: What is ATOVS?

Sorry for my carelessness.

"ATOVS (Advanced TOVS)" has been added. (L 424)

Thanks.

(34) L 440-443: Table 1 is not needed at all in this manuscript, I think. What is the reader supposed to do with it? Just provide the web link for reference.

Yes, we agree with you.

Table 1 and table 2 is not needed.

The two tables have been shifted to the Appendix A. (L 846-L 854)

Thanks.

(35) L 451-452: The phrase "The weight function matrix K ..." can be deleted, as this is clear.

Yes, you are right. The sentence has been deleted. (L 437)

Thanks.

(36) L 465: What is H(X0)? Is it needed for anything here?

Sorry for the confusion.

It has been explained "The RTTOV_K (the K mode), is used to calculate the matrix H(X0) (Eq. (1)) for a given atmospheric profile characteristic.”

(L 448-L 450)

Thanks.

(37) L 473-475: Which "products" are you referring to? Is there a reference for the NWPSAF requirements?

Sorry for this. This has been modified and a reference for the NWPSAF has been added.

“NCS is short for NWP channel selection in this paper. The products were released by the NWPSAF 1DVar (one-dimensional variational analysis) scheme, in accordance with the requirements of the NWPSAF.” has been modified to “NCS is short for NWP channel selection in this paper. NCS were released by the NWPSAF 1DVar (one-dimensional variational analysis) scheme, in accordance with the requirements of the NWPSAF (Saunders et al., 2018).” (L 456-L 460)

Thanks.

(38) L 492-495: At this point the reader does not know anything about the IFS-137 data set. It is introduced much later in the manuscript.

Yes, you are right. Because the main idea of this part is to introduce the channel selection experiment, we will introduce IFS-137 data set in Sect. 4.

It has been explained “The error covariance matrix of the background, S_a, is calculated using 5000 samples of the IFS-137 data provided by the

ECMWF dataset (The detailed information will be introduced in Sect. 4). The last access date is April 26th, 2019 (download address: https://www.nwpsaf.eu/site/update-137-level-nwp-profile-dataset/, 2019).” (L 476-L 482)

Thanks.

(39) L 500: What is causing the off-diagonal bands in the temperature covariance matrix? For instance, why is the temperature at 100 hPa closely correlated with temperature at about 60-70 hPa?

Yes, you are right. We have noticed the off-diagonal bands in the temperature covariance matrix, especially from 50hPa to 200hPa. There should be some dynamic processes here. But this study is aimed to examine the effectiveness of a channel selection method. As the temperature covariance matrix is the same, so we do not introduce it further here.

Thanks.

(40) L 516: The color bar unit is "Kˆ2", but shouldn’t this be "K/K", as it refers to a change of brightness temperature with respect to atmospheric temperature, i.e., dBT/dT? (Same for Fig. 7)

Sorry for this. This has been modified (Fig. 3: L 500; Fig.6: L 575-L 577)

Thanks.

(41) L 532-544: Wavenumbers are missing the unit "cmˆ-1". Replace "11 micron" by "10 micron".

Yes, you are right.

The wavenumber unit " cm^{-1}" has been added. (L 518; L 520; L 524; L 527; L 534)

"11μm" has been replaced by "10μm "(L 517)

Thanks.

(42) L 546: The term "high temperature zone" is used here and elsewhere in the manuscript, but what does it refer to? Please explain.

Sorry for this. We have added our explanations "Because 4.2 μm and 4.3 μm bands are sensitive to high temperature, the higher temperature is, the better observation can be obtained". (L 531-L 533)

"…in the high temperature zone." has been modified to "…to the higher temperature." (L 546-L 547)

"…the channel combination of ICS is superior to that of PCS and NCS for atmospheric temperature observation in the high temperature zone" has been modified to "…the channel combination of ICS is better than that of PCS and NCS for atmospheric temperature observation to the higher temperature" (L 775-L 778; L 834-L 836)

Thanks.

(43) L 575-576: "Moreover, the temperature profile of each layer can be retrieved." How can you retrieve a profile for a layer? Please clarify.

Sorry for this.

After 324 channels are selected for each layer, the temperature profile of each layer can be retrieved based on statistical inversion (see at Sect. 4).

"In this paper, the atmosphere is divided into 137 layers, and based on the information content and iteration, 324 channels are selected for each layer. Moreover, the temperature profile of each layer can be retrieved." has been modified to "In this paper, the atmosphere is divided into 137 layers, and based on the information content and iteration, 324 channels are selected for each layer. Then, the temperature profile of each layer can be retrieved based on statistical inversion (see at Sect. 4)" (L 560-L 564)

Thanks.

(44) L 569 and 583: Figs. 5 and 6 could be combined in a single figure to allow for a comparison.

Yes, we agree with you.

Figs.5 and Figs.6 has been combined in a single figure. (Figure 5: L 556)

The following figure numbers (Fig. 7-13) have been modified (Fig. 6-12).

Thanks.

(45) L 596-605: You are describing the PCS distribution as "scattered", but I would rather apply this word to the ICS distribution. The ICS distributions seems to jump or scatter

Thank you for your notice. Sorry for my carelessness.

In Fig.6 "(a) PCS. (b) ICS." should be "(a) ICS. (b) PCS." Which has been modified. (L 576-L 577)

Thanks.

(46) L 604-605: Sorry, but I don’t know what you mean by "scenario in the real atmosphere" in this context?

Sorry for the confusion.

“(2) regardless of the number of iterations, the maximum value of the weighting function is stable near 300–400 hPa and 600–700 hPa, without scattering, which resembles more closely the scenario in real atmosphere.” has been modified to “(2) regardless of the number of iterations, the maximum value of the weighting function is stable near 300–400 hPa and 600–700 hPa, without scattering, which is closer to the situation in real atmosphere.” (L 585-L 588)

Thanks.

(47) L 615-619: Please provide a reference for the IFS-137 data set here.

Sorry for my carelessness.

The corresponding references have been added.

“…(Eresmaa and McNally, 2014; Brath et al., 2018)” (L 603)

“Brath, M., Fox, S., Eriksson, P., Harlow, R. C., Burgdorf, M., and Buehler, S. A.: Retrieval of an ice water path over the ocean from ISMAR and MARSS millimeter and submillimeter brightness temperatures, Atmos. Meas. Tech., 11, 611–632, https://doi.org/10.5194/amt-11-611-2018, 2018.” (L 891-L 895)

“Eresmaa, R. and McNally, A. P.: Diverse profile datasets from the

ECMWF 137-level short-range forecasts, Tech. rep., ECMWF, 2014." " (L 919-L 921)

Thanks.

(48) L 620-623: Please replace the number of model grid points by something more meaningful such as horizontal resolution of the data. The list of the 137 individual pressure levels and Table 2 are not really needed, I think.

Yes, we agree with you.

"There are two operational analyses each day (at 00z and 12z), and the modeling grid contains 2,140,702 grid points. The pressure levels adopted for IFS-137 are shown in Table 2." has been modified to "There are two operational analyses each day (at 00z and 12z), and approximately 13 000 atmospheric profiles over the ocean. The pressure levels adopted for IFS-137 are shown in Table A2 (see Table A2 in Appendix A)." (L 604- L 608)

Thanks.

(49) L 647-664: As you are not going to make any use of the IFS-91 data set in this study, there is no need to introduce it and discuss the differences with respect to the IFS-137 data set. Section 4.1 could be shortened significantly, I think.

Yes, we agree with you.

"The temporal distribution of the selected profiles is illustrated in Fig. 9.

Again, the lack of randomized selection results in large variations from one month to the next in the case of the IFS-91 database (left panel). The different distributions come mainly from variations in the ozone subset (green parts of each column). Dominance of randomly-selected profiles in the IFS-137 database leaves little room for monthly variation in the data count (right panel). Moreover, the IFS-91 database also supports the mode with input parameters, such as detection angle, 2 m temperature, cloud information. Therefore, it is feasible to use the selected samples in a statistical multiple regression experiment." has been modified to "The temporal distribution of the selected profiles is illustrated in Fig. 8. The coverage of the IFS-137 data set is more homogeneous than the IFS-91 data set. Moreover, the IFS-137 database supports the mode with input parameters, such as detection angle, 2 m temperature, and cloud information. Therefore, it is feasible to use the selected samples in a statistical multiple regression experiment." (L 628-L 633)

Thanks.

(50) L 641: The axes labels in Fig. 8 are too small

Sorry for this.

It has been modified. (Fig. 7: L 622-L 626)

Thanks.

(51) L 658: Fig. 9 is not really needed, as it was already pointed out in the text that the coverage of the IFS-137 data set is rather

homogeneous.

Because the introduction of IFS-137 data set has been shortened, in order to introduce IFS-137 data set briefly and visually, Fig.8 (previous Fig. 9) can be remained.

Thanks.

(52) L 674: Why does the RTTOV model need 10 m wind speeds for the radiative transfer calculations?

According to RTTOV users' guide, the new physically-based model (RTTOV) depends on wind speed and skin temperature as well as zenith angle. Some parameters are put into the RTTOV mode. 10 m wind speeds are used to calculate emissivity (details can be seen at RTTOV users' guide).

Thanks.

(53) L 744-746: Did you also look at the southern hemisphere polar regions? The sentence "These regions' profiles can represent the global typical atmospheric temperature profiles" makes no sense to me because the regional means are different from the global mean. Delete this.

Sorry for my carelessness.

We haven't looked at the southern hemisphere polar regions. The sentence "The profiles of these regions can represent the global typical atmospheric temperature profiles." has been deleted. (L 720)

Thanks.

(54) L 746-748: I got very concerned about the mean temperature profiles shown in Fig. 11. If these are regional means of hundreds to thousands of profiles, how can they show wave oscillations and look that noisy? Shouldn't the mean profiles be rather smooth? Is this due to the original selection of the IFS-137 profiles focusing on cases with strong temperature gradients?

Sorry for my careless.

The figure actually is the temperature standard deviation of ICS in four typical regions (Figure 12). I put the wrong figure here. Wave oscillations in this figure is due to the number of profiles in each region are not hundreds to thousands of profiles. For example, in the arctic (80N -90 N), there are 45 samples. So in the figure, wave oscillation is obvious in arctic.

The average temperature profiles in these four regions have been modified (Fig.10). (L 727-L 731)

Thanks.

(55) L 774-775 and 813: It is okay to say that ICS works "better" than NCS or PCS, but saying it is "greatly superior" or "impressive" is overselling the results, I think. Suggest to rephrase this and use more moderate wording.

Yes, we agree with you.

"Generally, the retrieval temperature by ICS is greatly superior to that of NCS and PCS." has been modified to "Generally, the retrieval temperature by ICS is better than that of NCS and PCS." (L 750-L 751)

"According to Fig. 12, ICS takes channel sensitivity as a function of height into consideration, so its retrieval result is impressive." has been modified to "According to Fig. 11, ICS takes channel sensitivity as a function of height into consideration, so its retrieval result is better." (L 786-L 788)

Other similar problems have been modified.

"…the channel combination of PCS is superior to that of NCS for atmospheric temperature observation in the high temperature zone." has been modified to "…the channel combination of PCS is better than that of NCS for atmospheric temperature observation to the higher temperature." (L 546-L 547)

"…the ICS method is superior to that of PCS." has been modified to "the ICS method is better than that of PCS." (L 567-L 568)

"…the channel combination of ICS is superior to that of PCS and NCS for atmospheric temperature observation in the high temperature zone" has been modified to "…the channel combination of ICS is better than that of PCS and NCS for atmospheric temperature observation to the higher temperature" (L 775-L 778; L 834-L 836)

"…ICS is superior to PCS." has been modified to "…ICS is better than

PCS.” (L 821-L 822)

“Moreover, ICS takes channel sensitivity as a function of height into consideration, so its retrieval result is impressive.” has been modified to “Moreover, ICS takes channel sensitivity as a function of height into consideration, so its retrieval result is improved.” (L 703-L 704)

Thanks.

(56) L 819-834: Tables 4 to 7 are largely redundant and can be removed from the paper, I think.

Yes, we agree with you.

Tables 4 to 7 have been removed from the paper. And the corresponding indication has been modified. (L 795)

In abstract “Especially, from 100 hPa to 0.01 hPa, the accuracy of ICS can be improved by more than 11 %; (3) Statistical inversion comparison experiments in four typical regions indicate that ICS in this paper is significantly better than NCS (NWP Channel Selection) and PCS (Primary Channel Selection) in different regions and shows latitudinal variations. Especially, from 100 hPa to 0.01 hPa, the accuracy of ICS can be improved by 7% to 13%, which means the ICS method selected in this paper is feasible and shows great promise for applications.” has been modified to “(3) Statistical inversion comparison experiments in four typical regions indicate that ICS in this paper is significantly better than NCS (NWP Channel Selection) and PCS (Primary Channel Selection) in different regions and shows latitudinal variations, which shows potential for future applications.” (L 32-L 36)

Thanks.

(57) L 849 and 882: Suggest to simply delete the headings for Sects. 6.1 and 6.2, as they appear in the wrong order. The conclusions should follow the discussion.

Yes, you are right.

The headings and the correct order have been modified. (L 796-L 840)

Thanks.

Technical Corrections

(58) L30: remove "evidently"

Yes, you are right.

"evidently" has been deleted. (L 30)

Thanks.

(59) L 38-39: suggest to rephrase "... is feasible and shows great promise for application" as "... shows potential for future applications"

Yes, we agree with you.

“(3) Statistical inversion comparison experiments in four typical regions indicate that ICS in this paper is significantly better than NCS (NWP Channel Selection) and PCS (Primary Channel Selection) in different regions and shows latitudinal variations. Especially, from 100 hPa to 0.01

hPa, the accuracy of ICS can be improved by 7% to 13%, which means the ICS method selected in this paper is feasible and shows great promise for applications.” has been modified to “(3) Statistical inversion comparison experiments in four typical regions indicate that ICS in this paper is significantly better than NCS (NWP Channel Selection) and PCS (Primary Channel Selection) in different regions and shows latitudinal variations, which shows potential for future applications.” (L 32-L 36)

“…Especially, from 100 hPa to 0.01 hPa, the accuracy of ICS can be improved by 7% to 13%, which means the ICS method selected in this paper is feasible and shows great promise for applications.” has been modified to “…, which shows potential for future applications.” (L 839-L 840)

Thanks.

(60) L44: _the_ Earth’s

Yes, you are right

“…observe Earth’s atmosphere…” has been modified to “…observe the Earth’s atmosphere…” (L41)

Thanks.

(61) L 67-68: suggest to rephrase "AIRS has 2378 spectral channels with subpoint at 13 km and a detection height from the ground of up to 65 km" as "AIRS has 2378 spectral channels providing sensitivity from the ground to up to about 65 km of altitude"

Yes, you are right. This has been modified. (L 66-L 68)

Thanks.

(62) L 73: change "attaches" to "devotes" (or similar)

Yes, you are right. This has been modified. (L 72)

Thanks.

(63) L 76: change "detection" to "observations" (or similar)

Yes, you are right. This has been modified. (L 75)

The similar problems have been modified.

"…satellite detection technology has developed rapidly" has been modified to "…satellite observation technology has developed rapidly" (L 40-L 41)

"From the perspective of vertical atmospheric detection, satellite instruments are developing rapidly. In their infancy, the traditional infrared detection instruments for detecting atmospheric temperature and moisture profiles …" has been modified to "From the perspective of vertical atmospheric observation, satellite instruments are developing rapidly. In their infancy, the traditional infrared measurement instruments for detecting atmospheric temperature and moisture profiles …" (L 47-L 50)

" … in terms of detection accuracy … filter-based spectroscopic detection instrument, therefore, …To meet this challenge, …for the creation of high-spectral resolution atmospheric detection instruments …"

has been modified to "… in terms of observation accuracy … filter-based spectroscopic measurement instrument, therefore, …To meet this challenge,… for the creation of high-spectral resolution atmospheric measurement instruments…" (L 55-L 61)

"… such advanced detection technologies. … techniques of hyperspectral resolution atmospheric detection." has been modified to "… such advanced sounding technologies. … techniques of hyperspectral resolution atmospheric observations." (L 72-L 75)

"detection data" has been modified to "observation data" (L 80)

"…the general satellite detection instrument" has been modified to "…the typical satellite instruments" (L 85)

"With the development of detection technology…"has been modified to "With the development of measurement technology…" (L 88-L 89)

"temperature detection" has been modified to "temperature observation" (L 391; L 530; L 547; L 701-L 702; L 777-L 778; L 835)

Thanks.

(64) L 80: change "atmospheric detectors" to "instruments"

Yes, you are right. This has been modified. (L 79)

Thanks.

(65) L 83: delete "intense"

Yes, you are right. This has been deleted. (L 82)

Thanks.

(66) L 86: change "general satellite detection instrument" to "typical satellite instruments"

Yes, you are right. This has been modified. (L 85)

Thanks.

(67) L 89: change "the center frequency, bandwidth" to "center frequency and bandwidth"

Yes, you are right. This has been modified. (L 88)

Thanks.

(68) L 96: there is _often_ a close correlation between _the channels_

Yes, you are right. This has been modified. (L 94-L 95)

Thanks.

(69) L 106: demands of _simulating_ all the channels

Yes, you are right. This has been modified. (L 105)

Thanks.

(70) L 107: to _properly_ select

Yes, you are right. This has been modified. (L 106-L 107)

Thanks.

(71) L 151: ignoring _some_ factors

Yes, you are right. This has been modified. (L 151)

Thanks.

(72) L 183: change "\hat S" to "S_\epsilon"

Sorry for my careless.

"$\hat{S}$" has been modified to "S_ε". (L 185)

Thanks.

(73) L 186: delete "by hyperspectral data"

Yes, you are right. This has been deleted. (L 188)

Thanks.

(74) L 187-188: delete "which comes from the selected channel in hyperspectral data with respect to ..." or rephrase to clarify

Sorry for this. It has been deleted. (L 188)

Thanks.

(75) L 209-210: rephrase to "... combination making the information content..."

"This combination make the information content, H, or the ARI defined in this paper as large as possible, in order to maintain the highest possible accuracy in the retrieval results." has been modified to "This combination makes the information content, H, or the ARI defined in this paper as large as possible, in order to maintain the highest possible accuracy in the retrieval results." (L 205-L 208)

Thanks.

(76) L 235: change "single" to "scalar"

Yes, you are right. This has been modified. (L 230)

Thanks.

(77) L 242: rephrase to "Since S_a and S_nepsilon are ..."

Yes, you are right.

"Since S_a is a positive definite symmetric matrix..." has been modified to "Since S_a and S_ε are positive definite symmetric matrixes…" (L 237)

Thanks.

(78) L 248: change "pre-observation error" to "a priori uncertainty"

Yes, you are right. This has been modified. (L 243)

Thanks.

(79) L 275: delete "its"

Yes, you are right. This has been deleted. (L 266)

Thanks.

(80) L 288: method_s for_ the ... profile_s_

Yes, you are right.

"The inversion method of the atmospheric temperature profile…" has been modified to "The inversion methods for the atmospheric temperature profiles…" (L 281)

Thanks.

(81) L 297: _numerically_ stable

Yes, you are right. This has been added. (L 290)

Thanks.

(82) L 302: change "bright temperature" to "brightness temperature" (here and throughout the manuscript)

Sorry for my careless. Those have been modified. (L 296; L 321; L 503; L 512)

Thanks.

(83) L 303: expanded _as_

Yes, you are right. This has been modified. (L 297)

Thanks.

(84) L 367: Taking a derivative of Eq. (21) with respect to G,...

Yes, you are right.

"Equation (21) takes a derivative with respect to G…" has been modified to "Taking a derivative of Eq. (21) with respect to G…" (L 362)

Thanks.

(85) L 387: delete "instrument suite" and change to "is _primarily_ designed"

Yes, you are right.

"The Atmospheric Infrared Sounder (AIRS) instrument suite is designed to…" has been modified to "The Atmospheric Infrared Sounder (AIRS) is primarily designed to…" (L 381)

Thanks.

(86) L 415: few _channels_

Yes, you are right. This has been modified. (L 402-L 403)

Thanks.

(87) L 428: rephrase to "For the calculation of radiative transfer and

the weighting function matrix, K, the RTTOV..."

Yes, you are right. This has been modified. (L 417-L418)

Thanks.

(88) L 434: rephrase to "and _trace_ gas concentration_s_"

Yes, you are right. This has been modified. (L 427)

Thanks.

(89) L 439 and 440: delete "v12"

Yes, we agree with you. Those have been deleted. (L 431-L 432 and L 433)

Thanks.

(90) L 459 and 461: change "characteristic" to "variable"

Yes, you are right. This has been modified. (L 443 and L 445)

Thanks.

(91) L 460: delete "radiation"

Yes, you are right. This has been deleted. (L 444)

Thanks.

(92) L 481: selection __ in

Yes, you are right. This has been modified. (L 466)

Thanks.

(93) L 491: rephrase to "...of the AIRS channels"

Yes, you are right. This has been modified. (L 476)

Thanks.

(94) L 510: change "But due to" to "However,"

Yes, we agree with you.

“Therefore, when we select channels, the results differ because of the different observation angles. But due to the selection principle and method are exactly the same and our key is the selection method; we do not discuss, therefore, the variation in observation angle when making a selection.” has been modified to “The goal of this section is focusing on the selection methods of selecting channels; therefore the biases produced from different observation angles can be ignored.” (L 495-L 497)

Thanks.

(95) L 518: delete "of ICS"

Yes, you are right. This has been deleted. (L 502)

Thanks.

(96) L 563: change to "retrieval of temperature"

Yes, you are right. This has been modified. (L 550)

Thanks.

(97) L 611: was used _for the statistical inversion experiments_.

Yes, you are right. This has been added. (L 594-L 595)

Thanks.

(98) L 675: mode_l_. Then, the _simulated AIRS spectra are_ obtained

Yes, you are right. This has been modified. (L 651)

Thanks.

(99) L 696: delete "obviously"

Yes, you are right. This has been deleted. (L 671)

Thanks.

(100) L 704 and 719: _at_ different height_s_

Yes, you are right. Those have been modified. (L 679 and L 694)

Thanks.

(101) L 729: change "impressive" to "improved"

Yes, you are right.

This has been modified to "…its retrieval result is improved". (L 704)

Thanks.

(102) L 740: change "weather conditions" to "atmospheric conditions" (also elsewhere in the manuscript)

Yes, you are right. Those have been modified. (L 715 and L 722)

Thanks.

(103) L 743: change "and divides it" to "have been divided"

Yes, we agree with you.

"…the atmospheric profile is from the IFS-137 database introduced in Sect. 4, and divides it into four regions…" has been modified to "…this paper has divided the atmospheric profile from the IFS-137 database introduced in Sect. 4 into four regions…" (L 716-L 720)

Thanks.

(104) L 777: replace "optimized to" by "improved by"

Yes, you are right. This has been modified. (L 753)

Thanks.

(105) L 785: (_d_) Arctic

Sorry for my carelessness. This has been modified. (L 761)

Thanks.

(106) L 892: _is_ proposed

Yes, you are right. This has been modified. (L 806)

Thanks again for your careful review.

（b） **The list of all relevant changes made in the manuscript**

~~Channel~~A channel selection method for hyperspectral atmospheric infrared ~~sounder using AIRS data~~sounders based on layering

Shujie Chang[1, 2,3], Zheng Sheng[1,2], Huadong Du[1,2], Wei Ge[1,2] and Wei Zhang[1,2]

[1] College of Meteorology and Oceanography, National University of Defense Technology, Nanjing, China

[2] Collaborative Innovation Center on Forecast and Evaluation of Meteorological Disasters, Nanjing University of Information Science and Technology, Nanjing, China

[3] South China Sea Institute for Marine Meteorology, Guangdong Ocean University, Zhanjiang, China

Correspondence: Zheng Sheng (19994035@sina.com)

Abstract. Because a satellite channel's ability to resolve hyperspectral data varies with height, an improved channel selection method is proposed based on information content. An effective channel selection scheme for a hyperspectral atmospheric infrared sounder using AIRS data based on layering is proposed. The results are as follows: (1) Using the improved method, the atmospheric

retrievable index is more stable, the value reaching 0.54. The ~~distribution~~coverage of the ~~temperature weight function~~weighting functions is more ~~continuous, more closely approximating that of~~evenly distributed over height with this method and closer to the actual atmosphere; (2) Statistical inversion comparison experiments show that the accuracy of the retrieval temperature, using the improved channel selection method in this paper, is consistent with that of 1Dvar channel selection. In the ~~near space layer~~stratosphere and mesosphere especially, from 10 hPa to 0.02 hPa, the accuracy of the retrieval temperature of our improved channel selection method is ~~evidently~~ improved by about 1 K. In general, the accuracy of the retrieval temperature of ICS (Improved Channel Selection) is improved~~. Especially, from 100 hPa to 0.01 hPa, the accuracy of ICS can be improved by more than 11 %;~~; (3) Statistical inversion comparison experiments in four typical regions indicate that ICS in this paper is significantly better than NCS (NWP Channel Selection) and PCS (Primary Channel Selection) in different regions and shows latitudinal variations~~. Especially, from 100 hPa to 0.01 hPa, the accuracy of ICS can be improved by 7% to 13%,~~, which ~~means the ICS method selected in this paper is feasible and~~ shows ~~great promise~~potential for future applications.

1 Introduction

Since the successful launch of the first meteorological satellite, TIROS in the 1960s, satellite ~~detection~~observation technology has developed rapidly. Meteorological satellites observe the Earth's atmosphere from space and are able to record data from regions which are otherwise difficult to observe. Satellite data greatly enrich the content and range of meteorological observations, and consequently, atmospheric exploration technology and meteorological observations have taken us to a new stage in our understanding of weather systems and related phenomena (Fang, 2014). From the perspective of vertical atmospheric ~~detection~~observation, satellite instruments are developing rapidly. In their infancy, the traditional infrared ~~detection~~measurement instruments for detecting atmospheric temperature and moisture profiles, such as TOVS (Smith et al., 1991) or HIRS in ATOVS (Chahine, 1972; Li et al., 2000; Liu, 2007), usually employed filter spectrometry. Even though such instruments have played an important role in improving weather prediction, it is difficult to continue to build upon improvements in terms of ~~detection~~observation accuracy and vertical resolution due to the limitation of low spectral resolution. By using this kind of filter-based spectroscopic ~~detection~~measurement instrument, therefore, it is difficult to meet today's needs in numerical weather prediction (Eyre et al., 1993~~).~~; Prunet et al., 2010; Menzel et al., 2018). To meet this challenge, a series of plans for the creation of high-spectral resolution atmospheric ~~detection~~measurement instruments has been executed in the United States and in Europe in recent years: One example is the AIRS (Atmospheric ~~Infrared~~InfraRed Sounder) on the Earth Observation System, "Aqua", launched on May 4, 2002 from the United States. AIRS has 2378 spectral channels ~~with subpoint at 13 km and a detection height~~providing sensitivity from the ground ~~of~~ to up to about 65 km of altitude (Aumann et al., 2003; Hoffmann and Alexander, 2009; Gong et al., 2011). The United States and Europe, in 2010 and in 2007, also installed the CRIS (Cross-track Infrared Sounder) and the IASI (Inter-Attractive Atmospheric Sounding Interferometer) on polar-orbiting satellites.

China also ~~attaches~~devotes great importance to the development of such advanced ~~detection~~sounding technologies. In the early 1990s, the National Satellite Meteorological Center began to investigate the principles and techniques of hyperspectral resolution atmospheric ~~detection.~~observations. China's development of interferometric atmospheric vertical detectors eventually led to the launch of Fengyun No. 3, on May 27, 2008, and Fengyun No. 4 on December

11, 2016, both of which were equipped with infrared atmospheric ~~detectors.~~instruments. How best to use the hyperspectral resolution ~~detection~~observation data obtained from these instruments, to obtain reliable atmospheric temperature and humidity profiles, is an active area of ~~intense~~ study in atmospheric inversion theory.

Due to technical limitations, only a limited number of channels could at first be built into the ~~general~~typical satellite ~~detection instrument.~~instruments. In this case, channel selection generally involved controlling the channel ~~weight~~weighting function by utilizing the spectral response characteristics of the channel (such as ~~the~~ center frequency~~,~~ and bandwidth). With the development of ~~detection~~measurement technology, increasing numbers of hyperspectral detectors were carried on meteorological satellites. Due to the large number of channels and data supported by such instruments today (such as AIRS with 2378 channels and IASI with 8461 channels), it has proven extremely cumbersome to store, transmit, and process such data. Moreover, there is often a close correlation between ~~each~~the channel, causing an ill-posedness of the inversion, potentially compromising accuracy of the retrieval product based on hyperspectral resolution data.

However, hyperspectral detectors have many channels and provide real-time mode prediction systems with vast quantities of data, which can significantly improve prediction accuracy. But, if all the channels are used to retrieve data, the retrieval time considerably increases. Even more problematic are the glut of information produced, and the unsuitability of the calculations for real-time forecasting. Concurrently, the computer processing power must be large enough to meet the demands of simulating all the channels simultaneously within the forecast time. It is important to properly select a group of channels that can provide as much information as possible from the thousands of channels' observations to improve the calculation efficiency and retrieval quality.

Many researchers have studied the channel selection algorithm. Menke (1984) first chose channels using a data precision matrix method. Aires et al. (1999) made the selection using the Jacobian matrix, which has been widely used since then (Aires et al., 2002; Rabier et al., 2010). Rodgers (2000) indicated that there are two useful quantities in measuring the information provided by the observation data: Shannon information content and degrees of freedom. The concept of information capacity then became widely used in satellite channel selection. In 2007, Xu (2007) compared the Shannon information content with the relative entropy, analyzing the information loss and information redundancy. In 2008, Du et al. (2008) introduced the concept of the atmospheric retrievable index

(ARI) as a criterion for channel selection, and in 2010, Wakita et al. (2010) produced a scheme for calculating the information content of the various atmospheric parameters in remote sensing using Bayesian estimation theory. Kuai et al. (2010) analyzed both the Shannon information content and degrees of freedom in channel selection when retrieving CO_2 concentrations using thermal infrared remote sensing and indicated that 40 channels could contain 75% of the information from the total ~~of 1016~~ channels. Cyril et al. (2003) proposed the optimal sensitivity profile method based on the sensitivity of different atmospheric components. Lupu et al. (2012) used degrees of freedom for signals (DFS) to estimate the amount of information contained in observations in the context of observing system experiments. In addition, the singular value decomposition method has also been widely used for channel selection (Prunet et al., 2010; Zhang et al., 2011; Wang et al., 2014). In 2017, Chang et al. (2017) selected a new set of Infrared Atmospheric Sounding Interferometer (IASI) channels using the channel score index (CSI). Richardson et al. (2018) selected 75 from 853 channels based on the high spectral-resolution oxygen A-band instrument on NASA's Orbiting Carbon Observatory-2 (OCO-2), using information content analysis to retrieve the cloud optical depth, cloud properties, and position.

Today’s main methods for channel selection ~~(~~use only the weighting function to study appropriate numerical methods, such as the data precision matrix method (Menke, 1984), singular value decomposition method (Prunet et al., 2010; Zhang et al., 2011; Wang et al., 2014), and the Jacobi method (Aires et al., 1999; Rabier et al., 2010~~)~~). The use ~~only~~ of the ~~weight function to study appropriate numerical~~ methods~~, the use of which~~ allows sensitive channels to be selected. The above-mentioned studies also take into account the sensitivity of each channel to atmospheric parameters during channel selection, while ignoring some factors that impact retrieval results. The accuracy of retrieval results depends not only on the channel ~~weight~~weighting function but also on the channel noise, background field, and the retrieval algorithm.

Currently, information content is often employed in channel selection. During retrieval, this method delivers the largest amount of information for the selected channel combination (Rodgers, 1996; Du et al., 2008; He et al., 2012; Richardson et al., 2018). ~~Although this~~This method has made great breakthroughs in both theory and practice, ~~however, it does not take~~and the ~~sensitivity~~concept of ~~different channels at different heights into consideration.~~information content itself does consider all the height dependencies of the kernel matrix K (Rodgers, 2000). However, earlier works have neglected the height dependencies of K for simplicity. This paper uses the atmospheric retrievable index (ARI) as the index, which is based on information content (Du et al., 2008; Richardson et al. 2018). Channel selection is made at different heights, and an effective channel selection scheme is proposed which fully considers various factors, including the influence of different channels on the retrieval results at different heights. This ensures the best accuracy of the retrieval product when using the selected channel. In addition, statistical inversion comparison experiments are used to verify the effectiveness of the method.

2 Channel selection indicator ~~and~~, scheme and method

2.1 Channel selection indicator

According to the concept of information content, the information content contained in a selected channel of a hyperspectral instrument can be described as H (Rodgers, 1996; Rabier et al., 2010). The final expression of H is:

$$\mathrm{H} = -\frac{1}{2} ln\left|\hat{S} S_a^{-1}\right|$$

$$= -\frac{1}{2} ln|(S_a - S_a K^T (K S_a K^T + S_\varepsilon)^{-1} K S_a) S_a^{-1}|, \quad (1)$$

where S_a is the error covariance matrix of the background or the estimated value of atmospheric profile, $\cancel{\hat{S}}S_{\varepsilon}$ represents the observation error covariance matrix of each hyperspectral detector channel, $\hat{S} = (S_a - S_a K^T (K S_a K^T + S_{\varepsilon})^{-1} K S_a)$ denotes the covariance matrix after retrieval~~ by hyperspectral data~~, K is the ~~weight~~weighting function matrix~~, which comes from the selected channel in the hyperspectral data with respect to a specific atmospheric profile parameter~~.

In order to describe the accuracy of the retrieval results visually and quantitatively, the atmospheric retrievable index (ARI), p, (Du et al., 2008) is defined as follows:

$$p = 1 - \exp\left(\frac{1}{2n} ln\left|\hat{S} S_a^{-1}\right|\right), \qquad (2)$$

~~where S_a is the error covariance matrix of the background or the estimated value of the atmospheric profile, and $\hat{S}$ represents the observation error covariance matrix of each hyperspectral detector channel.~~ Assuming that before and after retrieval, the ratio of the root mean square error of each element in the atmospheric state vector is 1-p, then $\left|\hat{S} S_a^{-1}\right| = (1-p)^{2n}$ is derived. By inverting the equation, the ARI that is p can be obtained in Eq. (2), which indicates the relative portion of the error that is eliminated by retrieval. In fact, before and after retrieval, the ratio of the root mean square error of each element cannot be 1-p. Therefore, p defined by Eq. (1) is actually an overall evaluation of the retrieval result.

2.2 Channel selection scheme

The principle of channel selection is to find the optimum channel combination after numbering the channels. This combination ~~will make~~makes the information content, H, or the ARI defined in this paper as large as possible, in order to maintain the highest possible accuracy in the retrieval results.

Let there be M layers in the vertical direction of the atmosphere and N satellite channels. Selecting n from N channels, there will be C_N^n combinations in each layer, leading C_N^n calculations to get C_N^n kinds of p results. Furthermore, ~~under~~there are M layers in the ~~maximum one p-value,~~vertical direction of the ~~corresponding channel combination is used as the optimum channel combination; therefore~~atmosphere. Therefore, the entire atmosphere must be calculated $M \cdot \cancel{C_N^n} C_N^n$ times. However, the calculation $M \cdot C_N^n$ times will be particularly large, which makes this approach impractical in calculating p for all possible combinations. Therefore, it is necessary to design an effective calculation scheme, and such a scheme, i.e., a channel selection method, using iteration is proposed, called the "sequential absorption method"~~.~~ (Dudhia et al., 2002; Du et al., 2008). The method's main function is to select ("absorb") channels one by one, taking the channel with the maximum value of p. Through n iterations, n channels can be selected as the final channel combination. The steps are as follows:

(1) The expression of information content in a single channel:

First, we use only one channel for retrieval. A row vector, k, in the ~~weight~~weighting function matrix, K, is a ~~weight~~weighting function corresponding to the channel. ~~A diagonal element, $s_{\varepsilon}\frac{\partial^2 \Omega}{\partial v^2}$, in the S_{ε} matrix is the error variance in the channel.~~ After observation in this channel, the error covariance matrix is:

$$\hat{S} = S_a - S_a k^T (s_\varepsilon + k S_a k^T)^{-1} k S_a. \tag{3}$$

It should be noted that $(s_\varepsilon + k S_a k^T)$ is a ~~single~~scalar value in Eq. (3), so Eq. (3) can be converted to:

$$\hat{S} = \left(I - \frac{S_a k^T k}{(s_\varepsilon + k S_a k^T)}\right) S_a = \left(I - \frac{(k S_a)^T k}{(s_\varepsilon + k (k S_a)^T)}\right) S_a. \tag{4}$$

Substituting Eq. (4) into Eq. (2) gives:

$$\mathrm{p} = 1 - \exp\left(\frac{1}{2n} ln\left(\left|I - \frac{(k S_a)^T k}{(s_\varepsilon + k (k S_a)^T)}\right|\right)\right). \tag{5}$$

(2) Simplification of Eq. (5) p matrix:

Since S_a ~~is a~~and S_ε are positive definite symmetric ~~matrix~~matrixes, it can be decomposed into $S_a = (S_a^{1/2})^T (S_a^{1/2})$ and

$S_\varepsilon = (S_\varepsilon^{1/2})^T (S_\varepsilon^{1/2})$.

Define $\mathrm{R} = S_\varepsilon^{1/2} K S_a^{1/2}$. (6)

The matrix R can then be regarded as a ~~weight~~weighting function matrix, normalized by the observed error and ~~pre-observation error.~~a priori uncertainty. A row vector of R, $\mathrm{r} = s_\varepsilon^{-1/2} k S_a^{1/2}$, represents the normalized ~~weight~~weighting function matrix of a single channel.

Substituting r into Eq. (5) gives:

$$\mathrm{p} = 1 - \exp(\frac{1}{2n} ln\left(\left|I - \frac{rr^T}{1+r^T r}\right|\right)). \quad (7)$$

For arbitrary row vectors, a and b, using the matrix property $\det(\mathrm{I} + a^T \mathrm{b}) = 1 + \mathrm{b}a^T$, the new expression for p is:

$$\mathrm{p} = 1 - \exp\left(\frac{1}{2n} ln\left(1 - \frac{r^T r}{1 + r^T r}\right)\right)$$
$$= 1 - \exp\left(\frac{1}{2n} ln\left(\frac{1}{1+r^T r}\right)\right)$$
$$= 1 - \exp\left(-\frac{1}{2n} ln(1 + r^T r)\right). \quad (8)$$

(3) Iteration in a single layer:

First, the iteration in a single layer requires the calculation of R.

According to ~~S_a, S_ε~~ S_a, S_ε , K and Eq. (6), R~~, which is r corresponding to all the selected channels,~~ can be calculated. Second, using Eq. (8), p of each candidate channel can be calculated. Moreover, the channel corresponding to maximum p is the selected channel for this iteration. After a channel has been selected, according to Eq. (3) we can use $\hat{S}$ to get S_a for the next iteration. Finally, channels which are not selected during this iteration are used as the candidate channels for the next iteration.

When selecting n from N channels, it is necessary to calculate (N-n/2)n≈Nn p values, which is much smaller than C_N^n. ~~Of course, the combination selected by this method is not completely equivalent to the channel combination corresponding to the optimum value of C_N^n p, but it still satisfies the optimum value in a certain sense. In addition to its~~In addition to high computational efficiency by using this method, another advantage is that all channels can be recorded in the order in which they are selected. In the actual application, if n' channels are needed, and $n' < n$, we will not need to select the channel again, but record the selected channel only.

(4) Iteration for different altitudes:

Because satellite channel sensitivity varies with height, repeating the iterative process of step (3), selects the optimum channels at different heights. Assuming there are M layers in the atmosphere and selecting n from N channels, it is necessary to calculate $\mathrm{M}\cdot(\mathrm{N}-\mathrm{n}/2)\mathrm{n} \approx \mathrm{M}\cdot\mathrm{Nn}$ p values, a much smaller number than $\mathrm{M}\cdot\mathrm{C}_{N}^{n}$. In this way, different channel sets can be used to evaluate corresponding height in the retrieved profiles.

2.3 Statistical inversion method

The inversion ~~method of~~methods for the atmospheric temperature ~~profile~~profiles can be summarized in two categories: statistical inversion and physical inversion. Statistical inversion is essentially a linear regression model which uses a large number of satellite measurements and atmospheric parameters to match samples and calculate their correlation coefficient. Then, based on the correlation coefficient, the required parameters of the independent measurements obtained by the satellite are retrieved. Because the method does not directly solve the radiation transfer equation, it has the advantages of fast calculation speed. In addition, the solution is numerically stable, which makes it one of the highest precision methods (Chedin et al., 1985). Therefore, the statistical inversion method will be used for our channel selection experiment and a regression equation will be established.

According to an empirical orthogonal function, the atmospheric temperature (or humidity), T, and the ~~bright~~brightness temperature, T_b, are expanded ~~thus~~as:

$$\mathrm{T} = T^* \cdot A, \tag{9}$$

$$T_b = T_b^* \cdot A, \tag{10}$$

where T^* and T_b^* are the eigenvectors of the covariance matrix of temperature (or humidity) and brightness temperature, respectively. A and B stand for the corresponding expansion coefficient vectors of temperature (humidity) and brightness temperature.

Using the least squares method and the orthogonal property, the coefficient conversion matrix, V, is introduced:

$$\mathrm{A} = \mathrm{V} \cdot B, \tag{11}$$

where $V = AB^T(BB^T)^{-1}$. (12)

Using the orthogonality, we get:

$$\mathrm{B} = (T_b^*)^T T_b, \tag{13}$$

$$A = (T^*)^T T. \tag{14}$$

For convenience, the anomalies of the state vector (atmospheric temperature), T, and the observation vector (~~bright~~brightness temperature), T_b, are taken:

$$\hat{T} = \overline{T} + \hat{T}' = \overline{T} + GT_b' = \overline{T} + G(T_b - \overline{T_b}), \tag{15}$$

where $\hat{T}$ stands for the retrieval atmospheric temperature. $\overline{T}$ and ~~$\overline{T_b}$~~$\overline{T_b}$ are the corresponding average values of the elements, respectively. ~~T'~~$\hat{T}'$ and T_b' represent the corresponding anomalies of the elements, respectively.

Assuming there are k sets of observations, a sample anomaly matrix with k vectors can be constructed:

$$T' = (t_1', t_2', \cdots, t_k'), \tag{16}$$

$$T_b' = (t_{b1}', t_{b2}', \cdots, t_{bk}'). \tag{17}$$

Define the inversion error matrix as:

$$\delta = \overline{T} - \hat{T} = \hat{T}' - T'. \tag{18}$$

The retrieval error covariance matrix is:

$$
\begin{aligned}
S_\delta &= \frac{1}{k-n-1}\delta\delta^T \\
&= \frac{1}{k-n-1}(T' - GT_b')(T' - GT_b')^T \\
&= \frac{k-1}{k-n-1}(S_e - G^T S_{xy} - S_{xy}G^T + GS_yG^T), \qquad (19)
\end{aligned}
$$

where

$$
\begin{aligned}
S_e &= \frac{1}{k-1} T' T'^{T}, \\
S_y &= \frac{1}{k-1} T_b' T_b'^{T}, \\
S_{xy} &= \frac{1}{k-1} T' T_b'^{T}. \qquad (20)
\end{aligned}
$$

S_e stands for the sample covariance matrix of T, S_y denotes the sample covariance matrix of T_b, and S_{xy} represents the covariance matrix of T and T_b. The elements on the diagonal of the error covariance matrix, S_δ, represent the retrieval error variance of T. The matrix G that minimizes the overall error variance is the least squares coefficient matrix of the regression equation (15), which meets the criteria:

$$\delta^2 = \mathrm{tr}(S_\delta) = \mathrm{min}. \quad (21)$$

~~Equation (21) takes~~Taking a derivative of Eq. (21) with respect to G, $\frac{\partial}{\partial G}\mathrm{tr}(S_\delta) = 0 = (-2S_{xy} + 2GS_y)$, which means that:

$$G = S_{xy}S_y^{-1}. \quad (22)$$

Substituting Eq. (22) into Eq. (15) finally gives the least squares solution as:

$$\hat{T} = \overline{T} + S_{xy}S_y^{-1}(T_b - \overline{T_b}). \quad (23)$$

It should be noted that the least squares solution obtained here aims to minimize the sum of the error variance for each element in the atmospheric state vector after retrieval ~~of observations has been completed~~for several times. At present, statistical multiple regression is widely used in the retrieval of atmospheric profiles based on atmospheric remote sensing data. As long as there are enough data, S_{xy} and S_y can be determined.

3. Channel selection experiment

3.1 Data and model

The Atmospheric Infrared Sounder (AIRS) ~~instrument suite~~ is primarily designed to measure the Earth's atmospheric water vapor and temperature profiles on a global scale~~.~~ (Aumann et al., 2003; Hoffmann and Alexander, 2009). AIRS is a continuously operating cross-track scanning sounder, consisting of a telescope that feeds an echelle spectrometer. The AIRS infrared spectrometer acquires 2378 spectral samples at a resolution λ/Δλ, ranging from 1086 to 1570, in three bands: 3.74 μm to 4.61 μm, 6.20 μm to 8.22 μm, and 8.8 μm to 15.4 μm. The ~~spatial~~ footprint ~~of the infrared channels is 1.1° in diameter, which corresponds to about 15×15~~size 13.5 km at ~~the~~ nadir~~.~~ (Susskind et al., 2003). The spectral range includes 4.~~2~~3 μm and 15.5 μm for important temperature ~~detection, 15 μm for~~observation and CO_2, 6.3 μm for water vapor, and 9.6 μm for ozone absorption bands~~.~~ (Menzel et al., 2018). The ~~absolute accuracy~~root mean square error (RMSE) of the measured radiation is better than 0.2 K~~.~~ (Susskind et al., 2003). Moreover, global atmospheric profiles can be detected every day~~, and the four imaging channels of visible/near infrared are always filled.~~. Due to radiometer noise and faults, there are currently only 2047 effective channels. However, compared with previous infrared detectors, AIRS boasts a significant improvement in both the number of channels and spectral resolution (Aumann, 1994; Huang et al., 2005;

Li et al., 2005).

~~AIRS provides real-time mode prediction systems with vast quantities of data, which greatly improves prediction accuracy. However, if all the channels are used to retrieve data, the retrieval time becomes greatly extended. Even more problematic are the huge amounts of information and calculations not being suitable for real-time forecasting.~~

The root mean square error of an AIRS infrared channel is shown in Fig. 1, with black spots, indicating that not all the instrument channels possess a measurement error of less than 0.2 K. There are a few channels with extremely large measurement errors, which reduce the accuracy of prediction to some extent. ~~Moreover, not all channels possess the same~~Among them, some extremely large measurement ~~error.~~errors reduce the accuracy of prediction to some extent (Susskind et al., 2003). At present, more than 300 channels have not been used because their errors exceed 1 K. If data from these channels were to be used for retrieval, the accuracy of the retrieval could be reduced. Therefore, it is necessary to select a group of channels to improve the calculation efficiency and retrieval quality. In this paper we study channel selection for temperature profile retrieval by AIRS.

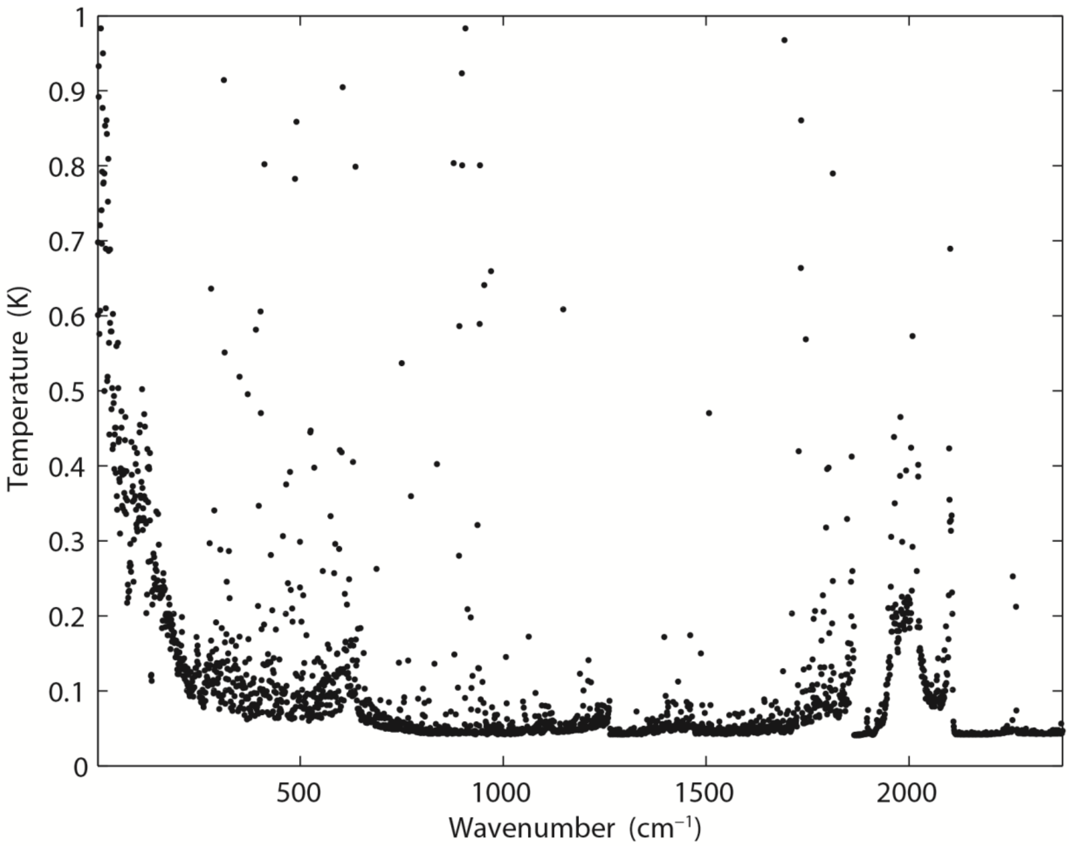

Figure 1. Root mean square error of AIRS infrared channel (black spots).

For the calculation of radiative transfer ~~model~~ and ~~its weight~~the weighting function matrix, K, the RTTOV (Radiative Transfer for TOVS) v12 fast radiative transfer model is used. Although initially developed for the TOVS (TIROS Operational Vertical Sounder) radiometers, RTTOV ~~is an evolution of RTTOV v11, adding~~can now simulate around 90 different satellite sensors measuring in the MW (microwave), IR (infrared) and ~~upgrading many features.~~VIS (visible) regions of the spectrum (Saunders et al., 2018). The model allows rapid simulations (1 ms for 40 channel ATOVS (Advanced TOVS) on a desktop PC) of radiances for satellite visible, infrared, or microwave nadir scanning radiometers given atmospheric profiles of temperature and ~~variable~~trace gas ~~concentration~~concentrations, and cloud and surface properties. The only mandatory gas included as a variable for RTTOV v12 is water vapor. Optionally, ozone, carbon dioxide, nitrous oxide, methane, carbon monoxide, and sulfur dioxide can be included, with all other constituents assumed to be constant. RTTOV ~~v12~~ can accept input profiles on any defined set of pressure levels. The majority of RTTOV ~~v12~~ coefficient files are based on the 54 levels ~~shown in~~ (see Table ~~1,~~A1 in Appendix A), ranking from 1050 hPa to 0.01 hPa, though coefficients for some hyperspectral sounders are also available on 101 levels.

~~**Table 1.** Pressure levels adopted for RTTOV v12 54 pressure level coefficients and profile limits within which the transmittance calculations are valid. Note that the gas units here are ppmv. (From https://www.nwpsaf.eu/site/software/rttov/, RTTOV Users guide, 2019).~~

~~Level~~	~~Pressure~~	~~Tmax~~	~~Tmin~~	~~Qmax~~	~~Qmin~~	~~Q_2max~~	~~Q_2min~~	~~Q_2Ref~~
~~Number~~	~~hPa~~	~~K~~	~~K~~	~~ppmv*~~	~~ppmv*~~	~~ppmv*~~	~~ppmv*~~	~~ppmv*~~
~~1~~	~~0.01~~	~~245.95~~	~~143.66~~	~~5.24~~	~~0.91~~	~~1.404~~	~~0.014~~	~~0.296~~
~~2~~	~~0.01~~	~~252.13~~	~~154.19~~	~~6.03~~	~~1.08~~	~~1.410~~	~~0.069~~	~~0.321~~
~~3~~	~~0.03~~	~~263.71~~	~~168.42~~	~~7.42~~	~~1.35~~	~~1.496~~	~~0.108~~	~~0.361~~
~~4~~	~~0.03~~	~~280.12~~	~~180.18~~	~~8.10~~	~~1.58~~	~~1.670~~	~~0.171~~	~~0.527~~

~~5~~	~~0.13~~	~~299.05~~	~~194.48~~	~~8.44~~	~~1.80~~	~~2.064~~	~~0.228~~	~~0.769~~
~~6~~	~~0.23~~	~~318.64~~	~~206.21~~	~~8.59~~	~~1.99~~	~~2.365~~	~~0.355~~	~~1.074~~
~~7~~	~~0.41~~	~~336.24~~	~~205.66~~	~~8.58~~	~~2.49~~	~~2.718~~	~~0.553~~	~~1.471~~
~~8~~	~~0.67~~	~~342.08~~	~~197.17~~	~~8.34~~	~~3.01~~	~~3.565~~	~~0.731~~	~~1.991~~
~~9~~	~~1.08~~	~~340.84~~	~~189.50~~	~~8.07~~	~~3.30~~	~~5.333~~	~~0.716~~	~~2.787~~
~~10~~	~~1.67~~	~~334.68~~	~~179.27~~	~~7.89~~	~~3.20~~	~~7.314~~	~~0.643~~	~~3.756~~
~~11~~	~~2.50~~	~~322.5~~	~~17627~~	~~7.75~~	~~2.92~~	~~9.191~~	~~0.504~~	~~4.864~~
~~12~~	~~3.65~~	~~312.51~~	~~175.04~~	~~7.69~~	~~2.83~~	~~10.447~~	~~0.745~~	~~5.953~~
~~13~~	~~5.19~~	~~303.89~~	~~173.07~~	~~7.58~~	~~2.70~~	~~12.336~~	~~1.586~~	~~6.763~~
~~14~~	~~7.22~~	~~295.48~~	~~168.38~~	~~7.53~~	~~2.54~~	~~12.936~~	~~1.879~~	~~7.109~~
~~15~~	~~9.84~~	~~293.33~~	~~166.30~~	~~7.36~~	~~2.46~~	~~12.744~~	~~1.322~~	~~7.060~~
~~16~~	~~13.17~~	~~287.05~~	~~16347~~	~~7.20~~	~~2.42~~	~~11.960~~	~~0.719~~	~~6.574~~
~~17~~	~~17.33~~	~~283.36~~	~~161.49~~	~~6.96~~	~~2.20~~	~~11.105~~	~~0.428~~	~~5.687~~
~~18~~	~~22.46~~	~~280.93~~	~~161.47~~	~~6.75~~	~~1.71~~	~~9.796~~	~~0.278~~	~~4.705~~
~~19~~	~~28.69~~	~~282.67~~	~~162.09~~	~~6.46~~	~~1.52~~	~~8.736~~	~~0.164~~	~~3.870~~
~~20~~	~~36.17~~	~~27993~~	~~162.49~~	~~6.14~~	~~1.31~~	~~7.374~~	~~0.107~~	~~3.111~~
~~21~~	~~45.04~~	~~27315~~	~~164.66~~	~~5.90~~	~~1.36~~	~~6.799~~	~~0.055~~	~~2.478~~
~~22~~	~~55.44~~	~~265.93~~	~~166.19~~	~~6.21~~	~~1.30~~	~~5.710~~	~~0.048~~	~~1.907~~
~~23~~	~~67.51~~	~~264.7~~	~~167.42~~	~~9.17~~	~~1.16~~	~~4.786~~	~~0.043~~	~~1.440~~
~~24~~	~~81.37~~	~~261.95~~	~~159.98~~	~~17.89~~	~~0.36~~	~~4.390~~	~~0.038~~	~~1.020~~
~~25~~	~~97.15~~	~~262.43~~	~~163.95~~	~~20.30~~	~~0.01~~	~~3.619~~	~~0.016~~	~~0.733~~
~~26~~	~~114.94~~	~~259.57~~	~~168.59~~	~~33.56~~	~~0.01~~	~~2.977~~	~~0.016~~	~~0.604~~
~~27~~	~~134.83~~	~~259.26~~	~~169.71~~	~~102.24~~	~~0.01~~	~~2.665~~	~~0.016~~	~~0.489~~
~~28~~	~~156.88~~	~~260.13~~	~~169.42~~	~~285.00~~	~~0.01~~	~~2.351~~	~~0.013~~	~~0.388~~
~~29~~	~~181.14~~	~~262.27~~	~~17063~~	~~714.60~~	~~0.01~~	~~1.973~~	~~0.010~~	~~0.284~~
~~30~~	~~207.61~~	~~264.45~~	~~174.11~~	~~1464.00~~	~~0.01~~	~~1.481~~	~~0.013~~	~~0.196~~
~~31~~	~~236.28~~	~~270.09~~	~~177.12~~	~~2475.60~~	~~0.01~~	~~1.075~~	~~0.016~~	~~0.145~~
~~32~~	~~267.10~~	~~277.93~~	~~181.98~~	~~4381.20~~	~~0.01~~	~~0.774~~	~~0.015~~	~~0.110~~
~~33~~	~~300.00~~	~~285.18~~	~~184.76~~	~~6631.20~~	~~0.01~~	~~0.628~~	~~0.015~~	~~0.086~~
~~34~~	~~334.86~~	~~293.68~~	~~187.69~~	~~9450.00~~	~~1.29~~	~~0.550~~	~~0.016~~	~~0.073~~

~~35~~	~~371.55~~	~~300.12~~	~~190.34~~	~~12432.00~~	~~1.52~~	~~0.447~~	~~0.015~~	~~0.063~~
~~36~~	~~409.89~~	~~302.63~~	~~194.40~~	~~15468.00~~	~~2.12~~	~~0.361~~	~~0.015~~	~~0.057~~
~~37~~	~~449.67~~	~~304.43~~	~~198.46~~	~~18564.00~~	~~2.36~~	~~0.284~~	~~0.015~~	~~0.054~~
~~38~~	~~490.85~~	~~307.2~~	~~201.53~~	~~21684.00~~	~~2.91~~	~~0.247~~	~~0.015~~	~~0.052~~
~~39~~	~~532.56~~	~~31217~~	~~202.74~~	~~24696.00~~	~~3.67~~	~~0.199~~	~~0.015~~	~~0.050~~
~~40~~	~~572.15~~	~~31556~~	~~201.61~~	~~27480.00~~	~~3.81~~	~~0.191~~	~~0.012~~	~~0.050~~
~~41~~	~~618.07~~	~~318.26~~	~~189.95~~	~~30288.00~~	~~6.82~~	~~0.171~~	~~0.010~~	~~0.049~~
~~42~~	~~661.00~~	~~321.71~~	~~189.95~~	~~32796.00~~	~~6.07~~	~~0.128~~	~~0.009~~	~~0.048~~
~~43~~	~~703.59~~	~~327.95~~	~~189.95~~	~~55328.00~~	~~6.73~~	~~0.124~~	~~0.009~~	~~0.047~~
~~44~~	~~745.48~~	~~333.77~~	~~189.95~~	~~37692.00~~	~~8.71~~	~~0.117~~	~~0.009~~	~~0.046~~
~~45~~	~~786.33~~	~~336.46~~	~~189.95~~	~~39984.00~~	~~8.26~~	~~0.115~~	~~0.008~~	~~0.045~~
~~46~~	~~825.75~~	~~338.54~~	~~189.95~~	~~42192.00~~	~~7.87~~	~~0.113~~	~~0.008~~	~~0.043~~
~~47~~	~~863.40~~	~~342.55~~	~~189.95~~	~~44220.00~~	~~7.53~~	~~0.111~~	~~0.007~~	~~0.041~~
~~48~~	~~898.93~~	~~346.23~~	~~189.95~~	~~46272.00~~	~~7.23~~	~~0.108~~	~~0.006~~	~~0.040~~
~~49~~	~~931.99~~	~~34924~~	~~189.95~~	~~47736.00~~	~~6.97~~	~~0.102~~	~~0.006~~	~~0.038~~
~~50~~	~~962.26~~	~~349.92~~	~~189.95~~	~~51264.00~~	~~6.75~~	~~0.099~~	~~0.006~~	~~0.034~~
~~51~~	~~989.45~~	~~350.09~~	~~189.95~~	~~49716.00~~	~~6.57~~	~~0.099~~	~~0.006~~	~~0.030~~
~~52~~	~~1013.29~~	~~360.09~~	~~189.95~~	~~47208.00~~	~~6.41~~	~~0.094~~	~~0.006~~	~~0.028~~
~~53~~	~~1033.54~~	~~350.09~~	~~189.95~~	~~47806.00~~	~~6.29~~	~~0.094~~	~~0.006~~	~~0.027~~
~~54~~	~~1050.00~~	~~350.09~~	~~189.95~~	~~47640.00~~	~~6.19~~	~~0.094~~	~~0.006~~	~~0.027~~

~~The weight function matrix, K (Jacobian matrix), in this paper is the weight function matrix of the atmospheric characteristics.~~ In order to correspond to the selected profiles, the atmosphere is divided into 137 layers, each of which contains corresponding atmospheric characteristics, such as temperature, pressure, and the humidity distribution. Each element in the ~~weight~~weighting function matrix can be written as ∂yi/∂xj. The subscript i is used to identify the satellite channel, and the subscript j is used to identify the atmospheric ~~characteristics.~~variable. Therefore, ∂yi/∂xj indicates the variation in ~~radiation~~ brightness temperature in a given satellite channel, when a given atmospheric ~~characteristic~~variable in a given layer changes. We are thus able to establish which layer of the satellite channel is particularly sensitive to which atmospheric characteristic (temperature, various gas contents) in the vertical atmosphere. The RTTOV_K (the K mode), is used to calculate the matrix H(X0) (Eq. (1)) for a given atmospheric profile characteristic.

3.2 Channel selection comparison experiment and results

In order to verify the effectiveness of the method, three sets of comparison experiments were conducted. First, 324 channels used by the EUMETSAT Satellite Application Facility on Numerical Weather Prediction (NWP SAF) were selected. NCS is short for NWP channel selection in this paper. ~~The products~~NCS were released by the NWPSAF 1DVar (one-dimensional variational analysis) scheme, in accordance with the requirements of the NWPSAF~~.~~ (Saunders et al., 2018). Second, 324 channels were selected using the information capacity method. This method was adopted by Du et al. (2008) without the consideration of layering. PCS is short for primary channel selection in this paper.

Third, 324×M channels were selected using the information capacity method for the M layer atmosphere. ICS is short for improved channel ~~selectionin~~selection in this paper. In order to verify the retrieval effectiveness after channel selection, statistical inversion comparison experiments were performed using 5000 temperature profiles provided by the ECMWF dataset, which will be introduced in Sect. 4.

The observation error covariance matrix, S_{ε}, in the experiment is provided by NWP SAF 1Dvar. In general, it can be converted to a diagonal matrix, the elements of which are the observation error standard deviation of each hyperspectral detector channel, which is the square of the root mean square error for each channel. The root mean square error of ~~an~~the AIRS ~~infrared channel~~channels is shown in Fig. 1. The error covariance matrix of the background, S_a, is calculated using 5000 samples of the IFS-137 data provided by the ECMWF dataset (The detailed information will be introduced in Sect. 4). The last access date is April 26th, 2019 (download address: https://www.nwpsaf.eu/site/update-137-level-nwp-profile-dataset/, 2019). The covariance matrix of temperature is shown in Fig. 2~~, the~~. The results are consistent with the previous study by Du et al. (2008).

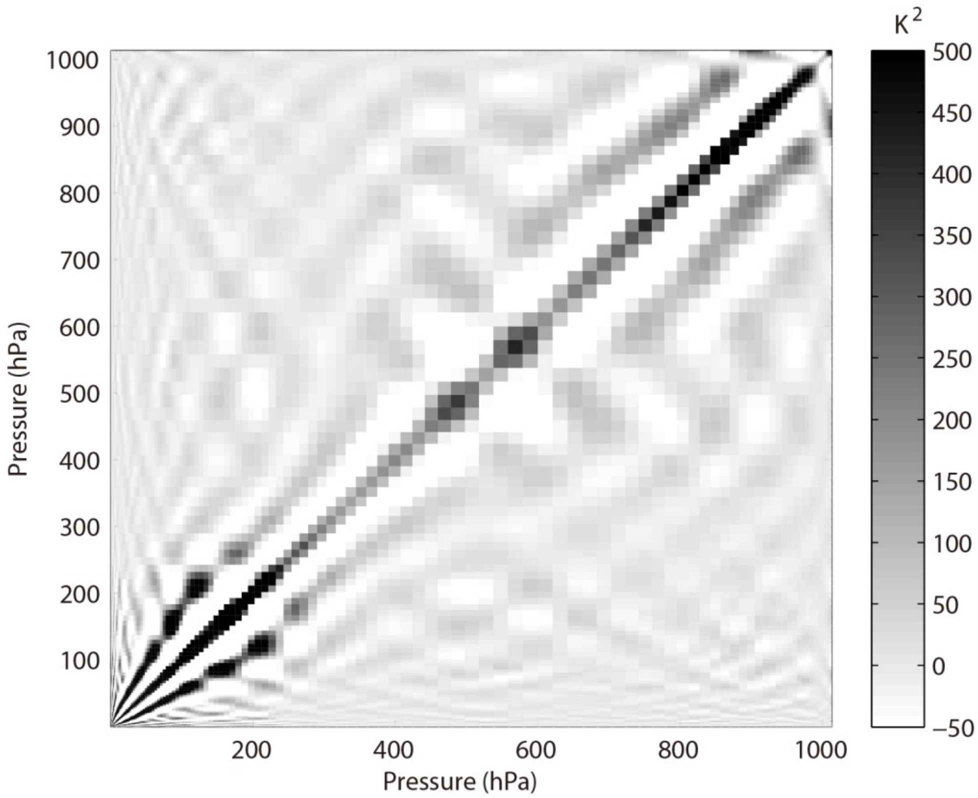

Figure 2. Error covariance matrix of temperature (shaded).

The reference atmospheric profiles are from the IFS-137 database, and the temperature ~~weight~~weighting function matrix is calculated using the RTTOV_K mode, as shown in Fig. 3; the results are consistent with those of the previous study by Du et al. (2008). For the air-based passive atmospheric remote sensing studied in this paper, when the same channel detects the atmosphere from different observation angles, the value of the ~~weight~~weighting function matrix K changes due to the limb effect. ~~Therefore, when we select~~The goal of this section is focusing on the selection methods of selecting channels~~, the results differ because of~~ ; therefore the biases produced from different observation angles~~. But due to the selection principle and method are exactly the same and our key is the selection method; we do not discuss, therefore, the variation in observation angle when making a selection~~ can be ignored.

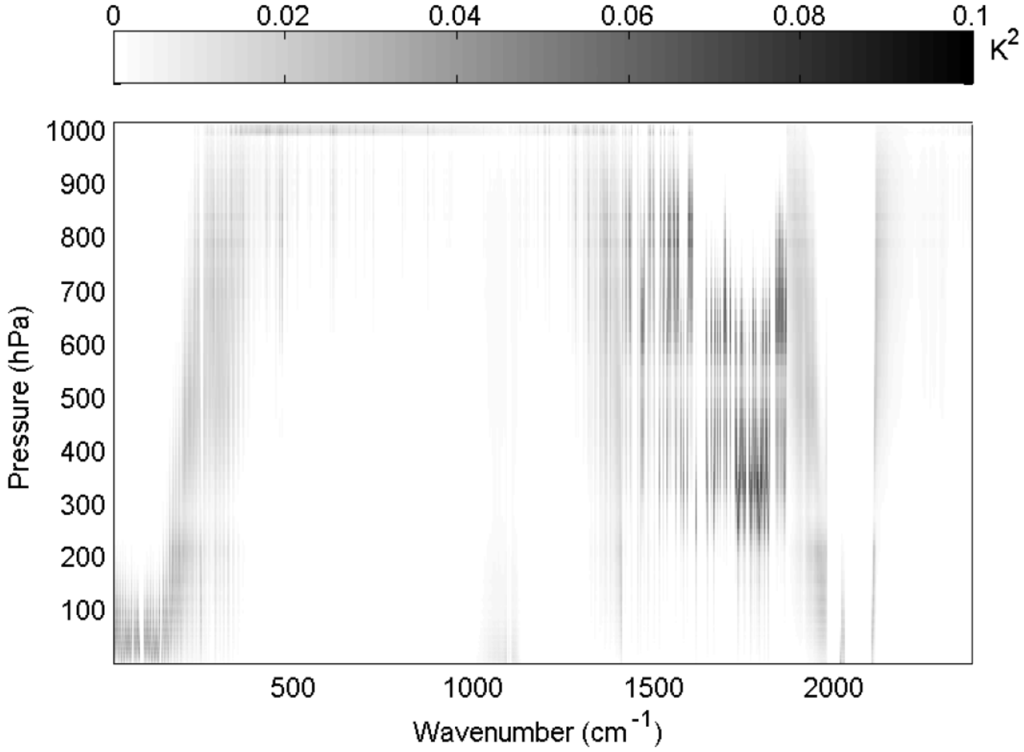

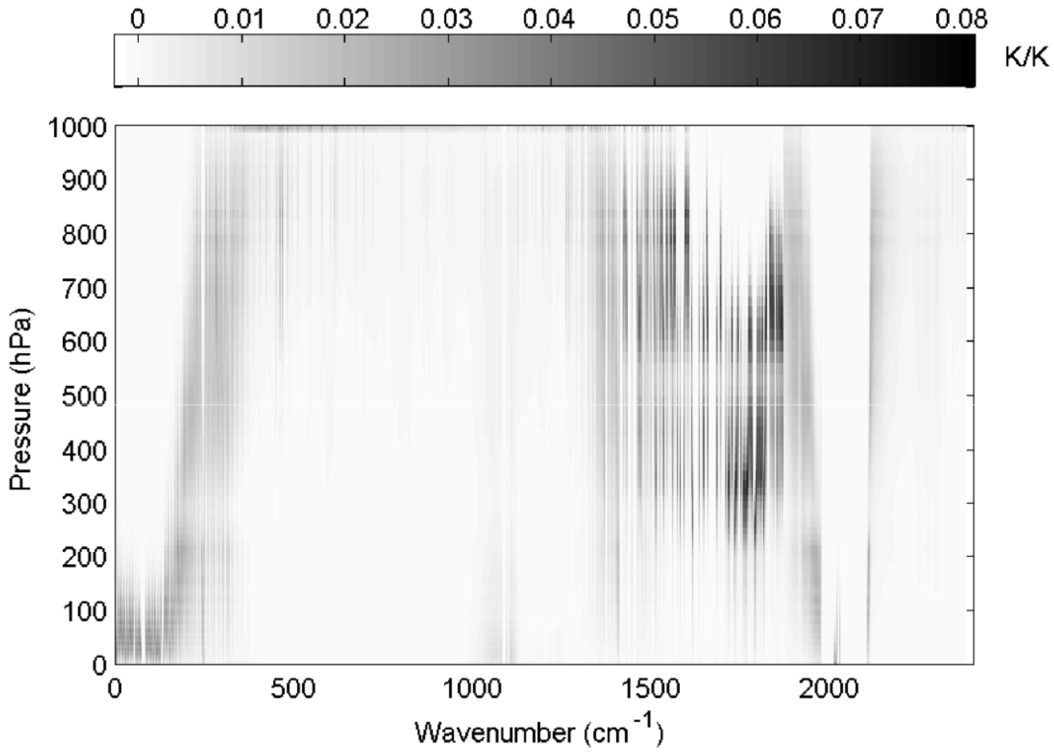

Figure 3. Temperature ~~weight~~weighting function matrix (shaded).

In order to verify the effectiveness ~~of ICS~~, the distribution of 324 channels, without considering layering, in the AIRS ~~bright~~brightness temperature spectrum is indicated in Fig. 4. The background brightness temperature is the simulated AIRS observation brightness temperature, which is from the atmospheric profile in RTTOV put into the model. Figure 4(a) shows the 324 channels selected by PCS, while Fig. 4(b) shows the 324 channels selected by NCS.

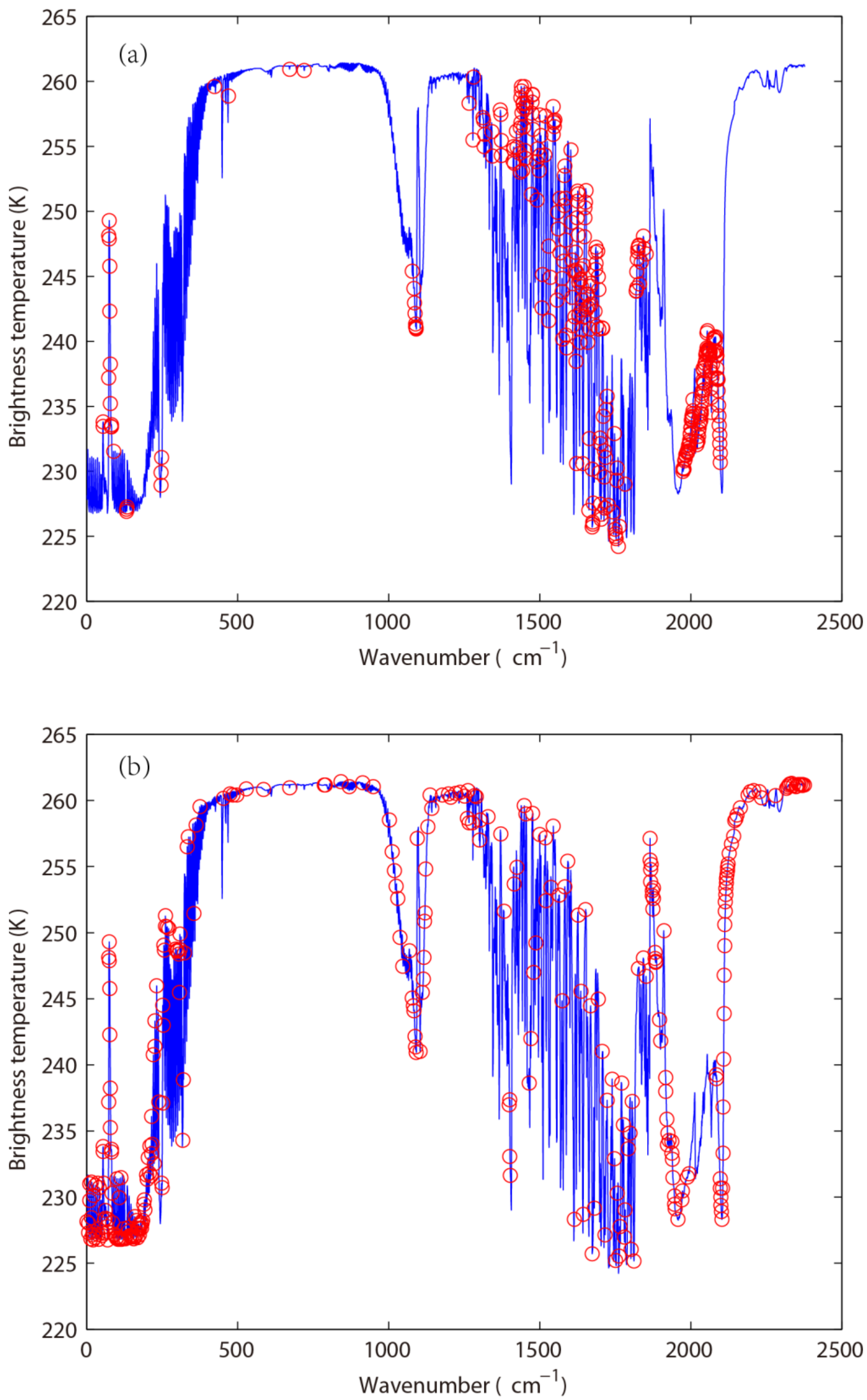

Figure 4. The distribution of different channel selection methods without considering layering in the AIRS ~~bright~~brightness

temperature spectrum (blue line). (a) 324 channels selected by PCS (red circles). (b) 324 channels selected by NCS (red circles).

Without considering layering, the main differences between the 324 channels selected by PCS and NCS are as follows: (1) When the wavenumber approaches 1000, the wavelength is ~~11~~10 μm (1/1000 cm^{-1}). Near this band, fewer channels are selected by PCS because the retrieval of ground temperature is considered by NCS; (2) When the wavenumber is near 1200, the wavelength is 9 μm (1/1200 cm^{-1}). Near this band, no channels are selected by PCS because the retrieval of O_3 is not considered in this paper; (3) When the wavenumber approaches 1500, the wavelength is 6.7 μm (1/1500 cm^{-1}). As is known, the spectral range from 6 μm to 7 μm corresponds to water vapor absorption bands, but fewer channels are selected by NCS; (4) When the wavenumber is close to 2000, it derives a wavelength of 5 μm (1/2000 cm^{-1}), which includes 4.2 μm for N_2O and 4.3 μm for CO_2 absorption bands. As is shown in Fig. 4, fewer channels are selected by PCS in those bands. PCS is favorable for atmospheric temperature ~~detection~~observation in the high temperature zone. Because 4.2 μm and 4.3 μm bands are sensitive to high temperature, the higher temperature is, the better observation can be obtained; (5) In the near infrared area, the wavenumber exceeds 2200, deriving a wavelength of less than 4 μm (1/2000 cm^{-1}).

A small number of channels is selected by NCS, but no channels are selected by PCS.

Above all, the information content used in this paper only takes the temperature profile retrieval into consideration, so the channel combination of PCS is inferior to that of NCS for the retrieval of surface temperature and the O_3 profile. The advantages of the channel selection method based on information content in this paper are mainly reflected in: (1) ~~Near space (20–100 km)~~Stratosphere and mesosphere is less affected by the ground surface, so the retrieval result of PCS is better than that of NCS. (2) Due to the method selected in this paper there are more channels at 4.2 μm for N_2O and 4.3 μm for CO_2 absorption bands; the channel combination of PCS is ~~superior to~~better than that of NCS for atmospheric temperature ~~detection in~~ observation to the ~~high~~higher temperature~~ zone.~~.

By comparing channel selection without considering layering, we note the general advantages and disadvantages of PCS and NCS for the retrieval of ~~atmosphere~~temperature and can improve the channel selection scheme. First, the retrieval of the temperature profile for 324 channels selected by PCS is obtained. The relationship between the number of iterations and the ARI is shown in Fig. 5.

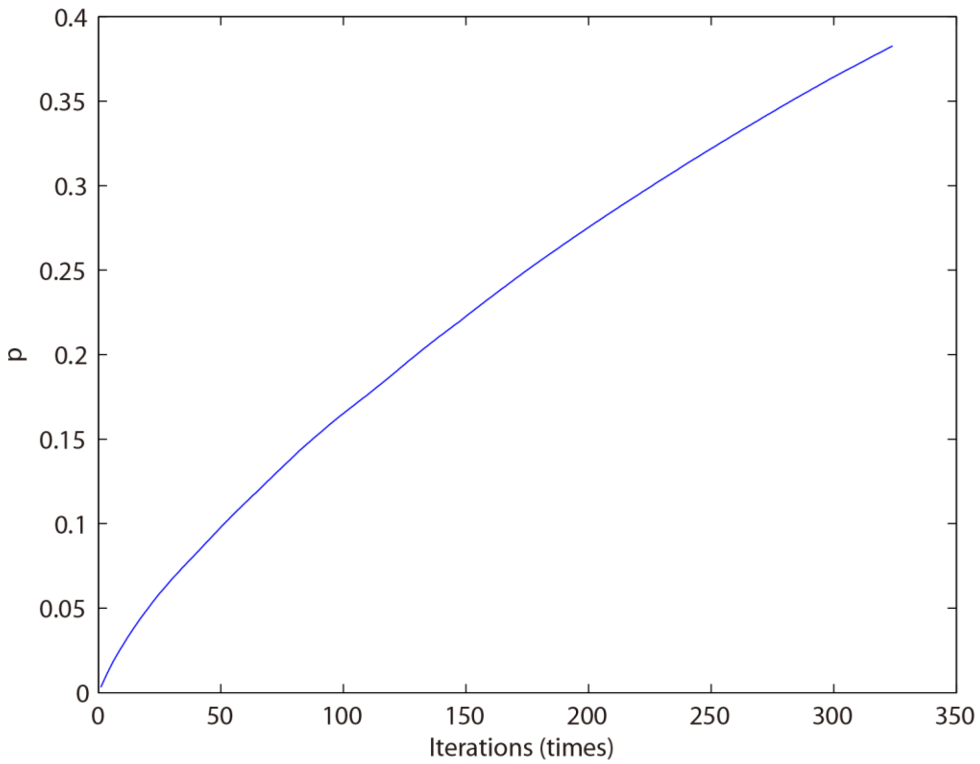
0.4
0.35
0.3
0.25
0.2
0.15
0.1
0.05
0
p
0
50
100
150
200
250
300
350
Iterations (times)

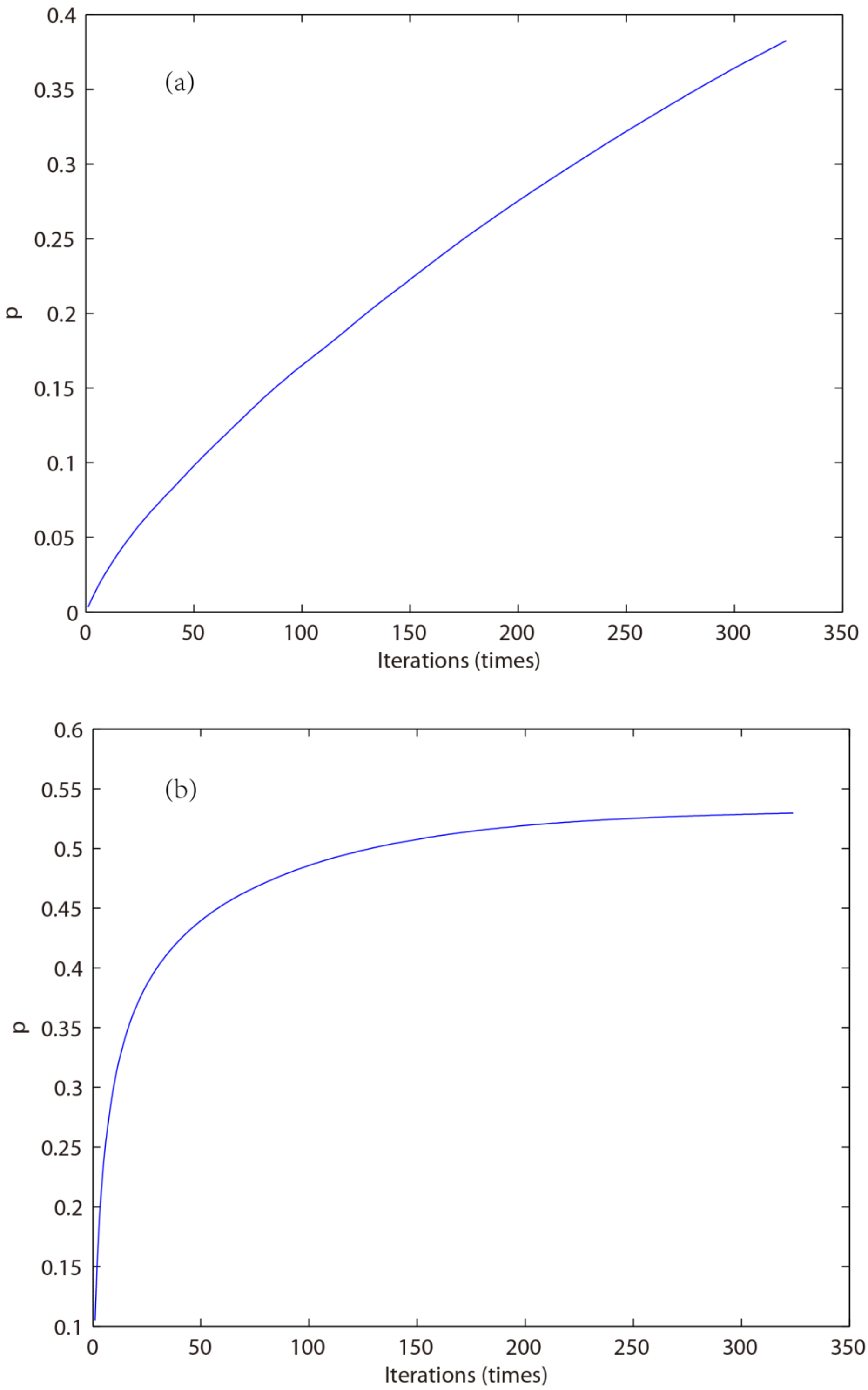

Figure 5. The relationship between the number of iterations and ARI ~~for~~. (a) PCS. (b) ICS.

The ARI for PCS tends to be 0.38 and is not convergent, so the PCS method needs to be improved. In this paper, the atmosphere is divided into 137 layers, and based on the information content and iteration, 324 channels are selected for each layer. ~~Moreover~~Then, the temperature profile of each layer can be retrieved~~.~~ based on statistical inversion (see at Sect. 4). The relationship between the number of iterations and the ARI for ICS is shown in Fig. ~~6.~~5b. When the number of iterations approaches 100, the ARI of ICS tends to be stable, ~~reaching~~and reach to 0.54. Thus, in terms of the ARI and convergence, the ICS method is ~~superior to~~better than that of PCS.

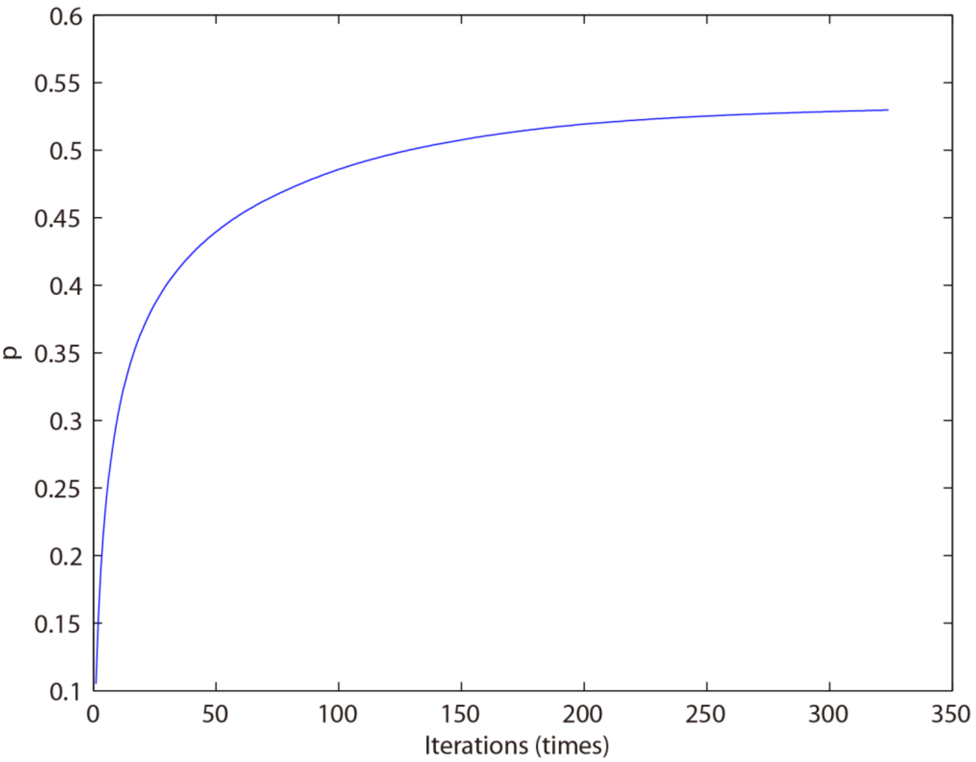

~~**Figure 6.** The relationship between the number of iterations and the ARI for ICS.~~

Furthermore, because an iterative method is used to select channels, the order of each selected channel is determined by the contribution from the ARI. The ~~weight~~weighting function matrix of the top 324 selected channels, according to channel order, is shown in Fig. ~~7~~6.

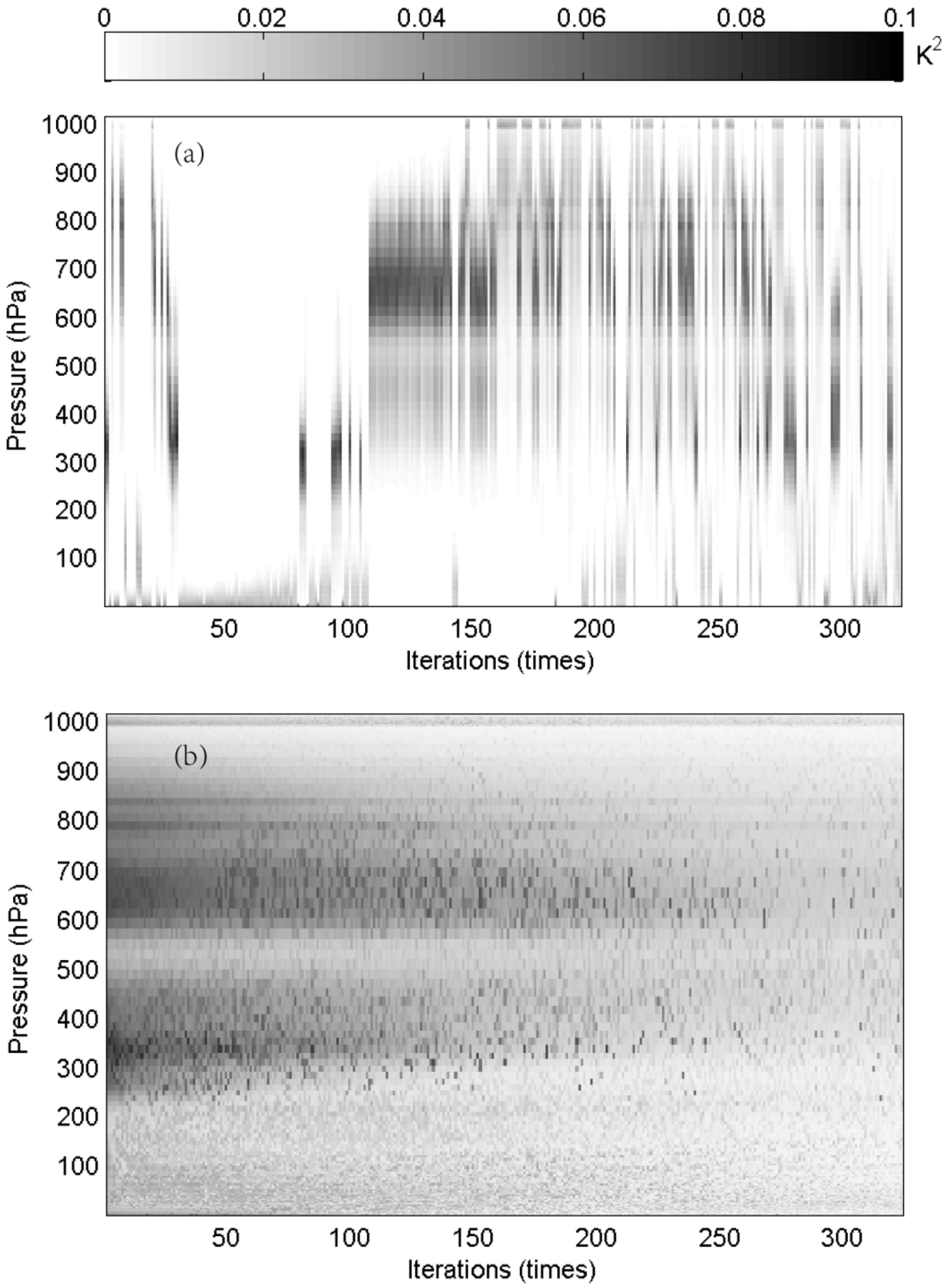
0 0.02 0.04 0.06 0.08 0.1
K^2
(a)
Pressure (hPa)
Iterations (times)
(b)
Pressure (hPa)
Iterations (times)

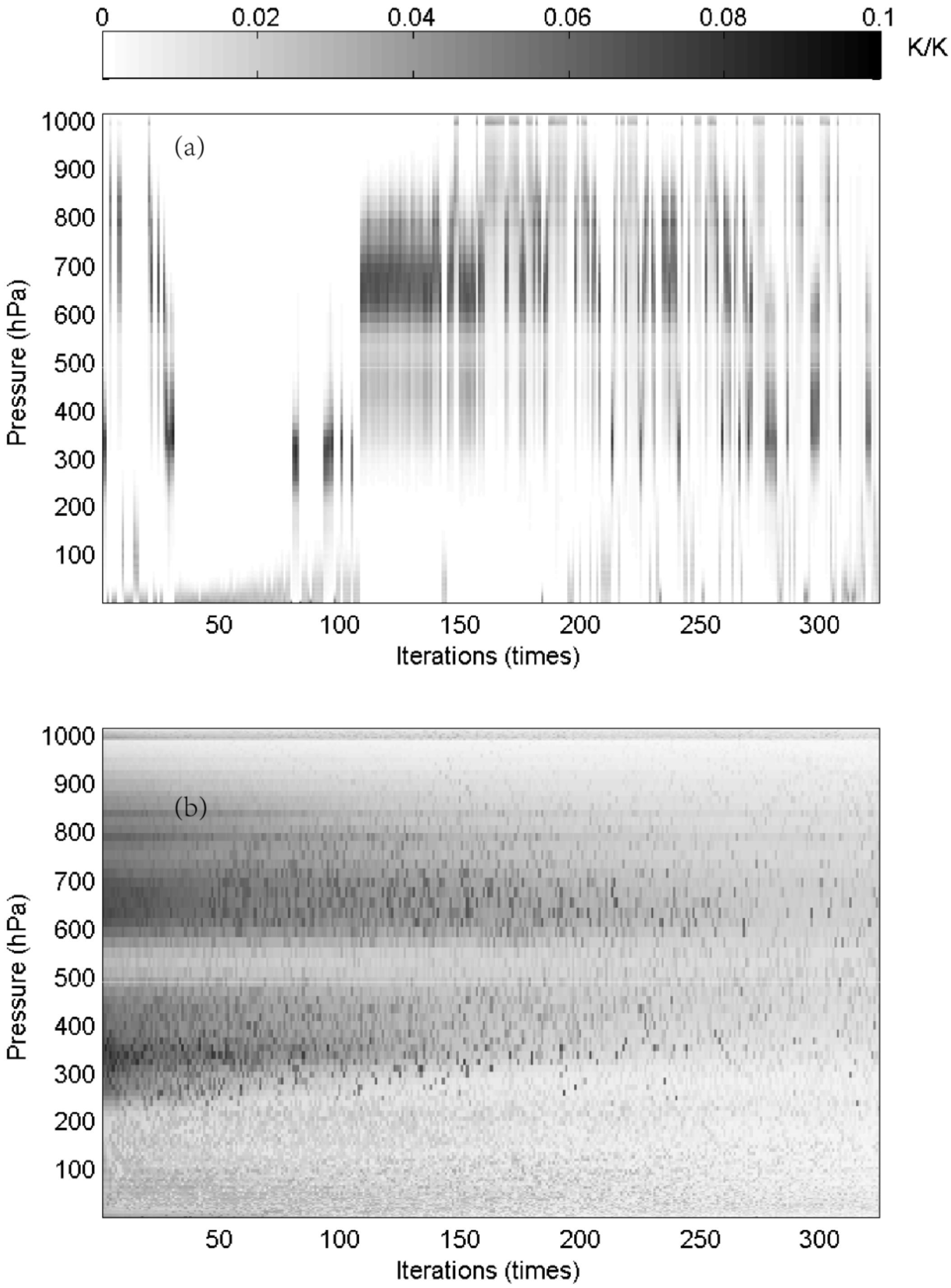

Figure ~~7~~6. The relationship between the number of iterations and the ~~weight~~weighting function of the top 324 selected channels (shaded). (a) ~~PCS.~~ICS. (b) ~~ICS~~PCS.

As illustrated in Fig. ~~7~~6, in the first 100 iterations, the distribution of the temperature ~~weight~~weighting function for PCS is relatively scattered; it does not reflect continuity between the adjacent layers of the atmosphere. Besides, the ICS result is better than that of PCS, showing that: (1) the distribution of the temperature ~~weight~~weighting function is more continuous and reflects the continuity between adjacent layers of the atmosphere; (2) regardless of the number of iterations, the maximum value of the ~~weight~~weighting function is stable near 300–400 hPa and 600–700 hPa, without scattering, which ~~resembles more closely~~is closer to the ~~scenario~~situation in real atmosphere.

4. Statistical multiple regression experiment

4.1 Temperature profile database

A new database including a representative collection of 25,000 atmospheric profiles from the European Centre for Medium-range Weather Forecasts (ECMWF) was used~~.~~ for the statistical inversion experiments. The profiles were given in a 137-level vertical grid extending from the surface up to 0.01 hPa. The database was divided into five subsets focusing on diverse sampling characteristics such as temperature, specific humidity, ozone mixing ratio, cloud condensates, and precipitation. In contrast with earlier releases of the ECMWF diverse profile database, the 137-level database places greater emphasis on preserving the statistical properties of sampled distributions produced by the Integrated Forecasting System (IFS~~).~~) (Eresmaa and McNally, 2014; Brath et al., 2018). IFS-137 spans the period from September 1, 2013 to August 31, 2014. There are two operational analyses each day (at 00z and 12z), and approximately 13 000 atmospheric profiles over the ~~modeling grid contains 2,140,702 grid points.~~ocean. The pressure levels adopted for IFS-137 are shown in Table ~~2.~~A2 (see Table A2 in Appendix A).

~~**Table 2**. Pressure levels adopted for IFS-137 137 pressure levels (in hPa).~~

Level number	pressure hPa	Level number	pressure hPa	Level number	pressure hPa	Level number	pressure hPa	Level number	pressure hPa
1	0.02	31	12.8561	61	106.4153	91	424.019	121	934.7666
2	0.031	32	14.2377	62	112.0681	92	441.5395	122	943.1399
3	0.0467	33	15.7162	63	117.9714	93	459.6321	123	950.9082
4	0.0683	34	17.2945	64	124.1337	94	478.3096	124	958.1037
5	0.0975	35	18.9752	65	130.5637	95	497.5845	125	964.7584
6	0.1361	36	20.761	66	137.2703	96	517.4198	126	970.9046
7	0.1861	37	22.6543	67	144.2624	97	537.7195	127	976.5737
8	0.2499	38	24.6577	68	151.5493	98	558.343	128	981.7968
9	0.3299	39	26.7735	69	159.1403	99	579.1926	129	986.6036
10	0.4288	40	29.0039	70	167.045	100	600.1668	130	991.023
11	0.5496	41	31.3512	71	175.2731	101	621.1624	131	995.0824
12	0.6952	42	33.8174	72	183.8344	102	642.0764	132	998.8081
13	0.869	43	36.4047	73	192.7389	103	662.8084	133	1002.225
14	1.0742	44	39.1149	74	201.9969	104	683.262	134	1005.356
15	1.3143	45	41.9493	75	211.6186	105	703.3467	135	1008.224
16	1.5928	46	44.9082	76	221.6146	106	722.9795	136	1010.849

~~17~~	~~1.9134~~	~~47~~	~~47.9915~~	~~77~~	~~231.9954~~	~~107~~	~~742.0855~~	~~137~~	~~1013.25~~
~~18~~	~~2.2797~~	~~48~~	~~51.199~~	~~78~~	~~242.7719~~	~~108~~	~~760.5996~~		
~~19~~	~~2.6954~~	~~49~~	~~54.5299~~	~~79~~	~~253.9549~~	~~109~~	~~778.4661~~		
~~20~~	~~3.1642~~	~~50~~	~~57.9834~~	~~80~~	~~265.5556~~	~~110~~	~~795.6396~~		
~~21~~	~~3.6898~~	~~51~~	~~61.5607~~	~~81~~	~~277.5852~~	~~111~~	~~812.0847~~		
~~22~~	~~4.2759~~	~~52~~	~~65.2695~~	~~82~~	~~290.0548~~	~~112~~	~~827.7756~~		
~~23~~	~~4.9262~~	~~53~~	~~69.1187~~	~~83~~	~~302.9762~~	~~113~~	~~842.6959~~		
~~24~~	~~5.6441~~	~~54~~	~~73.1187~~	~~84~~	~~316.3607~~	~~114~~	~~856.8376~~		
~~25~~	~~6.4334~~	~~55~~	~~77.281~~	~~85~~	~~330.2202~~	~~115~~	~~870.2004~~		
~~26~~	~~7.2974~~	~~56~~	~~81.6182~~	~~86~~	~~344.5663~~	~~116~~	~~882.791~~		
~~27~~	~~8.2397~~	~~57~~	~~86.145~~	~~87~~	~~359.4111~~	~~117~~	~~894.6222~~		
~~28~~	~~9.2634~~	~~58~~	~~90.8774~~	~~88~~	~~374.7666~~	~~118~~	~~905.7116~~		
~~29~~	~~10.372~~	~~59~~	~~95.828~~	~~89~~	~~390.645~~	~~119~~	~~916.0815~~		
~~30~~	~~11.5685~~	~~60~~	~~101.0047~~	~~90~~	~~407.0583~~	~~120~~	~~925.7571~~		

The locations of selected profiles of temperature, specific humidity, and cloud condensate subsets of the IFS-91 and IFS-137 databases are plotted on the map in Fig. ~~8~~7. In the IFS-91 database, the sampling is fully determined by the selection algorithm, which makes the geographical distributions very inhomogeneous. Selected profiles represent those regions where gradients of the sampled variable are the strongest: in the case of temperature, mid- and high-latitudes dominate, while humidity and cloud condensate subsets concentrate at low latitudes. However, the IFS-137 database shows a much more homogeneous spatial distribution in all the sampling subsets, which is a consequence of the randomized selection.

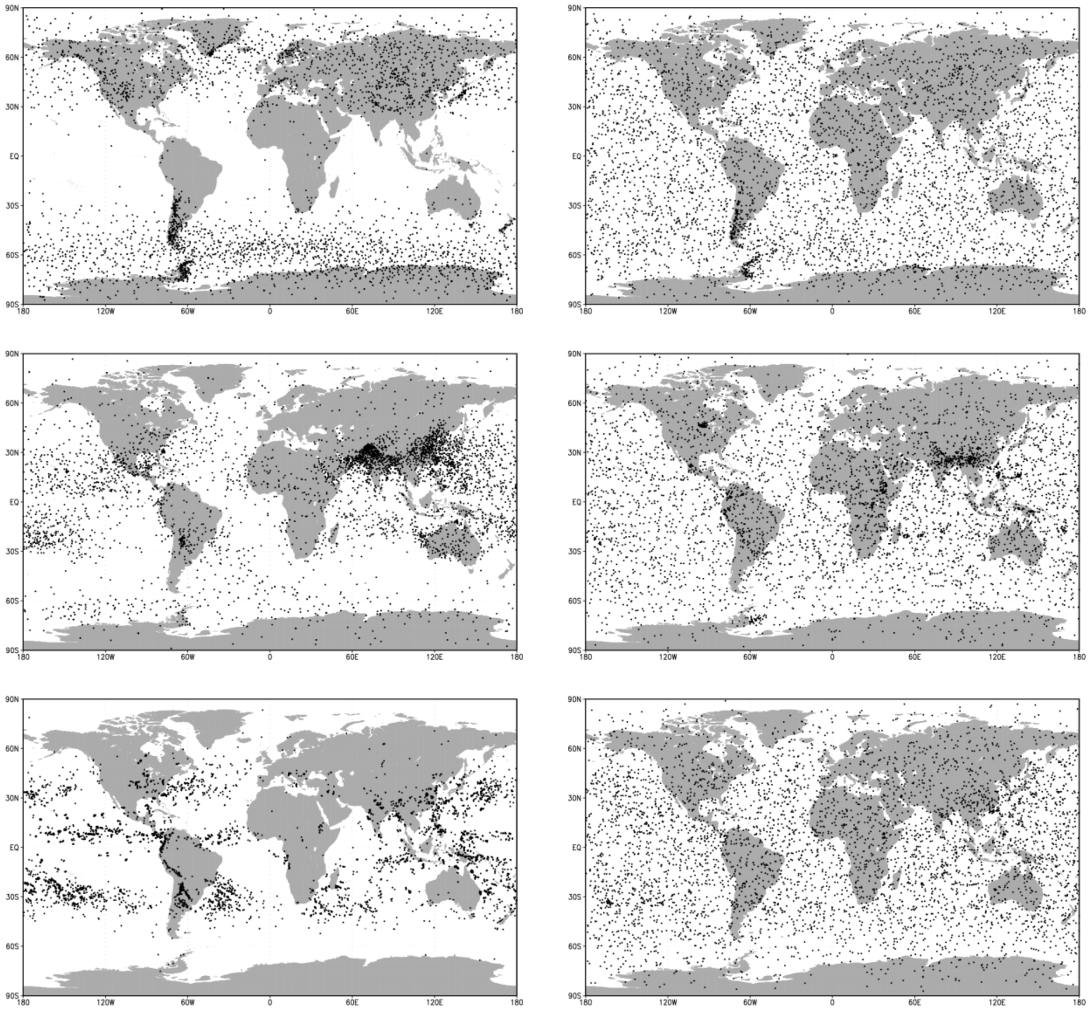
90N
60N
30N
EQ
30S
60S
90S
180
120W
60W
0
60E
120E
180

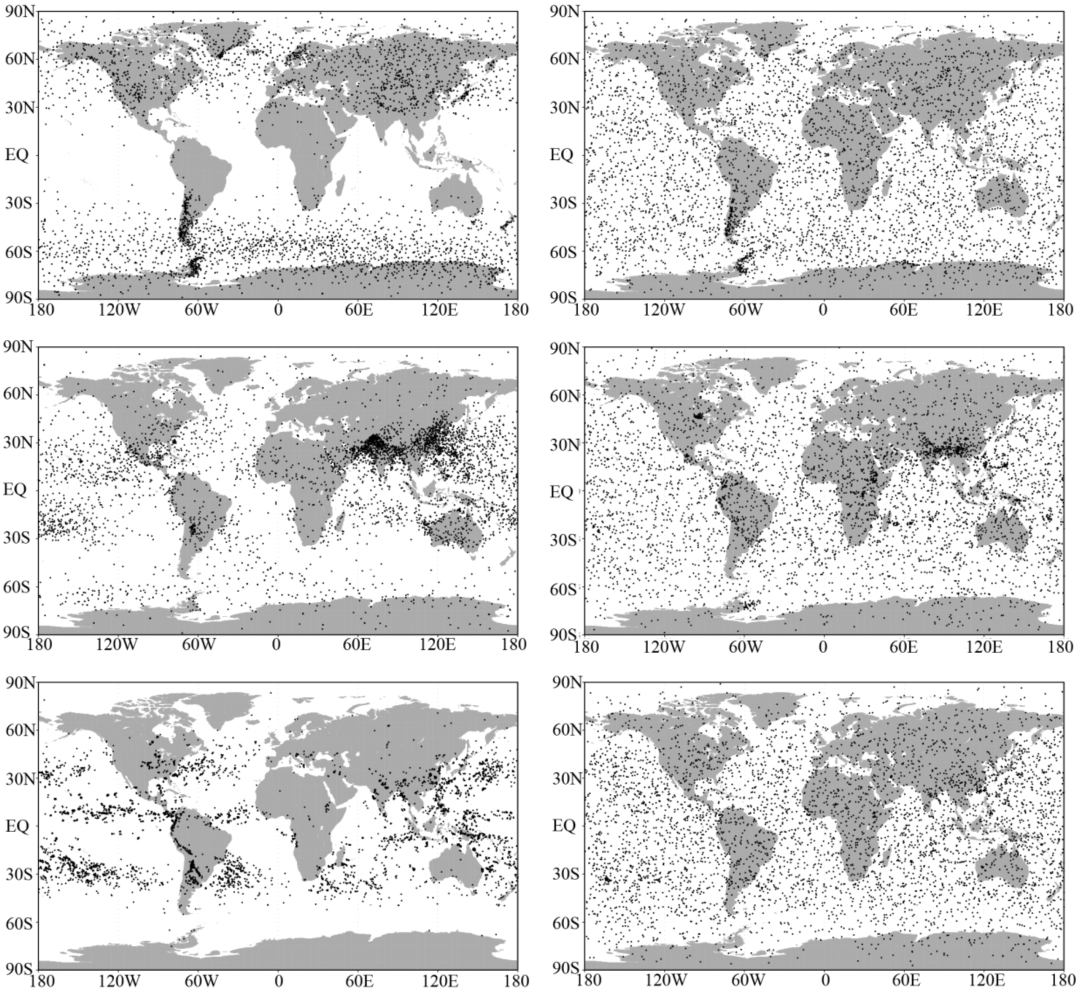

Figure ~~8.~~7. Locations of selected profiles in the temperature (top), specific humidity (middle), and cloud condensate (bottom), sampled subsets of the IFS-91 (left) and IFS-137 (right) databases (from https://www.nwpsaf.eu/site/update-137-level-nwp-profile-dataset/ , 2019).

The temporal distribution of the selected profiles is illustrated in Fig. ~~9. Again, the lack of randomized selection results in large variations~~

~~from one month to the next in the case~~8. The coverage of the IFS-~~91 database (left panel). The different distributions come mainly from variations in the ozone subset (green parts of each column). Dominance of randomly-selected profiles in the IFS-~~137 ~~database leaves little room for monthly variation in the~~ data ~~count (right panel).~~set is more homogeneous than the IFS-91 data set. Moreover, the IFS-~~91~~137 database ~~also~~ supports the mode with input parameters, such as detection angle, 2 m temperature, and cloud information~~, and so on~~. Therefore, it is feasible to use the selected samples in a statistical multiple regression experiment.

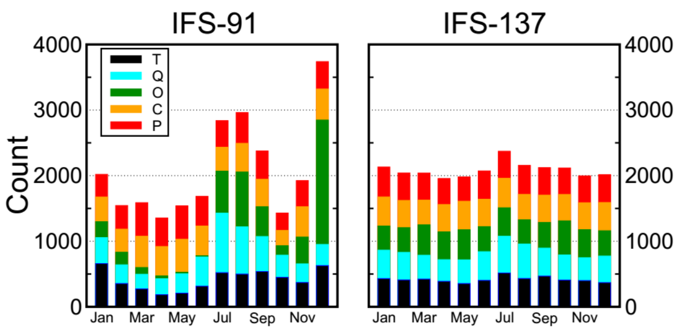

Figure ~~9.~~8. Distribution of profiles within the calendar months in IFS-91 (left) and IFS-137 (right) databases. Different subsets are shown in different colors.Black parts stand for temperature. Blue parts represent specific humidity. Green parts indicate ozone subset. Orange parts stand for cloud condensate. Red parts represent precipitation. ~~(from https://www.nwpsaf.eu/site/update-137-level-nwp-profile-dataset/Th~~

e last access date is April 26th, 2019. (from https://www.nwpsaf.eu/site/update-137-level-nwp-profile-dataset/ , 2019).

4.2 Experimental scheme

In order to verify the retrieval effectiveness of ICS, 5000 temperature profiles provided by the IFS-137 were used for statistical inversion comparison experiments. The steps are as follows:

(1) 5000 profiles and their corresponding surface factors, including surface air pressure, surface temperature, 2 m temperature, 2 m specific humidity, 10 m wind speed~~, etc~~. are put into the RTTOV mode. Then, the simulated AIRS ~~observation brightness temperature is~~spectra are obtained.

(2) The retrieval of temperature is carried out in accordance with Eq. (23). The 5000 profiles are divided into two groups. The first group of 2500 profiles is used to obtain the regression coefficient, and the second group of 2500 is used to test the result.

(3) Verification of the results. The test is carried out based on the standard deviation between the retrieval value and the true value.

4.3 Results and Discussion

For the statistical inversion comparison experiments, the standard deviation of temperature retrieval is shown in Fig. ~~10.~~9. First, because PCS does not take channel sensitivity as a function of height into consideration, the retrieval result of PCS is inferior to that of ICS. Second, by comparing the results of ICS and NCS we found that below 100 hPa, since the method used in this paper considers near ground to be less of an influencing factor, the channel combination of ICS is slightly inferior to that of NCS, but the difference is small.

From 100 hPa to10 hPa, the retrieval temperature of ICS in this paper is consistent with that of NCS, slightly better than the channel selected for NCS. From 10 hPa to 0.02 hPa, near the space layer, the retrieval temperature of ICS is ~~obviously~~ better than that of NCS. In terms of the standard deviation, the channel combination of ICS is slightly better than that of PCS from 100 hPa to 10 hPa. From 10 hPa to 0.02 hPa, the standard deviation of ICS is lower than that of NCS at about 1 K, meaning that the retrieval result of ICS is better than that of NCS.

In order to further illustrate the effectiveness of ICS, the mean improvement value of the ICS and its percentages compared with the PCS and NCS ~~in~~at different ~~height~~heights are shown in Table ~~3~~1. Because PCS does not take channel sensitivity as a function of height into consideration, the retrieval result of PCS is inferior to that of ICS. In general, the accuracy of the retrieval temperature of ICS is improved. Especially, from 100 hPa to 0.01 hPa, the mean value of ICS is evidently improved by more than 0.5 K which means the accuracy can be improved by more than 11%. By comparing the results of ICS and NCS we found that below 100 hPa, since the method used in this paper considers near ground to be less of an influencing factor, the channel combination of ICS is slightly inferior to that of NCS, but the difference is small. From 100 hPa to 0.01 hPa, the mean value of ICS is improved by more than 0.36 K which means the accuracy can be improved by more than 9.6%.

Table ~~3~~1. The mean improvement value of the ICS and its percentages compared with the PCS and NCS ~~in~~at different ~~height~~heights.

Pressure	Improved mean value /Percentage compared with PCS	Improved value /Percentage compared with NCS
hPa	K/%	K/%
surface-100hPa	0.24/10.77%	-0.04/-3.27%
100hPa-10hPa	0.15/5.08%	0.06/2.4%
10hPa-1hPa	0.04/0.64%	0.17/2.99%
1hPa-0.01hPa	0.52/11.92%	0.36/9.57%

This is because, as shown in Fig. 4: (1) ~~Near space (20–100 km)~~Stratosphere and mesosphere is less affected by the ground surface, so the retrieval result of PCS is better than that of NCS. (2)

Due to the method selected in this paper, there are more channels at 4.2 μm for N_2O and 4.3 μm for CO_2 absorption bands, and the channel combination of PCS is superior to that of NCS for atmospheric temperature ~~detection~~observation in the high temperature zone. Moreover, ICS takes channel sensitivity as a function of height into consideration, so its retrieval result is ~~impressive~~improved.

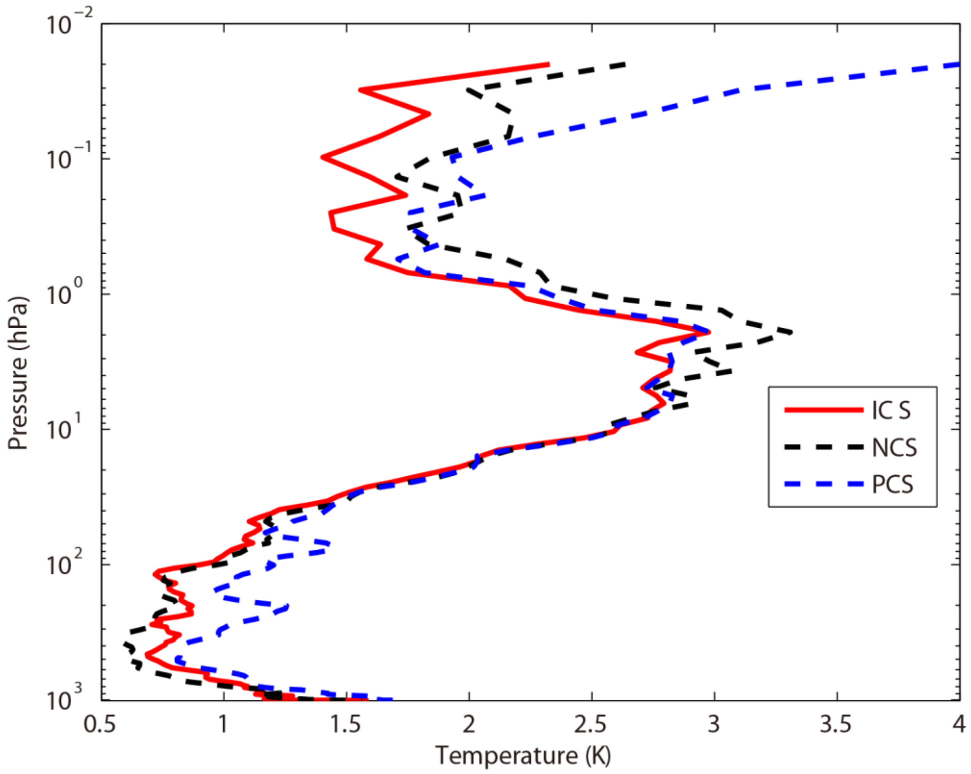

Figure ~~10.~~9. The temperature profile standard deviation of statistical inversion comparison experiments. Red line indicates the result of ICS. Black dotted line stands for the result of NCS. Blue dotted line represents the result of PCS.

5 Statistical inversion comparison experiments in four typical regions

The accuracy of the retrieval temperature varies from place to place and changes with ~~weather~~atmospheric conditions. Therefore, in order to further compare the inversion accuracy under different atmospheric conditions, this paper has divided the atmospheric profile ~~is~~ from the IFS-137 database introduced in Sect. ~~4, and divides it~~4 into four regions: equatorial zone, subtropical region, mid-latitude region and Arctic. ~~These regions' profiles can represent the global typical atmospheric temperature profiles.~~ The average temperature profiles in these four regions are shown in Fig. ~~11.~~10.
The retrieval temperature varies from place to place and changes with ~~weather~~ atmospheric conditions. In order to further compare the regional differences of inversion accuracy, the temperature standard deviations of ICS in four typical regions are compared in Sect. 5.2.

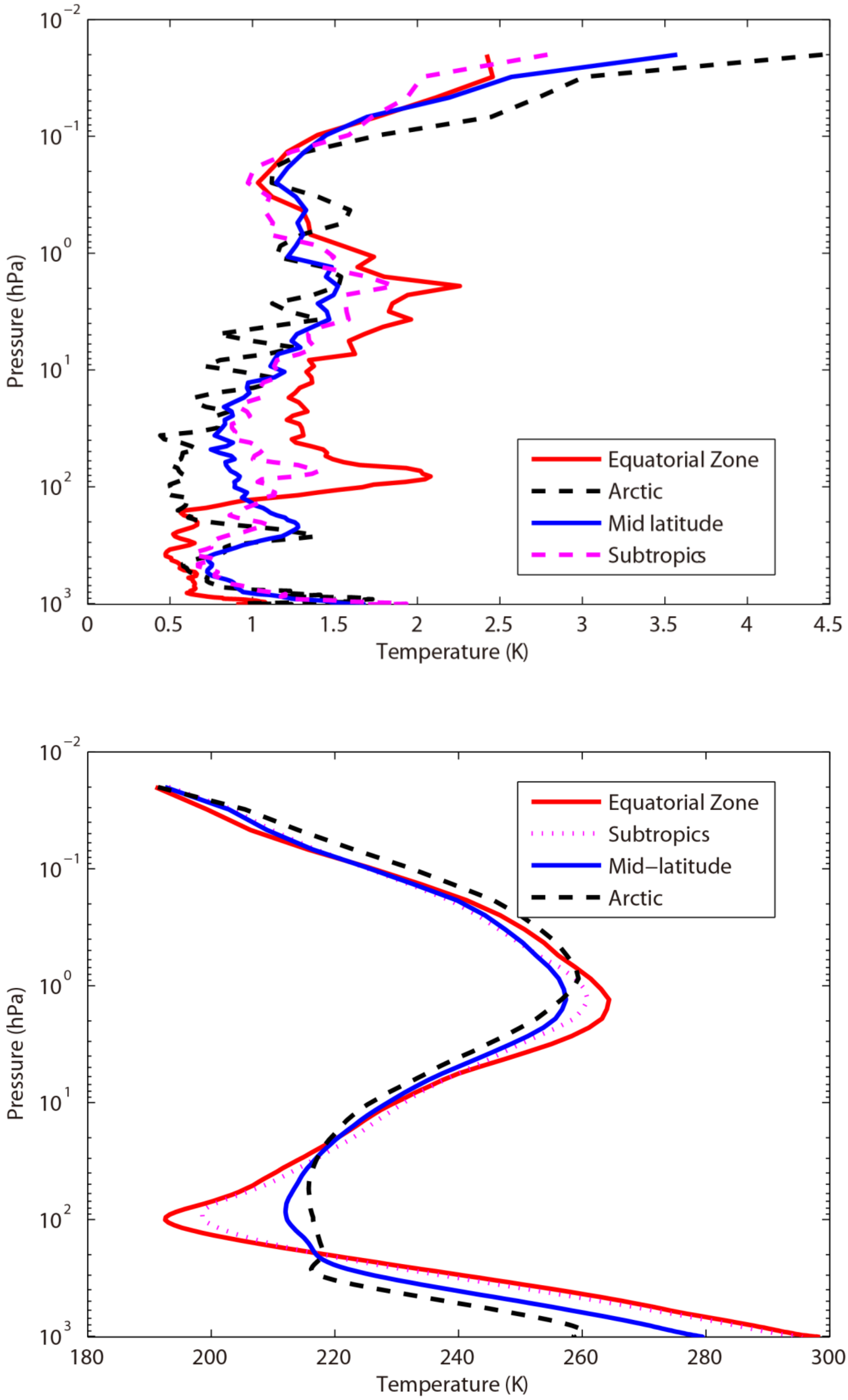

Figure ~~11.~~10. The average temperature profiles in four typical regions. Red line indicates the equatorial zone. Pink dotted line stands for the subtropics. Blue dotted line represents the mid-latitude region. Black dotted line stands for the Arctic.

5.1 Experimental scheme

In order to further illustrate the different accuracy of the retrieval temperature using our improved channel selection method under different atmospheric conditions, the profiles in four typical regions were used for statistical inversion comparison experiments. The experimental steps are as follows:

(1) 2500 profiles in Sect. 4 are used to work out the regression coefficient.

(2) The atmospheric profiles of the four typical regions: equatorial zone, subtropical region, mid-latitude region and Arctic are used for statistical inversion comparison experiments and test the result.(3) Verification of the results. The test is carried out based on the standard deviation between the retrieval value and the true value.

5.2 Results and Discussion

Using statistical inversion comparison experiments in four typical regions, the standard deviation of temperature retrieval is shown in Fig. ~~12~~11. Generally, the retrieval temperature by ICS is ~~greatly~~

~~superior to~~better than that of NCS and PCS. In particular, above 1 hPa (the ~~near space layer~~stratosphere and mesosphere), the standard deviation of atmospheric temperature can be ~~optimized to~~improved by 1 K with PCS and NCS. Thus, ICS shows a great improvement. The results were consistent with Sect. 4.

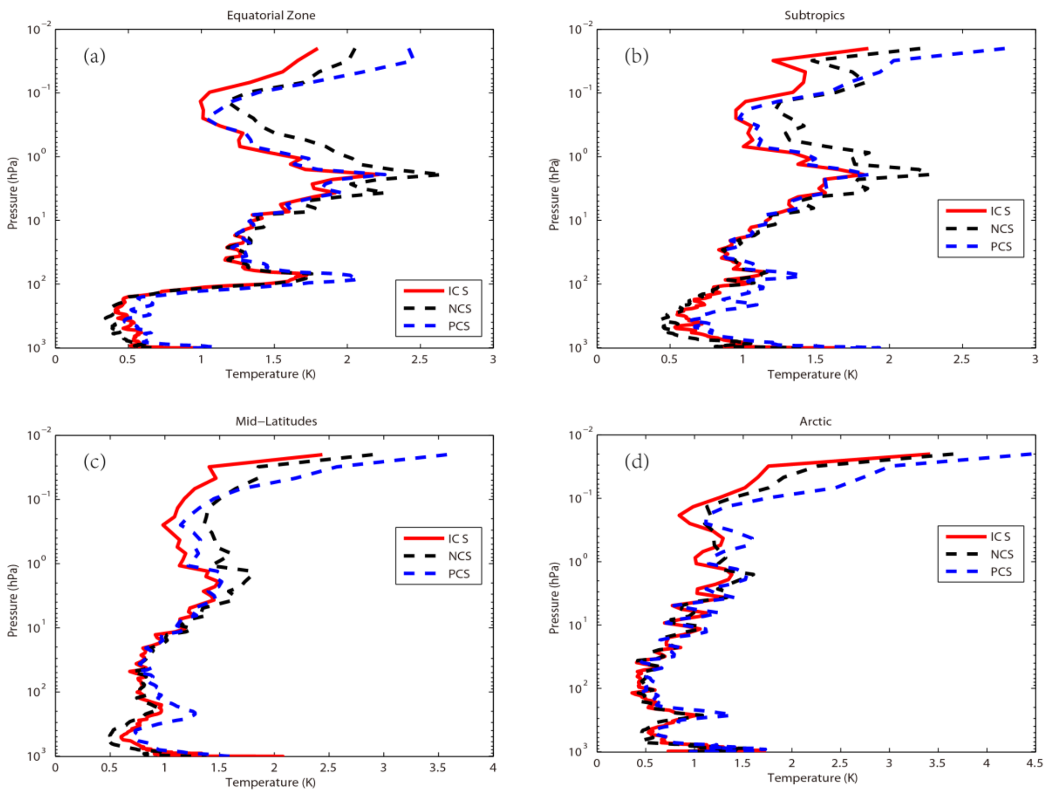

Figure ~~12~~11. The temperature profile standard deviation of statistical inversion comparison experiments in four typical regions. Red line indicates the result of ICS. Black dotted line stands for the result of NCS. Blue dotted line represents the result of PCS. (a) Equatorial zone. (b) Subtropics. (c) Mid-latitudes. (~~b~~d) Arctic.

In order to further compare the regional differences of inversion accuracy, the temperature standard deviation of ICS in four typical regions are compared in Fig. ~~13~~12.

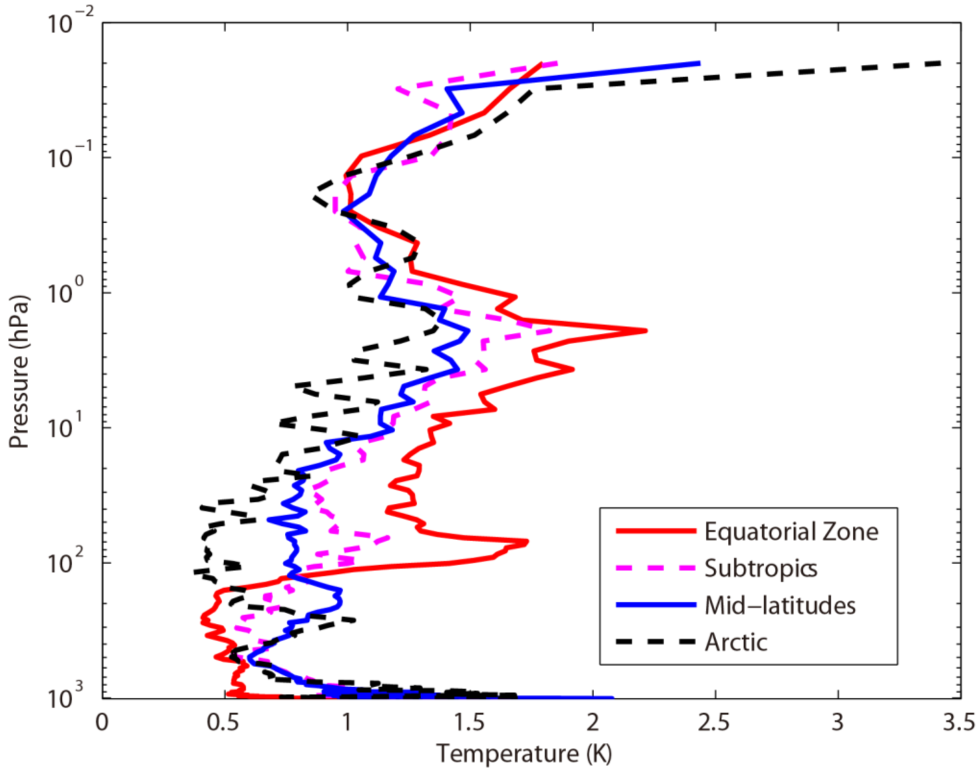

Figure ~~13.~~12. The temperature standard deviation of ICS in four typical regions. Red line indicates the result of equatorial zone. Pink dotted line represents the result of Subtropics. Blue line represents the result of Mid-latitudes. Black dotted line stands for the result of Arctic.

~~As can be seen from Fig. 13, the~~The temperature standard deviations of the ICS in the four typical regions are large~~.~~ (Fig. 12).

Below100 hPa, due to the high temperature in the equatorial zone, the channel combination of ICS is ~~superior to~~better than that of PCS and NCS for atmospheric temperature ~~detection in~~ observation to the ~~high~~higher temperature~~ zone~~. The standard deviation is 0.5K. Due to the method selected in this paper there are more channels at 4.2 µm for N_2O and 4.3 µm for CO_2 absorption bands which has been previously described in Sect. 3. Near the tropopause, the standard deviation of the equatorial zone increases sharply. It is also due to the sharp drops in temperature. However, the standard deviation of the Arctic is still around 0.5K. From 100hPa to 1hPa, the standard deviation of ICS is 0.5 K to 2K. With the increase of latitude, the effectiveness considerably increases. According to Fig. ~~12~~11, ICS takes channel sensitivity as a function of height into consideration, so its retrieval result is ~~impressive~~better.

~~In order to further illustrate the effectiveness of ICS, the mean improvement value of the ICS and its percentages compared with the PCS and NCS in different height of four typical regions are shown in Table 4 to Table 7.~~

~~**Table 4.** The mean improvement value of the ICS and its percentages compared with the PCS and NCS in different height in equatorial zone.~~

~~Pressure~~	~~Improved mean value /Percentage compared with PCS~~	~~Improved value /Percentage compared with NCS~~
~~hPa~~	~~K/%~~	~~K/%~~
~~surface-100hPa~~	~~0.18/12.25%~~	~~-0.06/-5.61%~~
~~100hPa-10hPa~~	~~0.13/4.23%~~	~~0.04/1.28%~~
~~10hPa-1hPa~~	~~0.03/0.09%~~	~~0.24/6.24%~~
~~1hPa-0.01hPa~~	~~0.24/7.41%~~	~~0.33/11.22%~~

~~**Table 5.** The mean improvement value of the ICS and its percentages compared with the PCS and NCS in different height in subtropics.~~

~~Pressure~~	~~Improved mean value /Percentage compared with PCS~~	~~Improved value /Percentage compared with NCS~~
~~hPa~~	~~K/%~~	~~K/%~~
~~surface-100hPa~~	~~0.26/12.49%~~	~~-0.08/-5.94%~~
~~100hPa-10hPa~~	~~0.08/3.55%~~	~~0.02/1.28%~~
~~10hPa-1hPa~~	~~0.02/0.56%~~	~~0.2/5.94%~~
~~1hPa-0.01hPa~~	~~0.25/7.73%~~	~~0.34/12.51%~~

~~**Table 6.** The mean improvement value of the ICS and its percentages compared with the PCS and NCS in different height in mid-latitudes.~~

~~Pressure~~	~~Improved mean value /Percentage compared with PCS~~	~~Improved value /Percentage compared with NCS~~
~~hPa~~	~~K/%~~	~~K/%~~
~~surface-100hPa~~	~~0. 18/9. 23%~~	~~-0. 13/-7. 41%~~
~~100hPa-10hPa~~	~~0. 06/3. 68%~~	~~0. 03/1. 84%~~
~~10hPa-1hPa~~	~~0. 03/1. 03%~~	~~0. 18/6. 01%~~
~~1hPa-0. 01hPa~~	~~0. 36/10. 64%~~	~~0. 36/12. 71%~~

~~**Table 7.** The mean improvement value of the ICS and its percentages compared with the PCS and NCS in different height in Arctic.~~

~~Pressure~~	~~Improved mean value /Percentage compared with PCS~~	~~Improved value /Percentage compared with NCS~~
~~hPa~~	~~K/%~~	~~K/%~~
~~surface-100hPa~~	~~0.12/6.52%~~	~~-0.05/-3.47%~~
~~100hPa-10hPa~~	~~0.08/6.59%~~	~~0.02/1.97%~~
~~10hPa-1hPa~~	~~0.09/3.64%~~	~~0.06/2.5%~~
~~1hPa-0.01hPa~~	~~0.49/13.72%~~	~~0.18/6.47%~~

Although the improvements of ICS in the four typical regions are different, in general, the accuracy of the retrieval temperature of ICS is improved. Because PCS does not take channel sensitivity as a function of height into consideration, the retrieval result of PCS is inferior to that of ICS. In general, the accuracy of the retrieval temperature of ICS is improved. ~~Especially, from 100 hPa to 0.01 hPa, the accuracy of ICS can be improved by 7% to 13%. By comparing the results of ICS and NCS we found that below 100 hPa, since the method used in this paper considers near ground to be less of an influencing factor, the channel combination of ICS is slightly inferior to that of NCS, but the difference is small. From 100 hPa to 0.01 hPa, the accuracy of ICS can be improved by 7% to 13%.~~

~~6.~~7 Conclusions ~~and discussion~~

~~6.1 Conclusions~~

~~An improved channel selection method is proposed, based on information content in this paper. A robust channel selection scheme and method are proposed, and a series of channel selection comparison experiments are conducted. The results are as follows:~~

~~(1) Since ICS takes channel sensitivity as a function of height into consideration, the ARI of PCS only tends to be 0.38 and is not convergent. However, as the 100th iteration is approached, the ARI of ICS tends to be stable, reaching 0.54, while the distribution of the temperature weight function is more continuous and closer to that of the actual atmosphere. Thus, in terms of the ARI, convergence, and the distribution of the temperature weight function, ICS is superior to PCS.~~

~~(2) Statistical inversion comparison experiments show that the retrieval temperature of ICS in this paper is consistent with that of NCS. In particular, from 10 hPa to 0.02 hPa (the near space layer), the retrieval temperature of ICS is obviously better than that of NCS at about 1 K. In general, the accuracy of the retrieval temperature of ICS is improved. Especially, from 100 hPa to 0.01 hPa, the accuracy of ICS can be improved by more than 11%. The reason is that near~~

~~space (20–100 km) is less affected by the ground surface, so the retrieval result of ICS is better than that of NCS. Additionally, due to the method selected in this paper there are more channels at 4.2 μm for the N_2O and 4.3 μm for the CO_2 absorption bands; the channel combination of ICS is superior to that of NCS for atmospheric temperature detection in the high temperature zone.~~

~~(3) Statistical inversion comparison experiments in four typical regions indicate that ICS in this paper is significantly better than NCS and PCS in different regions and shows latitudinal variations. Especially, from 100 hPa to 0.01 hPa, the accuracy of ICS can be improved by 7% to 13%, which means the ICS method selected in this paper is feasible and shows great promise for applications.~~

~~6.2 Discussion~~

In recent years, the atmospheric layer in the altitude range of about 20–100 km has been named “the near space layer” by aeronautical and astronautical communities. It is between the space-based satellite platform and the aerospace vehicle platform, which is the transition zone between aviation and aerospace. Its unique resource has attracted a lot of attention from many countries. Research and exploration, therefore, on and of the near space layer are of great importance. A new channel selection scheme and method for hyperspectral atmospheric infrared sounder AIRS data based on layering ~~are~~is proposed. The retrieval results of ICS concerning the near space atmosphere are particularly good. Thus, ICS aims to provide a new and an effective channel selection method for the study of the near space atmosphere using the hyperspectral atmospheric infrared sounder.

An improved channel selection method is proposed, based on information content in this paper. A robust channel selection scheme and method are proposed, and a series of channel selection comparison experiments are conducted. The results are as follows:

(1) Since ICS takes channel sensitivity as a function of height into consideration, the ARI of PCS only tends to be 0.38 and is not convergent. However, as the 100^{th} iteration is approached, the ARI of ICS tends to be stable, reaching 0.54, while the distribution of the temperature weighting function is more continuous and closer to that of the actual atmosphere. Thus, in terms of the ARI, convergence, and the distribution of the temperature weighting function, ICS is better than PCS.

(2) Statistical inversion comparison experiments show that the retrieval temperature of ICS in this paper is consistent with that of NCS. In particular, from 10 hPa to 0.02 hPa (the stratosphere and mesosphere), the retrieval temperature of ICS is obviously better

than that of NCS at about 1 K. In general, the accuracy of the retrieval temperature of ICS is improved. Especially, from 100 hPa to 0.01 hPa, the accuracy of ICS can be improved by more than 11%. The reason is that stratosphere and mesosphere are less affected by the ground surface, so the retrieval result of ICS is better than that of NCS. Additionally, due to the method selected in this paper there are more channels at 4.2 μm for the N_2O and at 4.3 μm for the CO_2 absorption bands; the channel combination of ICS is better than that of NCS for atmospheric temperature observation to the higher temperature.

(3) Statistical inversion comparison experiments in four typical regions indicate that ICS in this paper is significantly better than NCS and PCS in different regions and shows latitudinal variations, which shows potential for future applications.

Data availability. The data used in this paper are available from the corresponding author upon request.

Appendices

Appendix A

Table A1. Pressure levels adopted for RTTOV v12 54 pressure level coefficients and profile limits within which the transmittance calculations are valid. Note that the gas units here are ppmv. (From https://www.nwpsaf.eu/site/software/rttov/, RTTOV Users guide, 2019).

Level	Pressure	Tmax	Tmin	Qmax	Qmin	Q_2max	Q_2min	Q_2Ref
Number	hPa	K	K	ppmv*	ppmv*	ppmv*	ppmv*	ppmv*
1	0.01	245.95	143.66	5.24	0.91	1.404	0.014	0.296
2	0.01	252.13	154.19	6.03	1.08	1.410	0.069	0.321
3	0.03	263.71	168.42	7.42	1.35	1.496	0.108	0.361
4	0.03	280.12	180.18	8.10	1.58	1.670	0.171	0.527
5	0.13	299.05	194.48	8.44	1.80	2.064	0.228	0.769
6	0.23	318.64	206.21	8.59	1.99	2.365	0.355	1.074
7	0.41	336.24	205.66	8.58	2.49	2.718	0.553	1.471
8	0.67	342.08	197.17	8.34	3.01	3.565	0.731	1.991
9	1.08	340.84	189.50	8.07	3.30	5.333	0.716	2.787
10	1.67	334.68	179.27	7.89	3.20	7.314	0.643	3.756
11	2.50	322.5	17627	7.75	2.92	9.191	0.504	4.864
12	3.65	312.51	175.04	7.69	2.83	10.447	0.745	5.953
13	5.19	303.89	173.07	7.58	2.70	12.336	1.586	6.763
14	7.22	295.48	168.38	7.53	2.54	12.936	1.879	7.109
15	9.84	293.33	166.30	7.36	2.46	12.744	1.322	7.060
16	13.17	287.05	16347	7.20	2.42	11.960	0.719	6.574
17	17.33	283.36	161.49	6.96	2.20	11.105	0.428	5.687
18	22.46	280.93	161.47	6.75	1.71	9.796	0.278	4.705
19	28.69	282.67	162.09	6.46	1.52	8.736	0.164	3.870
20	36.17	27993	162.49	6.14	1.31	7.374	0.107	3.111
21	45.04	27315	164.66	5.90	1.36	6.799	0.055	2.478
22	55.44	265.93	166.19	6.21	1.30	5.710	0.048	1.907
23	67.51	264.7	167.42	9.17	1.16	4.786	0.043	1.440
24	81.37	261.95	159.98	17.89	0.36	4.390	0.038	1.020

25	97.15	262.43	163.95	20.30	0.01	3.619	0.016	0.733
26	114.94	259.57	168.59	33.56	0.01	2.977	0.016	0.604
27	134.83	259.26	169.71	102.24	0.01	2.665	0.016	0.489
28	156.88	260.13	169.42	285.00	0.01	2.351	0.013	0.388
29	181.14	262.27	17063	714.60	0.01	1.973	0.010	0.284
30	207.61	264.45	174.11	1464.00	0.01	1.481	0.013	0.196
31	236.28	270.09	177.12	2475.60	0.01	1.075	0.016	0.145
32	267.10	277.93	181.98	4381.20	0.01	0.774	0.015	0.110
33	300.00	285.18	184.76	6631.20	0.01	0.628	0.015	0.086
34	334.86	293.68	187.69	9450.00	1.29	0.550	0.016	0.073
35	371.55	300.12	190.34	12432.00	1.52	0.447	0.015	0.063
36	409.89	302.63	194.40	15468.00	2.12	0.361	0.015	0.057
37	449.67	304.43	198.46	18564.00	2.36	0.284	0.015	0.054
38	490.&5	307.2	201.53	21684.00	2.91	0.247	0.015	0.052
39	532.56	31217	202.74	24696.00	3.67	0.199	0.015	0.050
40	572.15	31556	201.61	27480.00	3.81	0.191	0.012	0.050
41	618.07	318.26	189.95	30288.00	6.82	0.171	0.010	0.049
42	661.00	321.71	189.95	32796.00	6.07	0.128	0.009	0.048
43	703.59	327.95	189.95	55328.00	6.73	0.124	0.009	0.047
44	745.48	333.77	189.95	37692.00	8.71	0.117	0.009	0.046
45	786.33	336.46	189.95	39984.00	8.26	0.115	0.008	0.045
46	825.75	338.54	189.95	42192.00	7.87	0.113	0.008	0.043
47	863.40	342.55	189.95	44220.00	7.53	0.111	0.007	0.041
48	898.93	346.23	189.95	46272.00	7.23	0.108	0.006	0.040
49	931.99	34924	189.95	47736.00	6.97	0.102	0.006	0.038
50	962.26	349.92	189.95	51264.00	6.75	0.099	0.006	0.034
51	989.45	350.09	189.95	49716.00	6.57	0.099	0.006	0.030
52	1013.29	360.09	189.95	47208.00	6.41	0.094	0.006	0.028
53	1033.54	350.09	189.95	47806.00	6.29	0.094	0.006	0.027
54	1050.00	350.09	189.95	47640.00	6.19	0.094	0.006	0.027

Table A2. Pressure levels adopted for IFS-137 137 pressure levels (in hPa).

Level number	pressure hPa	Level number	pressure hPa	Level number	pressure hPa	Level number	pressure hPa	Level number	pressure hPa
1	0.02	31	12.8561	61	106.4153	91	424.019	121	934.7666
2	0.031	32	14.2377	62	112.0681	92	441.5395	122	943.1399
3	0.0467	33	15.7162	63	117.9714	93	459.6321	123	950.9082
4	0.0683	34	17.2945	64	124.1337	94	478.3096	124	958.1037
5	0.0975	35	18.9752	65	130.5637	95	497.5845	125	964.7584
6	0.1361	36	20.761	66	137.2703	96	517.4198	126	970.9046
7	0.1861	37	22.6543	67	144.2624	97	537.7195	127	976.5737
8	0.2499	38	24.6577	68	151.5493	98	558.343	128	981.7968
9	0.3299	39	26.7735	69	159.1403	99	579.1926	129	986.6036
10	0.4288	40	29.0039	70	167.045	100	600.1668	130	991.023
11	0.5496	41	31.3512	71	175.2731	101	621.1624	131	995.0824
12	0.6952	42	33.8174	72	183.8344	102	642.0764	132	998.8081
13	0.869	43	36.4047	73	192.7389	103	662.8084	133	1002.225
14	1.0742	44	39.1149	74	201.9969	104	683.262	134	1005.356
15	1.3143	45	41.9493	75	211.6186	105	703.3467	135	1008.224
16	1.5928	46	44.9082	76	221.6146	106	722.9795	136	1010.849
17	1.9134	47	47.9915	77	231.9954	107	742.0855	137	1013.25
18	2.2797	48	51.199	78	242.7719	108	760.5996		
19	2.6954	49	54.5299	79	253.9549	109	778.4661		
20	3.1642	50	57.9834	80	265.5556	110	795.6396		
21	3.6898	51	61.5607	81	277.5852	111	812.0847		
22	4.2759	52	65.2695	82	290.0548	112	827.7756		
23	4.9262	53	69.1187	83	302.9762	113	842.6959		
24	5.6441	54	73.1187	84	316.3607	114	856.8376		
25	6.4334	55	77.281	85	330.2202	115	870.2004		
26	7.2974	56	81.6182	86	344.5663	116	882.791		
27	8.2397	57	86.145	87	359.4111	117	894.6222		
28	9.2634	58	90.8774	88	374.7666	118	905.7116		
29	10.372	59	95.828	89	390.645	119	916.0815		
30	11.5685	60	101.0047	90	407.0583	120	925.7571		

Author contributions. ZS contributed the central idea. SC, ZS and

HD conceived the method, developed the retrieval algorithm and discussed the results. SC analyzed the data, prepared the figures and wrote the paper. WG contributed to refining the ideas, carrying out additional analyses. All co-authors reviewed the paper.

Competing interests. The authors declare that they have no conflict of interest.

Acknowledgements. ~~The study was supported by the National Natural Science Foundation of China (Grant no. 41875045). The study was also partly~~The study was supported by the National Key Research Program of China: Development of high-resolution data assimilation technology and atmospheric reanalysis data set in East Asia (Research on remote sensing telemetry data assimilation technology, Grant no. ~~2017YFC1501802~~2017YFC1501802). The study was also supported by the National Natural Science Foundation of China (Grant no. 41875045) and Hunan Provincial Innovation Foundation for Postgraduate (Grant no. CX2018B033 and no. CX2018B034).

References

Aires, F., Schmitt, M., Chedin, A., and Scott, N.: The

"~~weight~~weighting smoothing" regularization of MLP for Jacobian stabilization, IEEE. T. Neural. Networks., 10, 1502-1510, https://doi.org/10.1109/72.809096, 1999.

Aires, F., Chédin, Alain., Scott, N. A., and Rossow, W. B.: A regularized neural net approach for retrieval of atmospheric and surface temperatures with the IASI instrument, J. Appl. Meteorol., 41,144-159, https://doi.org/10.1175/1520-0450(2002)041<0144:ARNNAF>2.0.CO;2, 2002.

Aumann, H. H.: Atmospheric infrared sounder on the earth observing system, Optl. Engr., 33, 776-784, https://doi.org/10.1117/12.159325, 1994.

Aumann, H. H., Chahine, M. T., Gautier, C., and Goldberg, M.: AIRS/AMSU/HSB on the Aqua mission: design, science objective, data products, and processing systems, IEEE. Trans. GRS., 41,253-264, http://dx.doi.org/10.1109/TGRS.2002.808356, 2003.

Brath, M., Fox, S., Eriksson, P., Harlow, R. C., Burgdorf, M., and Buehler, S. A.: Retrieval of an ice water path over the ocean from ISMAR and MARSS millimeter and submillimeter brightness temperatures, Atmos. Meas. Tech., 11, 611–632, https://doi.org/10.5194/amt-11-611-2018, 2018.

Chahine, M. I.: A general relaxation method for inverse solution of the full radiative transfer equation, J. Atmos. Sci., 29, 741-747, https://doi.org/10.1175/1520-0469(1972)029<0741:AGRMFI>2.0.CO;2, 1972.

Chang, K. W, L'Ecuyer, T. S., Kahn, B. H., and Natraj, V.: Information content of visible and midinfrared radiances for retrieving tropical ice cloud properties, J. Geophys. Res., 122, https://doi.org/10.1002/2016JD026357, 2017.

Chedin, A., Scott, N. A., Wahiche, C., and Moulinier, P.: The improved initialization inversion method: a high resolution physical method for temperature retrievals from satellites of the tiros-n series, J. Appl. Meteor., 24, 128-143, https://doi.org/10.1175/1520-0450(1985)024<0128:TIIIMA>2.0.CO;2, 1985.

Cyril, C., Alain, C., and Scott, N. A.: Airs channel selection for CO_2 and other trace-gas retrievals, Q. J. Roy. Meteor. Soc., 129, 2719-2740, https://doi.org/10.1256/qj.02.180, 2003.

Du, H. D., Huang, S. X., and Shi, H. Q.: Method and experiment of channel selection for high spectral resolution data, Acta. Physica. Sinica., 57, 7685-7692, 2008 .

Dudhia, A., Jay, V. L., and Rodgers, C. D.: Microwindow selection for high-spectral-resolution sounders, Appl. Opt. 41, 3665-3673, https://doi.org/10.1364/AO.41.003665, 2002.

Eresmaa, R. and McNally, A. P.: Diverse profile datasets from the ECMWF 137-level short-range forecasts, Tech. rep., ECMWF, 2014.

Eyre, J. R., Andersson E., and McNally, A. P.: Direct use of satellite sounding radiances in numerical weather prediction, High Spectral Resolution Infrared Remote Sensing for Earth's Weather and Climate Studies, Springer, Berlin, Heidelberg, https://doi.org/10.1007/978-3-642-84599-4_25, 1993.

Fang, Z. Y.: The evolution of meteorological satellites and the insight from it, Adv. Meteorol. Sci. Technol., 4, 27-34, https://doi.org/ 10.3969/j.issn.2095-1973.2014.06.003, 2014.

Gong, J., Wu, D. L., and Eckermann, S. D.: Gravity wave variances and propagation derived from AIRS radiances, Atmos. Chem. Phys., 11, 11691-11738, https://doi.org/10.5194/acp-12-1701-2012, 2011.

He, M. Y., Du, H. D., Long, Z. Y., and Huang, S. X.: Selection of regularization parameters using an atmospheric retrievable index in a retrieval of atmospheric profile, Acta. Physica Sinica., 61, 024205-160, 2012.

Hoffmann, L. and Alexander, M. J.: Retrieval of stratospheric temperatures from atmospheric infrared sounder radiance measurements for gravity wave studies, J. Geophys. Res. Atm., 114, https://doi.org/10.1029/2008JD011241, 2009.

Huang, H. L., Li, J., Baggett, K., Smith, W. L., and Guan, L.: Evaluation of cloud-cleared radiances for numerical weather prediction and cloud-contaminated sounding applications, Atmospheric and Environmental Remote Sensing Data Processing and Utilization: Numerical Atmospheric Prediction and Environmental Monitoring, I. S. O. Photonics., https://doi.org/10.1117/12.613027, 2005.

Kuai, L., Natraj, V., Shia, R. L., Miller, C., and Yung, Y. L.: Channel selection using information content analysis: a case study of CO_2 retrieval from near infrared measurements. J. Q. S. Radiative. Transfer., 111, 1296-1304, https://doi.org/10.1016/j.jqsrt.2010.02.011, 2010.

Li, J., Wolf, W. W., Menzel, W. P., Paul, Menzel. W., Zhang, W. J., Huang, H. L., and Achtor, T. H.: Global soundings of the atmosphere from ATOVS measurements: the algorithm and validation, J. Appl. Meteor., 39, 1248-1268, https://doi.org/10.1175/1520-0450(2000)039<1248:GSOTAF>2.0.CO;2, 2000.

Li, J., Liu, C. Y., Huang, H. L., Schmit, T. J., Wu, X., Menzel, W. P., and Gurka, J. J.: Optimal cloud-clearing for AIRS radiances using MODIS, IEEE. Trans. GRS. , 43, 1266-1278, http://dx.doi.org/

10.1109/tgrs.2005.847795, 2005.

Liu, Z. Q.: A regional ATOVS radiance-bias correction scheme for rediance assimilation, Acta. Meteorologica. Sinica., 65, 113-123, 2007.

Lupu, C., Gauthier, P., and Laroche, Stéphane.: Assessment of the impact of observations on analyses derived from observing system experiments, Mon. Weather. Rev., 140, 245-257, https://doi.org/10.1175/MWR-D-10-05010.1, 2012.

Menke, W.: Geophysical Data Analysis: Discrete Inverse Theory, Acad. Press., Columbia University, New York, https://doi.org/10.1016/B978-0-12-397160-9.00019-9, 1984.

Menzel, W. P., Schmit, T. J., Zhang, P. and Li, J.: Satellite-based atmospheric infrared sounder development and applications, Bull. Amer. Meteor. Soc., 99, 583–603, https://doi.org/10.1175/BAMS-D-16-0293.1, 2018.

Prunet, P., Thépaut J. N., and Cass, V.: The information content of clear sky IASI radiances and their potential for numerical weather prediction, Q. J. Roy. Meteor. Soc., 124, 211-241, https://doi.org/10.1002/qj.49712454510, 2010.

Xu, Q.: Measuring information content from observations for data assimilation: relative entropy versus shannon entropy difference, Tellus. A., 59, 198-209, https://doi.org/10.1111/j.1600-0870.2006.00222.x, 2007.

Rabier, F., Fourrié, N., and Chafäi, D.: Channel selection methods for infrared atmospheric sounding interferometer radiances, Q. J. Roy. Meteor. Soc., 128, 1011-1027, https://doi.org/10.1256/0035900021643638, 2010.

Richardson, M. and Stephens, G. L.: Information content of oco-2 oxygen a-band channels for retrieving marine liquid cloud properties, Atmospheric Measurement Techniques, 11, 1-19, https://doi.org/10.5194/amt-11-1515-2018, 2018.

Rodgers, C. D.: Information content and optimisation of high spectral resolution remote measurements, Adv. Spa. Research, 21, 136-147, https://doi.org/10.1016/S0273-1177(97)00915-0, 1996.

Rodgers, C. D.: Inverse Methods for Atmospheric Sounding, Inverse methods for atmospheric sounding, World Scientific, https://doi.org/10.1142/3171, 2000.

Saunders, R., Hocking, J., Turner, E., Rayer, P., Rundle, D., Brunel, P., Vidot, J., Roquet, P., Matricardi, M., Geer, A., Bormann, N., and Lupu, C.: An update on the RTTOV fast radiative transfer model (currently at version 12), Geosci. Model Dev., 11, 2717-2737, https://doi.org/10.5194/gmd-11-2717-2018, 2018.

Susskind, J., Barnet, C. D. and Blaisdell, J. M.: Retrieval of atmospheric and surface parameters from AIRS/AMSU/HSB data in the presence of clouds, IEEE Trans. Geosci. Remote Sensing, 41, 390-409, https://doi.org/10.1109/TGRS.2002.808236, 2003.

Smith, W. L., Woolf, H. M., and Revercomb, H. E.: Linear simultaneous solution for temperature and absorbing constituent profiles from radiance spectra, Appl. Optics., 30, 1117, https://doi.org/10.1364/AO.30.001117, 1991.

Wakita, H., Tokura, Y., Furukawa, F., and Takigawa, M.: Study of the information content contained in remote sensing data of atmosphere, Acta. Physica. Sinica., 59, 683-691, 2010.

Wang, G., Lu, Q. F., Zhang, J. W., and Wang, H. Y.,.: Study on method and experiment of hyper-spectral atmospheric infrared sounder channel selection, Remote Sensing Technology and Application., 29, 795-802 , 2014.

Zhang, J. W., Wang, G., Zhang, H., Huang J., Chen J., and Wu, L. L.: Experiment on hyper-spectral atmospheric infrared sounder channel selection based on the cumulative effect coefficient of principal component, Journal of Nanjing Institute of meteorology, 1, 36-42, http://dx.doi.org/10.3969/j.issn.1674-7097.2011.01.005, 2011.

（c） **The marked-up manuscript version**

A channel selection method for hyperspectral atmospheric infrared sounders based on layering

Shujie Chang[1, 2,3], Zheng Sheng[1,2], Huadong Du[1,2], Wei Ge[1,2] and Wei Zhang[1,2]

[1] College of Meteorology and Oceanography, National University of Defense Technology, Nanjing, China

[2] Collaborative Innovation Center on Forecast and Evaluation of Meteorological Disasters, Nanjing University of Information Science and Technology, Nanjing, China

[3] South China Sea Institute for Marine Meteorology, Guangdong Ocean University, Zhanjiang, China

Correspondence: Zheng Sheng (19994035@sina.com)

Abstract. Because a satellite channel's ability to resolve hyperspectral data varies with height, an improved channel selection method is proposed based on information content. An effective channel selection scheme for a hyperspectral atmospheric infrared sounder using AIRS data based on layering is proposed. The results

are as follows: (1) Using the improved method, the atmospheric retrievable index is more stable, the value reaching 0.54. The coverage of the weighting functions is more evenly distributed over height with this method and closer to the actual atmosphere; (2) Statistical inversion comparison experiments show that the accuracy of the retrieval temperature, using the improved channel selection method in this paper, is consistent with that of 1Dvar channel selection. In the stratosphere and mesosphere especially, from 10 hPa to 0.02 hPa, the accuracy of the retrieval temperature of our improved channel selection method is improved by about 1 K. In general, the accuracy of the retrieval temperature of ICS (Improved Channel Selection) is improved; (3) Statistical inversion comparison experiments in four typical regions indicate that ICS in this paper is significantly better than NCS (NWP Channel Selection) and PCS (Primary Channel Selection) in different regions and shows latitudinal variations, which shows potential for future applications.

1 Introduction

Since the successful launch of the first meteorological satellite, TIROS in the 1960s, satellite observation technology has developed rapidly. Meteorological satellites observe the Earth's atmosphere from space and are able to record data from regions which are otherwise difficult to observe. Satellite data greatly enrich the content and range of meteorological observations, and consequently, atmospheric exploration technology and meteorological observations have taken us to a new stage in our understanding of weather systems and related phenomena (Fang, 2014). From the perspective of vertical atmospheric observation, satellite instruments are developing rapidly. In their infancy, the traditional infrared measurement instruments for detecting atmospheric temperature and moisture profiles, such as TOVS (Smith et al., 1991) or HIRS in ATOVS (Chahine, 1972; Li et al., 2000; Liu, 2007), usually employed filter spectrometry. Even though such instruments have played an important role in improving weather prediction, it is difficult to continue to build upon improvements in terms of observation accuracy and vertical resolution due to the limitation of low spectral resolution. By using this kind of filter-based spectroscopic measurement instrument, therefore, it is difficult to meet today's needs in numerical weather prediction (Eyre et al., 1993; Prunet et al., 2010; Menzel et al., 2018). To meet this challenge, a series of plans for the creation of high-spectral resolution atmospheric measurement instruments has been executed in the United States and in Europe in recent years: One example is the AIRS (Atmospheric InfraRed Sounder) on the Earth Observation

System, “Aqua”, launched on May 4, 2002 from the United States. AIRS has 2378 spectral channels providing sensitivity from the ground to up to about 65 km of altitude (Aumann et al., 2003; Hoffmann and Alexander, 2009; Gong et al., 2011). The United States and Europe, in 2010 and in 2007, also installed the CRIS (Cross-track Infrared Sounder) and the IASI (Inter-Attractive Atmospheric Sounding Interferometer) on polar-orbiting satellites.

China also devotes great importance to the development of such advanced sounding technologies. In the early 1990s, the National Satellite Meteorological Center began to investigate the principles and techniques of hyperspectral resolution atmospheric observations. China’s development of interferometric atmospheric vertical detectors eventually led to the launch of Fengyun No. 3, on May 27, 2008, and Fengyun No. 4 on December 11, 2016, both of which were equipped with infrared atmospheric instruments. How best to use the hyperspectral resolution observation data obtained from these instruments, to obtain reliable atmospheric temperature and humidity profiles, is an active area of study in atmospheric inversion theory.

Due to technical limitations, only a limited number of channels could at first be built into the typical satellite instruments. In this case, channel selection generally involved controlling the channel weighting function by utilizing the spectral response characteristics of the channel (such as center frequency and bandwidth). With the development of measurement technology, increasing numbers of hyperspectral detectors were carried on meteorological satellites. Due to the large number of channels and data supported by such instruments today (such as AIRS with 2378 channels and IASI with 8461 channels), it has proven extremely cumbersome to store, transmit, and process such data. Moreover, there is often a close correlation between the channel, causing an ill-posedness of the inversion, potentially compromising accuracy of the retrieval product based on hyperspectral resolution data.

However, hyperspectral detectors have many channels and provide real-time mode prediction systems with vast quantities of data, which can significantly improve prediction accuracy. But, if all the channels are used to retrieve data, the retrieval time considerably increases. Even more problematic are the glut of information produced, and the unsuitability of the calculations for real-time forecasting. Concurrently, the computer processing power must be large enough to meet the demands of simulating all the channels simultaneously within the forecast time. It is important to properly select a group of channels that can provide as much information as possible from the thousands of channels' observations to improve the calculation efficiency and retrieval quality.

Many researchers have studied the channel selection algorithm. Menke (1984) first chose channels using a data precision matrix method. Aires et al. (1999) made the selection using the Jacobian matrix, which has been widely used since then (Aires et al., 2002; Rabier et al., 2010). Rodgers (2000) indicated that there are two useful quantities in measuring the information provided by the observation data: Shannon information content and degrees of freedom. The concept of information capacity then became widely used in satellite channel selection. In 2007, Xu (2007) compared the Shannon information content with the relative entropy, analyzing the information loss and information redundancy. In 2008, Du et al. (2008) introduced the concept of the atmospheric retrievable index (ARI) as a criterion for channel selection, and in 2010, Wakita et al. (2010) produced a scheme for calculating the information content of the various atmospheric parameters in remote sensing using Bayesian estimation theory. Kuai et al. (2010) analyzed both the Shannon information content and degrees of freedom in channel selection when retrieving CO_2 concentrations using thermal infrared remote sensing and indicated that 40 channels could contain 75% of the information from the total channels. Cyril et al. (2003) proposed the optimal sensitivity profile method based on the sensitivity of different atmospheric components. Lupu et al. (2012) used degrees of freedom for signals (DFS) to estimate the amount of information contained in observations in the context of observing system experiments. In addition, the singular value decomposition method has also been widely used for channel selection (Prunet et al., 2010; Zhang et al., 2011; Wang et al., 2014). In 2017, Chang et al. (2017) selected a new set of Infrared Atmospheric Sounding Interferometer (IASI) channels using the channel score index (CSI). Richardson et al. (2018) selected 75 from 853 channels based on the high spectral-resolution oxygen A-band instrument on NASA's Orbiting Carbon Observatory-2 (OCO-2), using information content analysis to retrieve the cloud optical depth, cloud properties, and position.

Today's main methods for channel selection use only the weighting function to study appropriate numerical methods, such as the data precision matrix method (Menke, 1984), singular value decomposition method (Prunet et al., 2010; Zhang et al., 2011; Wang et al., 2014), and the Jacobi method (Aires et al., 1999; Rabier et al., 2010). The use of the methods allows sensitive channels to be selected. The above-mentioned studies also take into account the sensitivity of each channel to atmospheric parameters during channel selection, while ignoring some factors that impact retrieval results. The accuracy of retrieval results depends not only on the channel weighting function but also on the channel noise, background field, and the retrieval algorithm.

Currently, information content is often employed in channel selection. During retrieval, this method delivers the largest amount of information for the selected channel combination (Rodgers, 1996; Du et al., 2008; He et al., 2012; Richardson et al., 2018). This method has made great breakthroughs in both theory and practice, and the concept of information content itself does consider all the height dependencies of the kernel matrix K (Rodgers, 2000). However, earlier works have neglected the height dependencies of K for simplicity. This paper uses the atmospheric retrievable index (ARI) as the index, which is based on information content (Du et al., 2008; Richardson et al. 2018). Channel selection is made at different heights, and an effective channel selection scheme is proposed which fully considers various factors, including the influence of different channels on the retrieval results at different heights. This ensures the best accuracy of the retrieval product when using the selected channel. In addition, statistical inversion comparison experiments are used to verify the effectiveness of the method.

2 Channel selection indicator, scheme and method

2.1 Channel selection indicator

According to the concept of information content, the information content contained in a selected channel of a hyperspectral instrument can be described as H (Rodgers, 1996; Rabier et al., 2010). The final expression of H is:

$$\mathrm{H} = -\frac{1}{2} ln\left|\hat{S} S_a^{-1}\right|$$

$$= -\frac{1}{2} ln|(S_a - S_a K^T (K S_a K^T + S_\varepsilon)^{-1} K S_a) S_a^{-1}|, \qquad (1)$$

where S_a is the error covariance matrix of the background or the estimated value of atmospheric profile, S_ε represents the observation error covariance matrix of each hyperspectral detector channel, $\hat{S} = (S_a - S_a K^T (K S_a K^T + S_\varepsilon)^{-1} K S_a)$ denotes the covariance matrix after retrieval, K is the weighting function matrix.

In order to describe the accuracy of the retrieval results visually and quantitatively, the atmospheric retrievable index (ARI), p, (Du et al., 2008) is defined as follows:

$$\mathrm{p} = 1 - \exp\left(\frac{1}{2n} ln\left|\hat{S} S_a^{-1}\right|\right), \qquad (2)$$

Assuming that before and after retrieval, the ratio of the root mean square error of each element in the atmospheric state vector is 1-p, then $\left|\hat{S}S_a^{-1}\right| = (1 - \mathrm{p})^{2n}$ is derived. By inverting the equation, the ARI that is p can be obtained in Eq. (2), which indicates the relative portion of the error that is eliminated by retrieval. In fact, before and after retrieval, the ratio of the root mean square error of each element cannot be 1-p. Therefore, p defined by Eq. (1) is actually an overall evaluation of the retrieval result.

2.2 Channel selection scheme

The principle of channel selection is to find the optimum channel combination after numbering the channels. This combination makes the information content, H, or the ARI defined in this paper as large as possible, in order to maintain the highest possible accuracy in the retrieval results.

Let there be M layers in the vertical direction of the atmosphere and N satellite channels. Selecting n from N channels, there will be C_N^n combinations in each layer, leading C_N^n calculations to get C_N^n kinds of p results. Furthermore, there are M layers in the vertical direction of the atmosphere. Therefore, the entire atmosphere must be calculated $\mathrm{M} \cdot \mathrm{C}_\mathrm{N}^\mathrm{n}$ times. However, the calculation $\mathrm{M} \cdot \mathrm{C}_N^n$ times will be particularly large, which makes this approach impractical in calculating p for all possible combinations. Therefore, it is necessary to design an effective calculation scheme, and such a scheme, i.e., a channel selection method, using iteration is proposed, called the "sequential absorption method" (Dudhia et al., 2002; Du et al., 2008). The method's main function is to select ("absorb") channels one by one, taking the channel with the maximum value of p. Through n iterations, n channels can be selected as the final channel combination. The steps are as follows:

(1) The expression of information content in a single channel:

First, we use only one channel for retrieval. A row vector, k, in the weighting function matrix, K, is a weighting function corresponding to the channel. After observation in this channel, the error covariance matrix is:

$$\hat{S} = S_a - S_a k^T (s_\varepsilon + k S_a k^T)^{-1} k S_a. \tag{3}$$

It should be noted that $(s_\varepsilon + k S_a k^T)$ is a scalar value in Eq. (3), so Eq. (3) can be converted to:

$$\hat{S} = \left(I - \frac{S_a k^T k}{(s_\varepsilon + k S_a k^T)}\right) S_a = \left(I - \frac{(k S_a)^T k}{(s_\varepsilon + k (k S_a)^T)}\right) S_a. \tag{4}$$

Substituting Eq. (4) into Eq. (2) gives:

$$\mathrm{p} = 1 - \exp\left(\frac{1}{2n} ln\left(\left|I - \frac{(k S_a)^T k}{(s_\varepsilon + k (k S_a)^T)}\right|\right)\right). \tag{5}$$

(2) Simplification of Eq. (5) p matrix:

Since S_a and S_ε are positive definite symmetric matrixes, it can be decomposed into $S_a = (S_a^{1/2})^T (S_a^{1/2})$ and $S_\varepsilon = (S_\varepsilon^{1/2})^T (S_\varepsilon^{1/2})$.

Define $\mathrm{R} = S_{\varepsilon}^{1/2} K S_{a}^{1/2}$. (6)

The matrix R can then be regarded as a weighting function matrix, normalized by the observed error and a priori uncertainty. A row vector of R, $\mathrm{r} = s_{\varepsilon}^{-1/2} k S_{a}^{1/2}$, represents the normalized weighting function matrix of a single channel. Substituting r into Eq. (5) gives:

$$\mathrm{p} = 1 - \exp\left(\frac{1}{2n} ln \left(\left| I - \frac{rr^T}{1+r^T r}\right|\right)\right). \tag{7}$$

For arbitrary row vectors, a and b, using the matrix property $\det(\mathrm{I} + a^T \mathrm{b}) = 1 + \mathrm{b}a^T$, the new expression for p is:

$$\begin{aligned}
\mathrm{p} &= 1 - \exp\left(\frac{1}{2n} ln\left(1 - \frac{r^T r}{1 + r^T r}\right)\right) \\
&= 1 - \exp\left(\frac{1}{2n} ln\left(\frac{1}{1+r^T r}\right)\right) \\
&= 1 - \exp\left(-\frac{1}{2n} ln(1 + r^T r)\right).
\end{aligned} \tag{8}$$

(3) Iteration in a single layer:

First, the iteration in a single layer requires the calculation of R. According to $\mathrm{S_a}$, $\mathrm{S_\varepsilon}$, K and Eq. (6), R can be calculated. Second, using Eq. (8), p of each candidate channel can be calculated.

Moreover, the channel corresponding to maximum p is the selected channel for this iteration. After a channel has been selected, according to Eq. (3) we can use $\hat{S}$ to get S_a for the next iteration. Finally, channels which are not selected during this iteration are used as the candidate channels for the next iteration.

When selecting n from N channels, it is necessary to calculate (N-n/2)n≈Nn p values, which is much smaller than C_N^n. In addition to high computational efficiency by using this method, another advantage is that all channels can be recorded in the order in which they are selected. In the actual application, if n' channels are needed, and $n' < n$, we will not need to select the channel again, but record the selected channel only.

(4) Iteration for different altitudes:

Because satellite channel sensitivity varies with height, repeating the iterative process of step (3), selects the optimum channels at different heights. Assuming there are M layers in the atmosphere and selecting n from N channels, it is necessary to calculate $M \cdot (N - n/2)n \approx M \cdot Nn$ p values, a much smaller number than $M \cdot C_N^n$. In this way, different channel sets can be used to evaluate corresponding height in the retrieved profiles.

2.3 Statistical inversion method

The inversion methods for the atmospheric temperature profiles can be summarized in two categories: statistical inversion and physical inversion. Statistical inversion is essentially a linear regression model which uses a large number of satellite measurements and atmospheric parameters to match samples and calculate their correlation coefficient. Then, based on the correlation coefficient, the required parameters of the independent measurements obtained by the satellite are retrieved. Because the method does not directly solve the radiation transfer equation, it has the advantages of fast calculation speed. In addition, the solution is numerically stable, which makes it one of the highest precision methods (Chedin et al., 1985). Therefore, the statistical inversion method will be used for our channel selection experiment and a regression equation will be established.

According to an empirical orthogonal function, the atmospheric temperature (or humidity), T, and the brightness temperature, T_b, are expanded as:

$$\mathrm{T} = T^{*} \cdot A, \tag{9}$$

$$T_b = T_b^{*} \cdot A, \tag{10}$$

where T^* and T_b^* are the eigenvectors of the covariance matrix of temperature (or humidity) and brightness temperature, respectively. A and B stand for the corresponding expansion coefficient vectors of temperature (humidity) and brightness temperature.

Using the least squares method and the orthogonal property, the coefficient conversion matrix, V, is introduced:

$$\mathrm{A} = \mathrm{V} \cdot B, \tag{11}$$

where $V = AB^T(BB^T)^{-1}$. (12)

Using the orthogonality, we get:

$$\mathrm{B} = (T_b^*)^T T_b, \tag{13}$$

$$\mathrm{A} = (T^*)^T T. \tag{14}$$

For convenience, the anomalies of the state vector (atmospheric temperature), T, and the observation vector (brightness temperature), T_b, are taken:

$$\widehat{\mathrm{T}} = \overline{\mathrm{T}} + \widehat{\mathrm{T}}' = \overline{\mathrm{T}} + \mathrm{G}\mathrm{T}_\mathrm{b}' = \overline{\mathrm{T}} + \mathrm{G}(\mathrm{T}_\mathrm{b} - \overline{\mathrm{T}_\mathrm{b}}), \tag{15}$$

where $\widehat{T}$ stands for the retrieval atmospheric temperature. $\overline{T}$ and $\overline{T_b}$ are the corresponding average values of the elements, respectively. $\widehat{T}'$ and T_b' represent the corresponding anomalies of the elements, respectively.

Assuming there are k sets of observations, a sample anomaly matrix with k vectors can be constructed:

$$T' = (t_1', t_2', \cdots, t_k'), \tag{16}$$

$$T_b' = (t_{b1}', t_{b2}', \cdots, t_{bk}'). \tag{17}$$

Define the inversion error matrix as：

$$\delta = \overline{T} - \widehat{T} = \widehat{T}' - T'. \tag{18}$$

The retrieval error covariance matrix is:

$$\begin{aligned} S_\delta &= \frac{1}{k-n-1}\delta\delta^T \\ &= \frac{1}{k-n-1}(T' - GT_b')(T' - GT_b')^T \\ &= \frac{k-1}{k-n-1}(S_e - G^T S_{xy} - S_{xy}G^T + GS_yG^T), \end{aligned} \tag{19}$$

where

$$S_e = \frac{1}{k-1} T' \, {T'}^{T} \, ,$$

$$S_y = \frac{1}{k-1} T_b' \, {T_b'}^{T} \, ,$$

$$S_{xy} = \frac{1}{k-1} T' \, {T_b'}^{T} . \qquad (20)$$

S_e stands for the sample covariance matrix of T, S_y denotes the sample covariance matrix of T_b, and S_{xy} represents the covariance matrix of T and T_b. The elements on the diagonal of the error covariance matrix, S_δ, represent the retrieval error variance of T. The matrix G that minimizes the overall error variance is the least squares coefficient matrix of the regression equation (15), which meets the criteria:

$$\delta^2 = \mathrm{tr}(S_\delta) = \min. \qquad (21)$$

Taking a derivative of Eq. (21) with respect to G, $\frac{\partial}{\partial G}\mathrm{tr}(S_\delta) = 0 = (-2S_{xy} + 2GS_y)$, which means that:

$$G = S_{xy} S_y^{-1}. \qquad (22)$$

Substituting Eq. (22) into Eq. (15) finally gives the least squares solution as:

$$\hat{T} = \overline{T} + S_{xy} S_y^{-1} (T_b - \overline{T_b}). \tag{23}$$

It should be noted that the least squares solution obtained here aims to minimize the sum of the error variance for each element in the atmospheric state vector after retrieval for several times. At present, statistical multiple regression is widely used in the retrieval of atmospheric profiles based on atmospheric remote sensing data. As long as there are enough data, S_{xy} and S_y can be determined.

3. Channel selection experiment

3.1 Data and model

The Atmospheric Infrared Sounder (AIRS) is primarily designed to measure the Earth's atmospheric water vapor and temperature profiles on a global scale (Aumann et al., 2003; Hoffmann and Alexander, 2009). AIRS is a continuously operating cross-track scanning sounder, consisting of a telescope that feeds an echelle spectrometer. The AIRS infrared spectrometer acquires 2378 spectral samples at a resolution λ/Δλ, ranging from 1086 to 1570, in three bands: 3.74 μm to 4.61 μm, 6.20 μm to 8.22 μm, and 8.8 μm to 15.4

μm. The footprint size 13.5 km at nadir (Susskind et al., 2003). The spectral range includes 4.3 μm and 15.5 μm for important temperature observation and CO_2, 6.3 μm for water vapor, and 9.6 μm for ozone absorption bands (Menzel et al., 2018). The root mean square error (RMSE) of the measured radiation is better than 0.2 K (Susskind et al., 2003). Moreover, global atmospheric profiles can be detected every day. Due to radiometer noise and faults, there are currently only 2047 effective channels. However, compared with previous infrared detectors, AIRS boasts a significant improvement in both the number of channels and spectral resolution (Aumann, 1994; Huang et al., 2005; Li et al., 2005).

The root mean square error of an AIRS infrared channel is shown in Fig. 1, with black spots, indicating that not all the instrument channels possess a measurement error of less than 0.2 K. There are a few channels with extremely large measurement errors, which reduce the accuracy of prediction to some extent. Among them, some extremely large measurement errors reduce the accuracy of prediction to some extent (Susskind et al., 2003). At present, more than 300 channels have not been used because their errors exceed 1 K. If data from these channels were to be used for retrieval, the accuracy of the retrieval could be reduced. Therefore, it is necessary to select a group of channels to improve the calculation efficiency and retrieval quality. In this paper we study channel selection for temperature profile retrieval by AIRS.

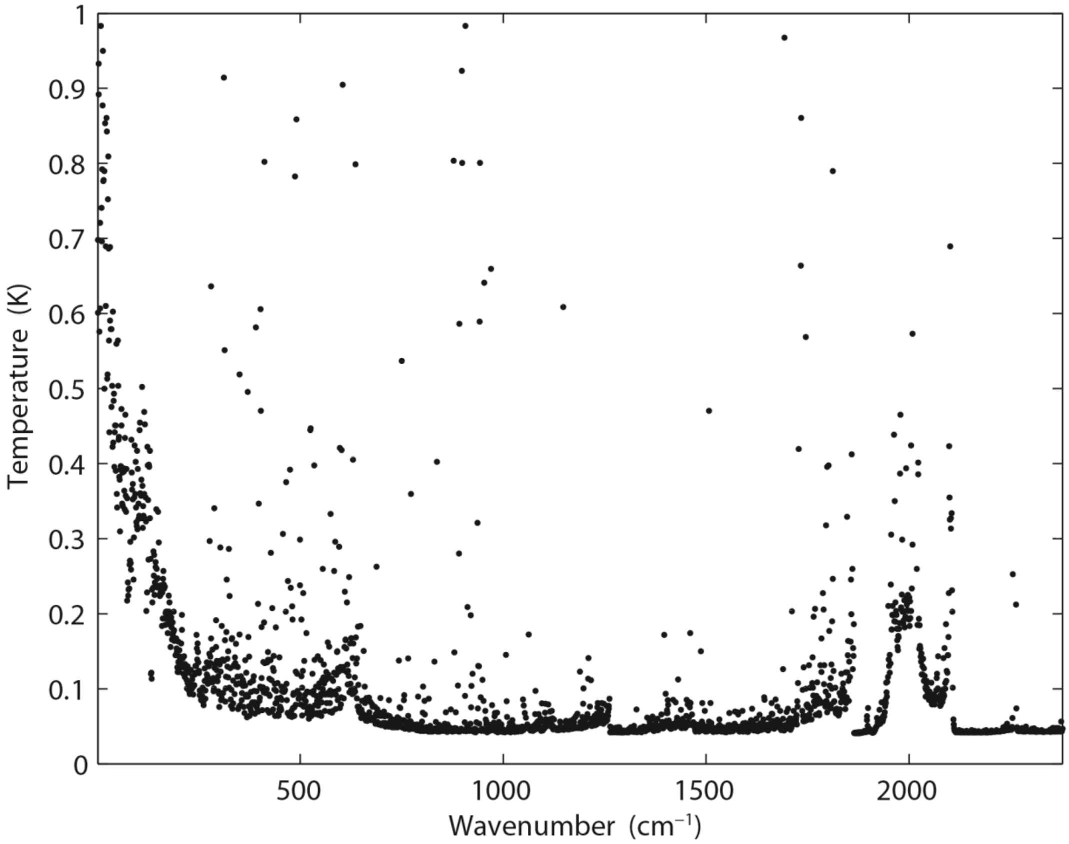

Figure 1. Root mean square error of AIRS infrared channel (black spots).

For the calculation of radiative transfer and the weighting function matrix, K, the RTTOV (Radiative Transfer for TOVS) v12 fast radiative transfer model is used. Although initially developed for the TOVS (TIROS Operational Vertical Sounder) radiometers, RTTOV can now simulate around 90 different satellite sensors measuring in the MW (microwave), IR (infrared) and VIS (visible) regions of the spectrum (Saunders et al., 2018). The model allows rapid simulations (1 ms for 40 channel ATOVS (Advanced TOVS) on a desktop PC) of radiances for satellite visible, infrared, or microwave nadir scanning radiometers given atmospheric profiles of temperature and trace gas concentrations, and cloud and surface properties. The only mandatory gas included as a variable for RTTOV v12 is water vapor. Optionally, ozone, carbon dioxide, nitrous oxide, methane, carbon monoxide, and sulfur dioxide can be included, with all other constituents assumed to be constant. RTTOV can accept input profiles on any defined set of pressure levels. The majority of RTTOV coefficient files are based on the 54 levels (see Table A1 in Appendix A), ranking from 1050 hPa to 0.01 hPa, though coefficients for some hyperspectral sounders are also available on 101 levels.

In order to correspond to the selected profiles, the atmosphere is divided into 137 layers, each of which contains corresponding atmospheric characteristics, such as temperature, pressure, and the humidity distribution. Each element in the weighting function matrix can be written as $\partial yi/\partial xj$. The subscript i is used to identify the satellite channel, and the subscript j is used to identify the atmospheric variable. Therefore, $\partial yi/\partial xj$ indicates the variation in brightness temperature in a given satellite channel, when a given atmospheric variable in a given layer changes. We are thus able to establish which layer of the satellite channel is particularly sensitive to which atmospheric characteristic (temperature, various gas contents) in the vertical atmosphere. The RTTOV_K (the K mode), is used to calculate the matrix H(X0) (Eq. (1)) for a given atmospheric profile characteristic.

3.2 Channel selection comparison experiment and results

In order to verify the effectiveness of the method, three sets of comparison experiments were conducted. First, 324 channels used by the EUMETSAT Satellite Application Facility on Numerical Weather Prediction (NWP SAF) were selected. NCS is short for NWP channel selection in this paper. NCS were released by the NWPSAF 1DVar (one-dimensional variational analysis) scheme, in accordance with the requirements of the NWPSAF (Saunders et al., 2018). Second, 324 channels were selected using the information capacity method. This method was adopted by Du et al. (2008) without the consideration of layering. PCS is short for primary channel selection in this paper.

Third, 324×M channels were selected using the information capacity method for the M layer atmosphere. ICS is short for improved channel selection in this paper. In order to verify the retrieval effectiveness after channel selection, statistical inversion comparison experiments were performed using 5000 temperature profiles provided by the ECMWF dataset, which will be introduced in Sect. 4.

The observation error covariance matrix, S_{ε}, in the experiment is provided by NWP SAF 1Dvar. In general, it can be converted to a diagonal matrix, the elements of which are the observation error standard deviation of each hyperspectral detector channel, which is the square of the root mean square error for each channel. The root mean square error of the AIRS channels is shown in Fig. 1. The error covariance matrix of the background, S_a, is calculated using 5000 samples of the IFS-137 data provided by the ECMWF dataset (The detailed information will be introduced in Sect. 4). The last access date is April 26th, 2019 (download address: https://www.nwpsaf.eu/site/update-137-level-nwp-profile-dataset/, 2019). The covariance matrix of temperature is shown in Fig. 2. The results are consistent with the previous study by Du et al. (2008).

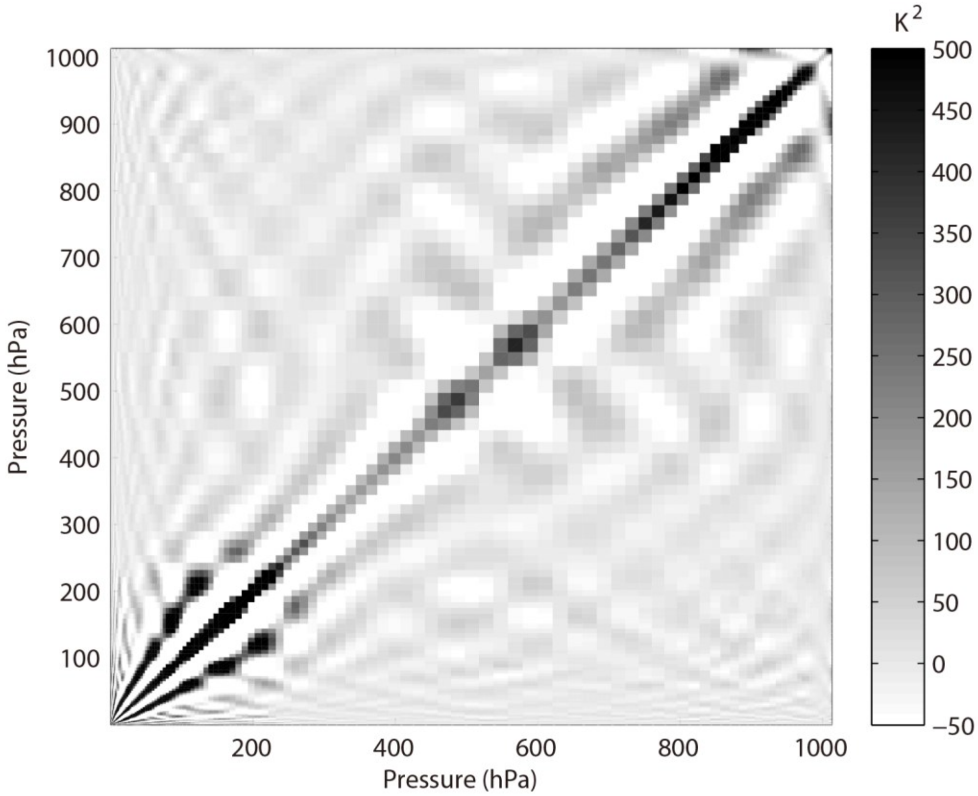

Figure 2. Error covariance matrix of temperature (shaded).

The reference atmospheric profiles are from the IFS-137 database, and the temperature weighting function matrix is calculated using the RTTOV_K mode, as shown in Fig. 3; the results are consistent with those of the previous study by Du et al. (2008). For the air-based passive atmospheric remote sensing studied in this paper, when the same channel detects the atmosphere from different observation angles, the value of the weighting function matrix K changes due to the limb effect. The goal of this section is focusing on the selection methods of selecting channels; therefore the biases produced from different observation angles can be ignored.

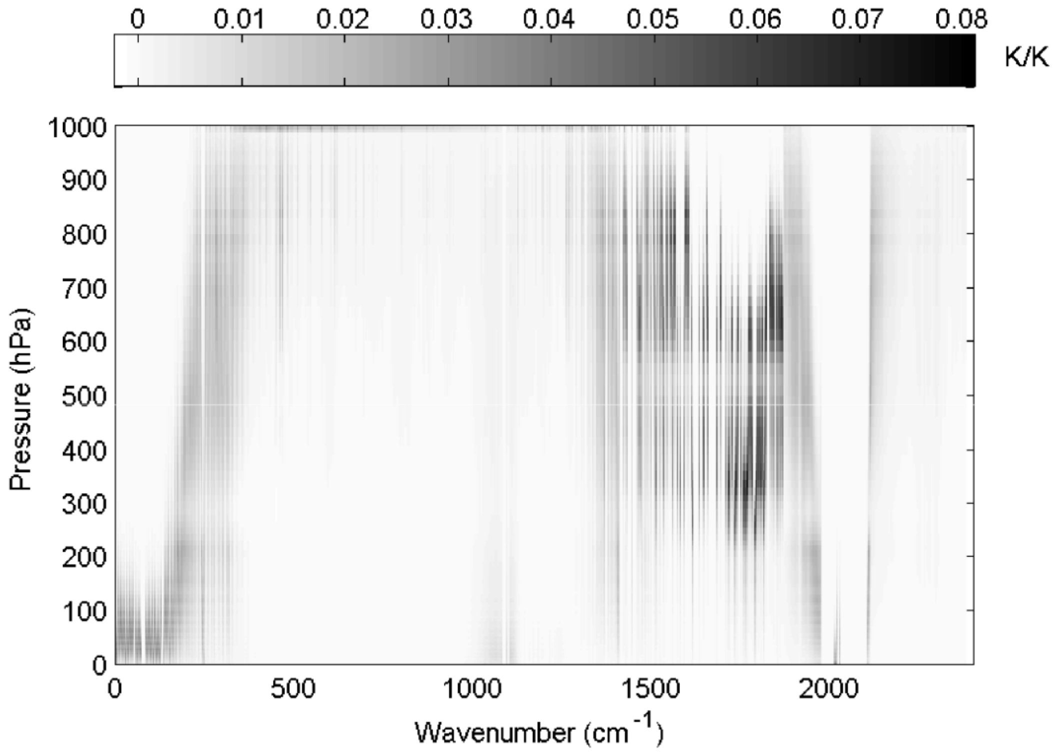

Figure 3. Temperature weighting function matrix (shaded).

In order to verify the effectiveness, the distribution of 324 channels, without considering layering, in the AIRS brightness temperature spectrum is indicated in Fig. 4. The background brightness temperature is the simulated AIRS observation brightness temperature, which is from the atmospheric profile in RTTOV put into the model. Figure 4(a) shows the 324 channels selected by PCS, while Fig. 4(b) shows the 324 channels selected by NCS.

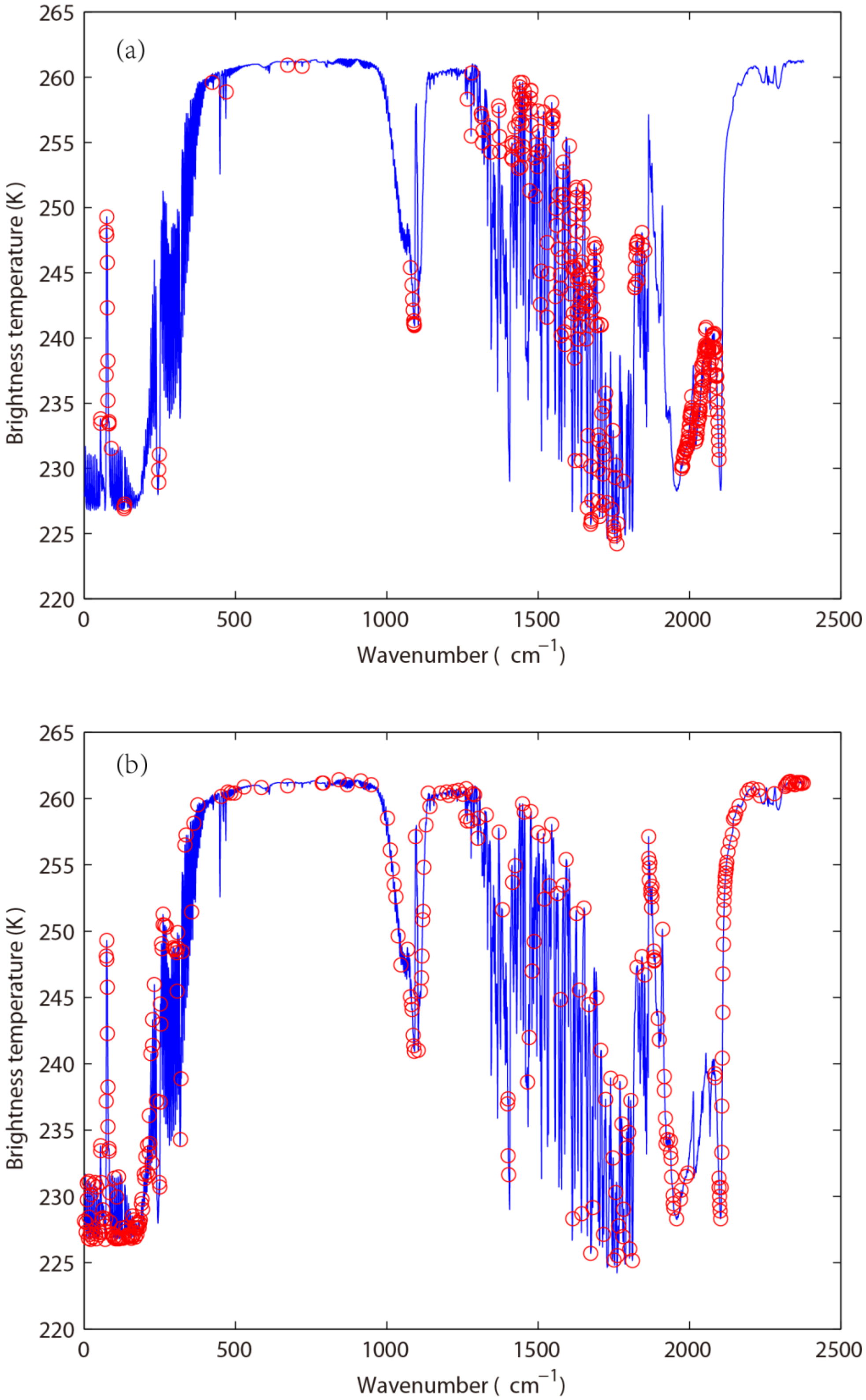

Figure 4. The distribution of different channel selection methods without considering layering in the AIRS brightness temperature

spectrum (blue line). (a) 324 channels selected by PCS (red circles). (b) 324 channels selected by NCS (red circles).

Without considering layering, the main differences between the 324 channels selected by PCS and NCS are as follows: (1) When the wavenumber approaches 1000, the wavelength is 10 μm (1/1000 cm^{-1}). Near this band, fewer channels are selected by PCS because the retrieval of ground temperature is considered by NCS; (2) When the wavenumber is near 1200, the wavelength is 9 μm (1/1200 cm^{-1}). Near this band, no channels are selected by PCS because the retrieval of O_3 is not considered in this paper; (3) When the wavenumber approaches 1500, the wavelength is 6.7 μm (1/1500 cm^{-1}). As is known, the spectral range from 6 μm to 7 μm corresponds to water vapor absorption bands, but fewer channels are selected by NCS; (4) When the wavenumber is close to 2000, it derives a wavelength of 5 μm (1/2000 cm^{-1}), which includes 4.2 μm for N_2O and 4.3 μm for CO_2 absorption bands. As is shown in Fig. 4, fewer channels are selected by PCS in those bands. PCS is favorable for atmospheric temperature observation in the high temperature zone. Because 4.2 μm and 4.3 μm bands are sensitive to high temperature, the higher temperature is, the better observation can be obtained; (5) In the near infrared area, the wavenumber exceeds 2200, deriving a wavelength of less than 4 μm (1/2000 cm^{-1}). A small number of channels is selected by NCS, but no channels are selected by PCS.

Above all, the information content used in this paper only takes the temperature profile retrieval into consideration, so the channel combination of PCS is inferior to that of NCS for the retrieval of surface temperature and the O_3 profile. The advantages of the channel selection method based on information content in this paper are mainly reflected in: (1) Stratosphere and mesosphere is less affected by the ground surface, so the retrieval result of PCS is better than that of NCS. (2) Due to the method selected in this paper there are more channels at 4.2 μm for N_2O and 4.3 μm for CO_2 absorption bands; the channel combination of PCS is better than that of NCS for atmospheric temperature observation to the higher temperature.

By comparing channel selection without considering layering, we note the general advantages and disadvantages of PCS and NCS for the retrieval of temperature and can improve the channel selection scheme. First, the retrieval of the temperature profile for 324 channels selected by PCS is obtained. The relationship between the number of iterations and the ARI is shown in Fig. 5.

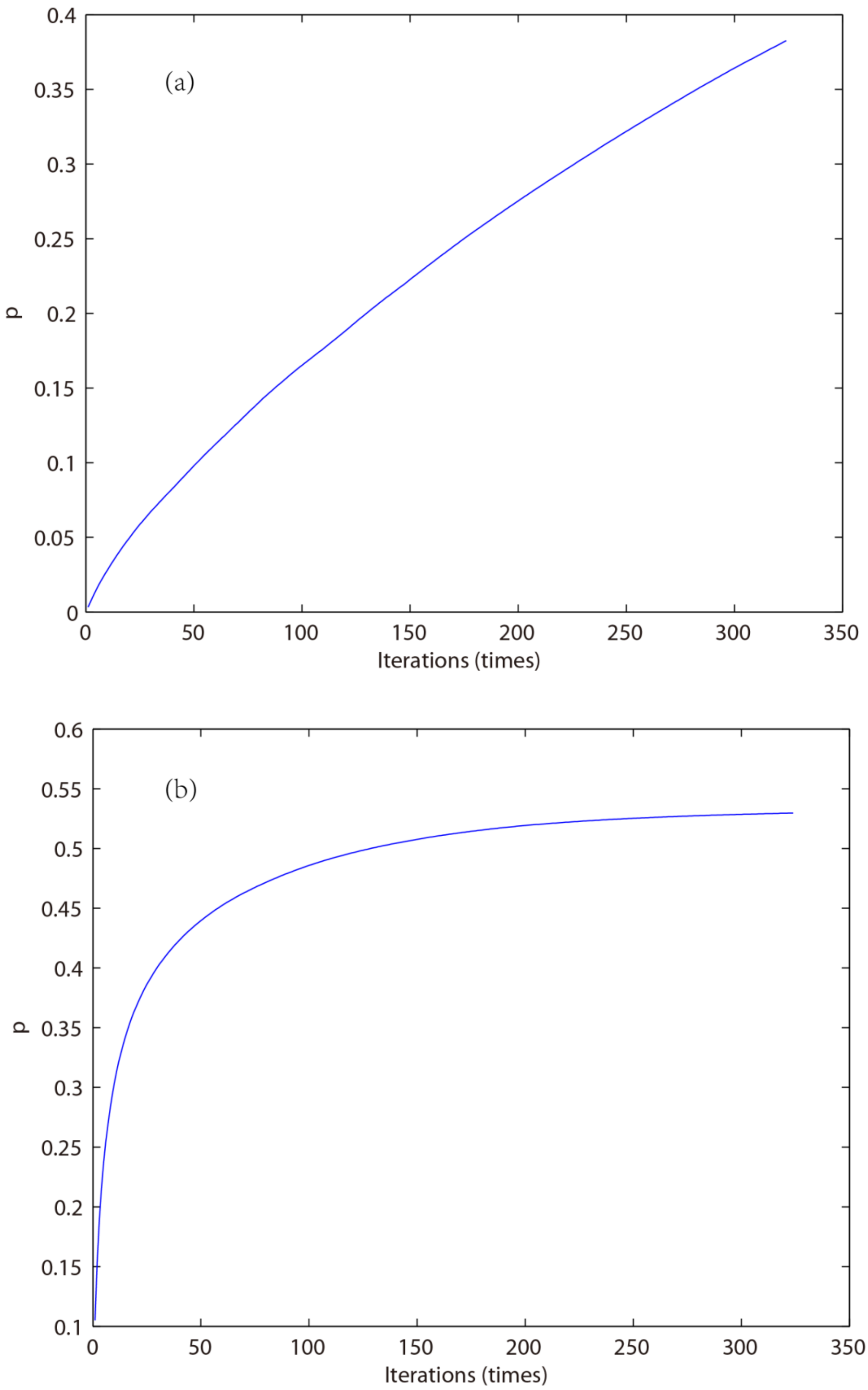

Figure 5. The relationship between the number of iterations and ARI.
(a) PCS. (b) ICS.

The ARI for PCS tends to be 0.38 and is not convergent, so the PCS method needs to be improved. In this paper, the atmosphere is divided into 137 layers, and based on the information content and iteration, 324 channels are selected for each layer. Then, the temperature profile of each layer can be retrieved based on statistical inversion (see at Sect. 4). The relationship between the number of iterations and the ARI for ICS is shown in Fig. 5b. When the number of iterations approaches 100, the ARI of ICS tends to be stable, and reach to 0.54. Thus, in terms of the ARI and convergence, the ICS method is better than that of PCS.

Furthermore, because an iterative method is used to select channels, the order of each selected channel is determined by the contribution from the ARI. The weighting function matrix of the top 324 selected channels, according to channel order, is shown in Fig. 6.

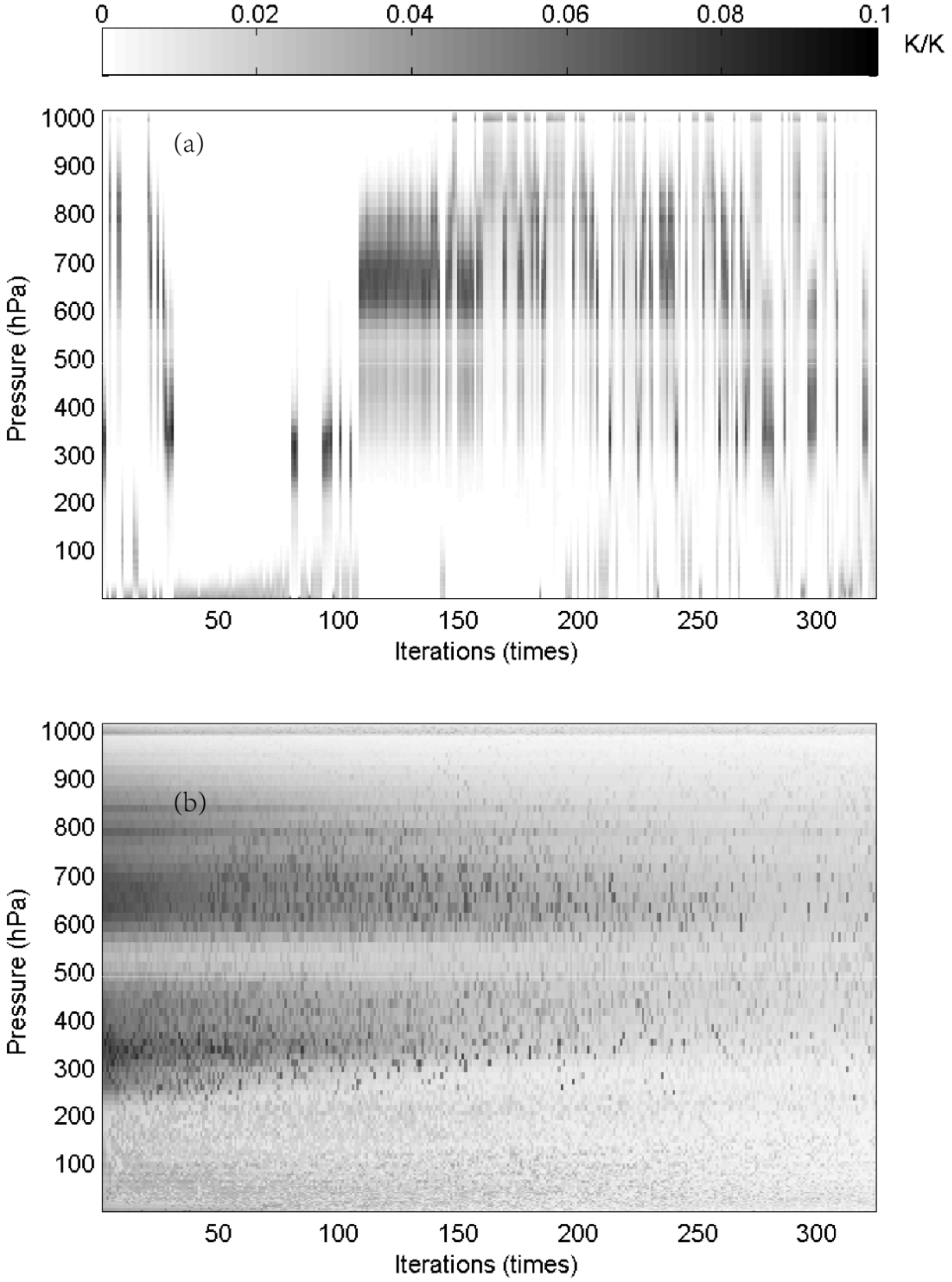

Figure 6. The relationship between the number of iterations and the weighting function of the top 324 selected channels (shaded). (a) ICS. (b) PCS.

As illustrated in Fig. 6, in the first 100 iterations, the distribution of the temperature weighting function for PCS is relatively scattered; it does not reflect continuity between the adjacent layers of the atmosphere. Besides, the ICS result is better than that of PCS, showing that: (1) the distribution of the temperature weighting function is more continuous and reflects the continuity between adjacent layers of the atmosphere; (2) regardless of the number of iterations, the maximum value of the weighting function is stable near 300–400 hPa and 600–700 hPa, without scattering, which is closer to the situation in real atmosphere.

4. Statistical multiple regression experiment

4.1 Temperature profile database

A new database including a representative collection of 25,000 atmospheric profiles from the European Centre for Medium-range Weather Forecasts (ECMWF) was used for the statistical inversion experiments. The profiles were given in a 137-level vertical grid extending from the surface up to 0.01 hPa. The database was divided into five subsets focusing on diverse sampling characteristics such as temperature, specific humidity, ozone mixing ratio, cloud condensates, and precipitation. In contrast with earlier releases of the

ECMWF diverse profile database, the 137-level database places greater emphasis on preserving the statistical properties of sampled distributions produced by the Integrated Forecasting System (IFS) (Eresmaa and McNally, 2014; Brath et al., 2018). IFS-137 spans the period from September 1, 2013 to August 31, 2014. There are two operational analyses each day (at 00z and 12z), and approximately 13 000 atmospheric profiles over the ocean. The pressure levels adopted for IFS-137 are shown in Table A2 (see Table A2 in Appendix A).

The locations of selected profiles of temperature, specific humidity, and cloud condensate subsets of the IFS-91 and IFS-137 databases are plotted on the map in Fig. 7. In the IFS-91 database, the sampling is fully determined by the selection algorithm, which makes the geographical distributions very inhomogeneous. Selected profiles represent those regions where gradients of the sampled variable are the strongest: in the case of temperature, mid- and high-latitudes dominate, while humidity and cloud condensate subsets concentrate at low latitudes. However, the IFS-137 database shows a much more homogeneous spatial distribution in all the sampling subsets, which is a consequence of the randomized selection.

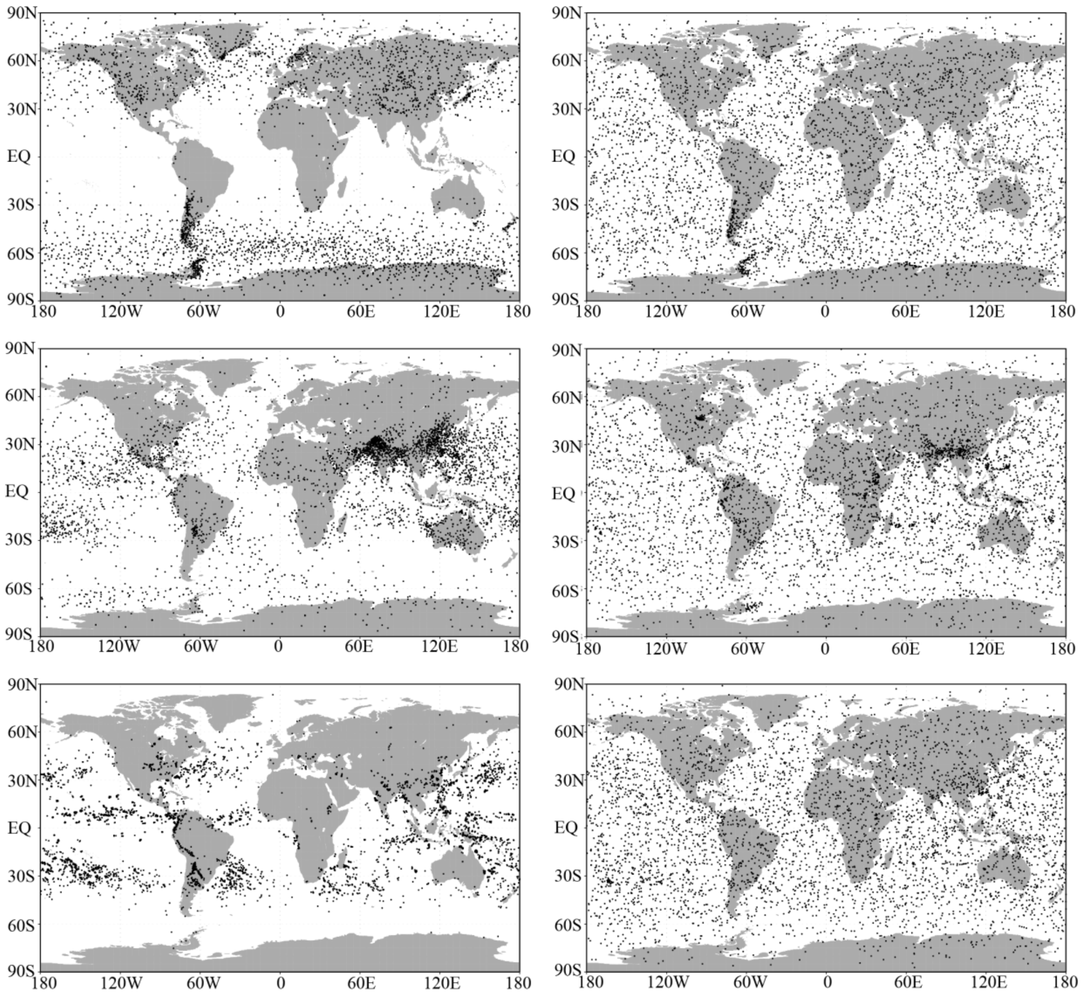

Figure 7. Locations of selected profiles in the temperature (top), specific humidity (middle), and cloud condensate (bottom), sampled subsets of the IFS-91 (left) and IFS-137 (right) databases (from https://www.nwpsaf.eu/site/update-137-level-nwp-profile-dataset/ , 2019).

The temporal distribution of the selected profiles is illustrated in Fig. 8. The coverage of the IFS-137 data set is more homogeneous than the IFS-91 data set. Moreover, the IFS-137 database supports the mode with input parameters, such as detection angle, 2 m temperature, and cloud information. Therefore, it is feasible to use the selected samples in a statistical multiple regression experiment.

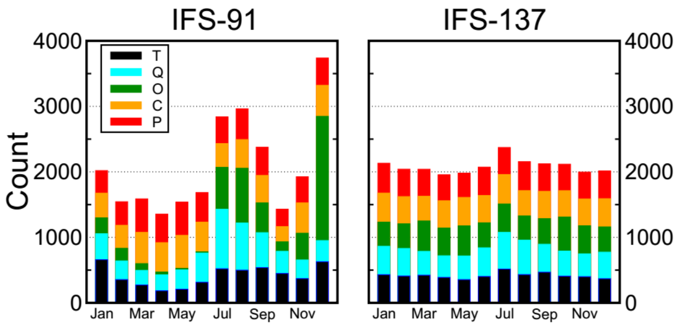

Figure 8. Distribution of profiles within the calendar months in IFS-91 (left) and IFS-137 (right) databases. Different subsets are shown in different colors.Black parts stand for temperature. Blue parts represent specific humidity. Green parts indicate ozone subset. Orange parts stand for cloud condensate. Red parts represent precipitation. The last access date is April 26th, 2019. (from https://www.nwpsaf.eu/site/update-137-level-nwp-profile-dataset/ , 2019).

4.2 Experimental scheme

In order to verify the retrieval effectiveness of ICS, 5000 temperature profiles provided by the IFS-137 were used for statistical inversion comparison experiments. The steps are as follows:

(1) 5000 profiles and their corresponding surface factors, including surface air pressure, surface temperature, 2 m temperature, 2 m specific humidity, 10 m wind speed. are put into the RTTOV mode. Then, the simulated AIRS spectra are obtained.

(2) The retrieval of temperature is carried out in accordance with Eq. (23). The 5000 profiles are divided into two groups. The first group of 2500 profiles is used to obtain the regression coefficient, and the second group of 2500 is used to test the result.

(3) Verification of the results. The test is carried out based on the standard deviation between the retrieval value and the true value.

4.3 Results and Discussion

For the statistical inversion comparison experiments, the standard deviation of temperature retrieval is shown in Fig. 9. First, because PCS does not take channel sensitivity as a function of height into consideration, the retrieval result of PCS is inferior to that of ICS. Second, by comparing the results of ICS and NCS we found that below 100 hPa, since the method used in this paper considers near ground to be less of an influencing factor, the channel combination of ICS is slightly inferior to that of NCS, but the difference is small.

From 100 hPa to10 hPa, the retrieval temperature of ICS in this paper is consistent with that of NCS, slightly better than the channel selected for NCS. From 10 hPa to 0.02 hPa, near the space layer, the retrieval temperature of ICS is better than that of NCS. In terms of the standard deviation, the channel combination of ICS is slightly better than that of PCS from 100 hPa to 10 hPa. From 10 hPa to 0.02 hPa, the standard deviation of ICS is lower than that of NCS at about 1 K, meaning that the retrieval result of ICS is better than that of NCS.

In order to further illustrate the effectiveness of ICS, the mean improvement value of the ICS and its percentages compared with the PCS and NCS at different heights are shown in Table 1. Because PCS does not take channel sensitivity as a function of height into consideration, the retrieval result of PCS is inferior to that of ICS. In general, the accuracy of the retrieval temperature of ICS is improved. Especially, from 100 hPa to 0.01 hPa, the mean value of ICS is evidently improved by more than 0.5 K which means the accuracy can be improved by more than 11%. By comparing the results of ICS and NCS we found that below 100 hPa, since the method used in this paper considers near ground to be less of an influencing factor, the channel combination of ICS is slightly inferior to that of NCS, but the difference is small. From 100 hPa to 0.01 hPa, the mean value of ICS is improved by more than 0.36 K which means the accuracy can be improved by more than 9.6%.

Table 1. The mean improvement value of the ICS and its percentages compared with the PCS and NCS at different heights.

Pressure	Improved mean value /Percentage compared with PCS	Improved value /Percentage compared with NCS
hPa	K/%	K/%
surface-100hPa	0.24/10.77%	-0.04/-3.27%
100hPa-10hPa	0.15/5.08%	0.06/2.4%
10hPa-1hPa	0.04/0.64%	0.17/2.99%
1hPa-0.01hPa	0.52/11.92%	0.36/9.57%

This is because, as shown in Fig. 4: (1) Stratosphere and mesosphere is less affected by the ground surface, so the retrieval result of PCS is better than that of NCS. (2) Due to the method selected in this paper, there are more channels at 4.2 μm for N_2O and 4.3 μm for CO_2 absorption bands, and the channel combination of PCS is superior to that of NCS for atmospheric temperature observation in the high temperature zone. Moreover, ICS takes channel sensitivity as a function of height into consideration, so its retrieval result is improved.

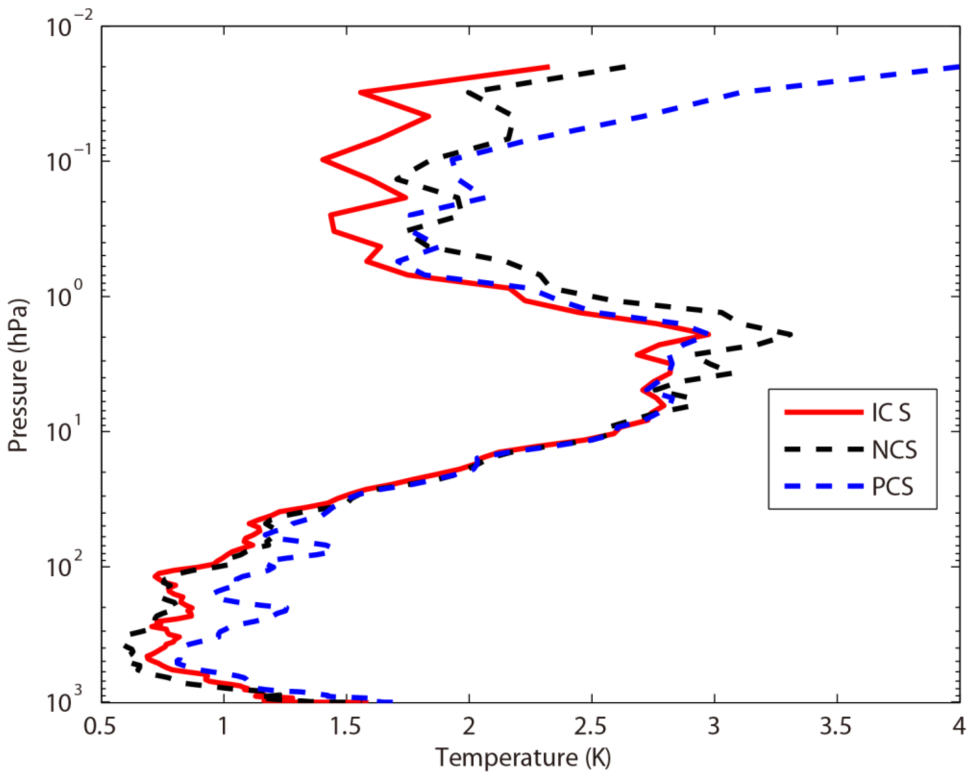

Figure 9. The temperature profile standard deviation of statistical inversion comparison experiments. Red line indicates the result of ICS. Black dotted line stands for the result of NCS. Blue dotted line represents the result of PCS.

5 Statistical inversion comparison experiments in four typical regions

The accuracy of the retrieval temperature varies from place to place and changes with atmospheric conditions. Therefore, in order to further compare the inversion accuracy under different atmospheric conditions, this paper has divided the atmospheric profile from the IFS-137 database introduced in Sect. 4 into four regions: equatorial zone, subtropical region, mid-latitude region and Arctic. The average temperature profiles in these four regions are shown in Fig. 10. The retrieval temperature varies from place to place and changes with atmospheric conditions. In order to further compare the regional differences of inversion accuracy, the temperature standard deviations of ICS in four typical regions are compared in Sect. 5.2.

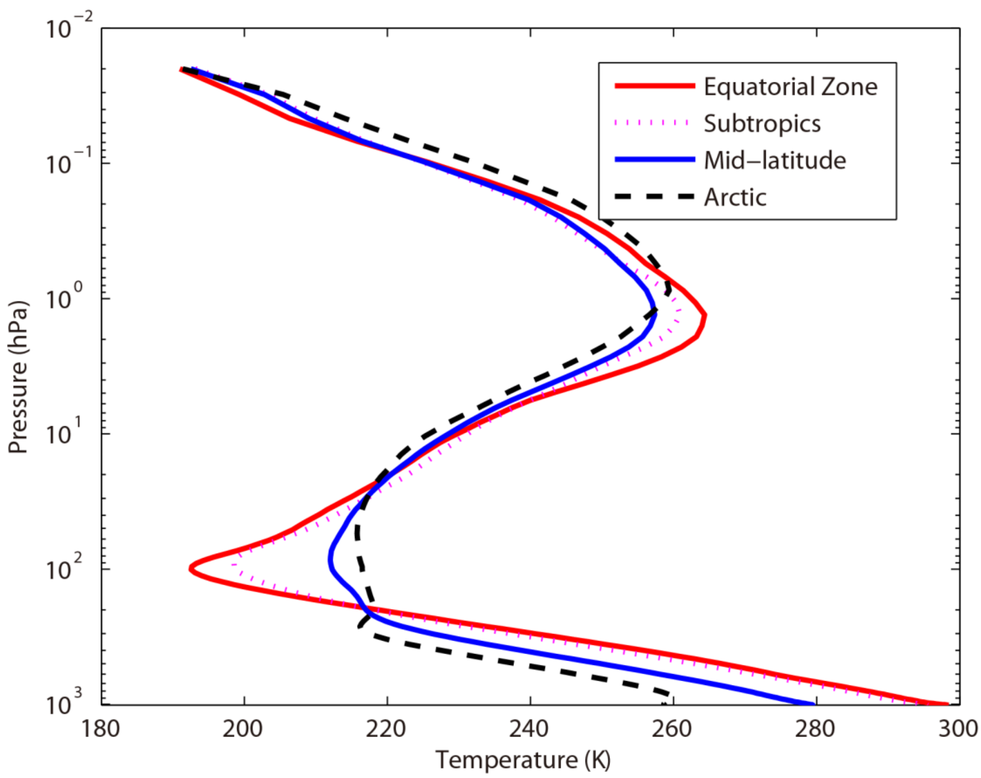

Figure 10. The average temperature profiles in four typical regions. Red line indicates the equatorial zone. Pink dotted line stands for the subtropics. Blue dotted line represents the mid-latitude region. Black dotted line stands for the Arctic.

5.1 Experimental scheme

In order to further illustrate the different accuracy of the retrieval temperature using our improved channel selection method under different atmospheric conditions, the profiles in four typical regions were used for statistical inversion comparison experiments. The experimental steps are as follows:

(1) 2500 profiles in Sect. 4 are used to work out the regression coefficient.

(2) The atmospheric profiles of the four typical regions: equatorial zone, subtropical region, mid-latitude region and Arctic are used for statistical inversion comparison experiments and test the result.(3) Verification of the results. The test is carried out based on the standard deviation between the retrieval value and the true value.

5.2 Results and Discussion

Using statistical inversion comparison experiments in four typical regions, the standard deviation of temperature retrieval is shown in Fig. 11. Generally, the retrieval temperature by ICS is better than that of NCS and PCS. In particular, above 1 hPa (the stratosphere and mesosphere), the standard deviation of atmospheric temperature can be improved by 1 K with PCS and NCS. Thus, ICS shows a great improvement. The results were consistent with Sect. 4.

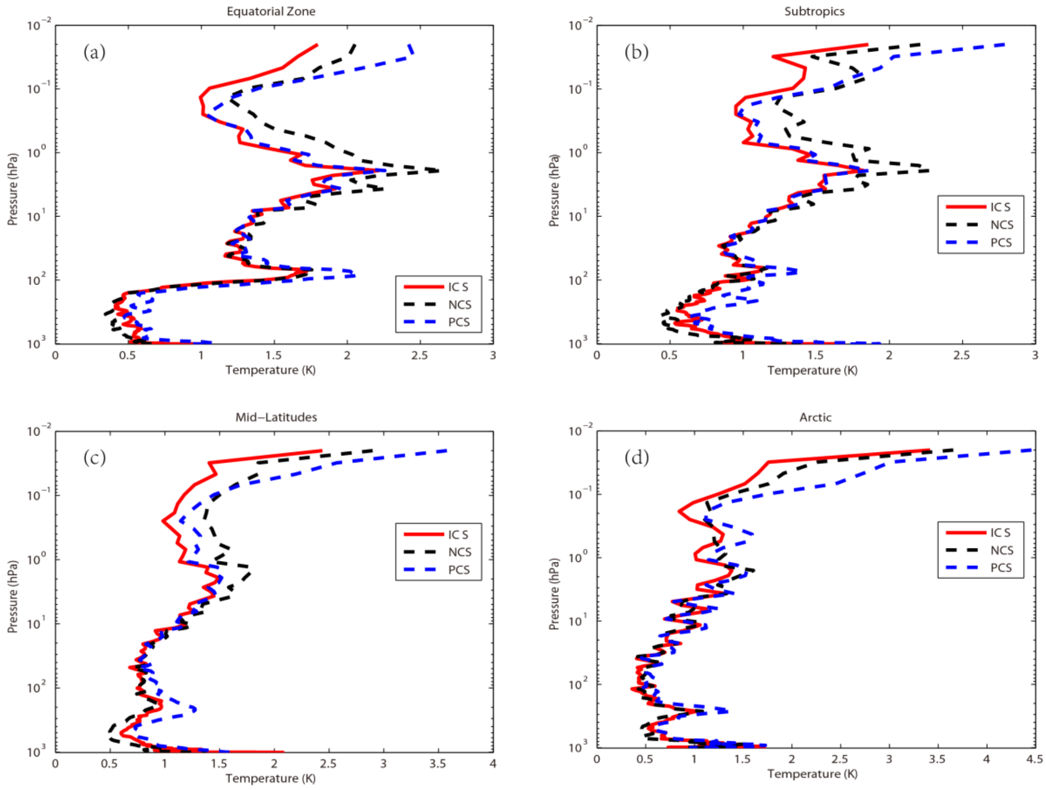

Figure 11. The temperature profile standard deviation of statistical inversion comparison experiments in four typical regions. Red line indicates the result of ICS. Black dotted line stands for the result of NCS. Blue dotted line represents the result of PCS. (a) Equatorial zone. (b) Subtropics. (c) Mid-latitudes. (d) Arctic.

In order to further compare the regional differences of inversion accuracy, the temperature standard deviation of ICS in four typical regions are compared in Fig. 12.

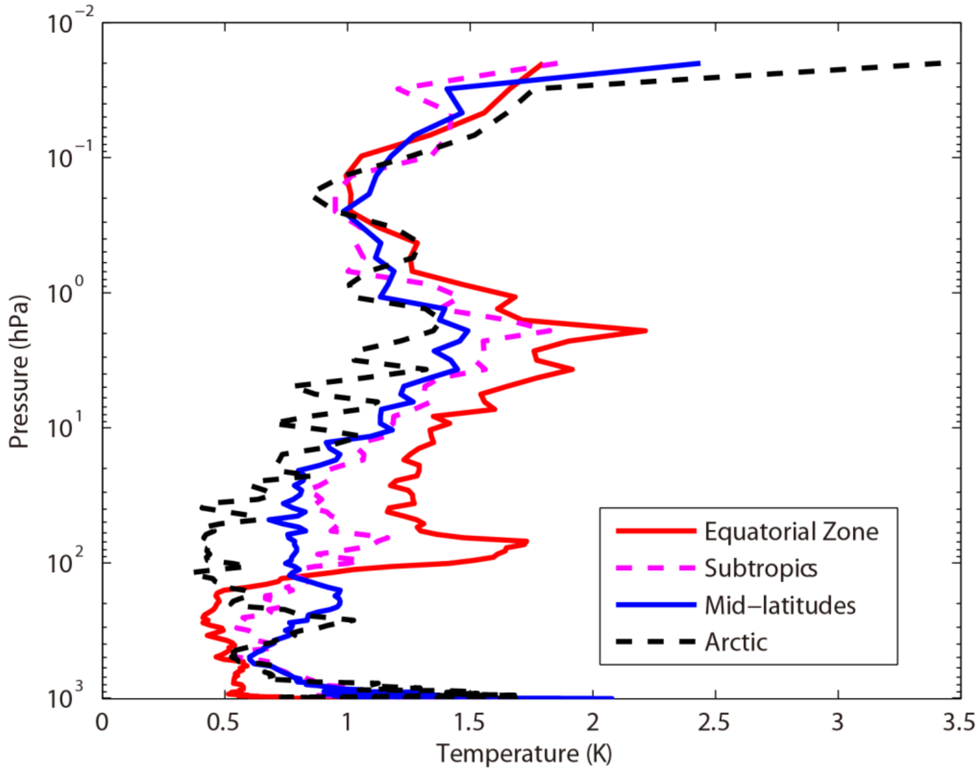

Figure 12. The temperature standard deviation of ICS in four typical regions. Red line indicates the result of equatorial zone. Pink dotted line represents the result of Subtropics. Blue line represents the result of Mid-latitudes. Black dotted line stands for the result of Arctic.

The temperature standard deviations of the ICS in the four typical regions are large (Fig. 12). Below100 hPa, due to the high temperature in the equatorial zone, the channel combination of ICS is better than that of PCS and NCS for atmospheric temperature observation to the higher temperature. The standard deviation is 0.5K. Due to the method selected in this paper there are more channels at 4.2 μm for N_2O and 4.3 μm for CO_2 absorption bands which has been previously described in Sect. 3. Near the tropopause, the standard deviation of the equatorial zone increases sharply. It is also due to the sharp drops in temperature. However, the standard deviation of the Arctic is still around 0.5K. From 100hPa to 1hPa, the standard deviation of ICS is 0.5 K to 2K. With the increase of latitude, the effectiveness considerably increases. According to Fig. 11, ICS takes channel sensitivity as a function of height into consideration, so its retrieval result is better.

Although the improvements of ICS in the four typical regions are different, in general, the accuracy of the retrieval temperature of ICS is improved. Because PCS does not take channel sensitivity as a function of height into consideration, the retrieval result of PCS is inferior to that of ICS. In general, the accuracy of the retrieval temperature of ICS is improved.

7 Conclusions

In recent years, the atmospheric layer in the altitude range of about 20–100 km has been named "the near space layer" by aeronautical and astronautical communities. It is between the space-based satellite platform and the aerospace vehicle platform, which is the transition zone between aviation and aerospace. Its unique resource has attracted a lot of attention from many countries. Research and exploration, therefore, on and of the near space layer are of great importance. A new channel selection scheme and method for hyperspectral atmospheric infrared sounder AIRS data based on layering is proposed. The retrieval results of ICS concerning the near space atmosphere are particularly good. Thus, ICS aims to provide a new and an effective channel selection method for the study of the near space atmosphere using the hyperspectral atmospheric infrared sounder.

An improved channel selection method is proposed, based on information content in this paper. A robust channel selection scheme and method are proposed, and a series of channel selection comparison experiments are conducted. The results are as follows:

(1) Since ICS takes channel sensitivity as a function of height into consideration, the ARI of PCS only tends to be 0.38 and is not convergent. However, as the 100^{th} iteration is approached, the ARI of ICS tends to be stable, reaching 0.54, while the distribution of the temperature weighting function is more continuous and closer to that of the actual atmosphere. Thus, in terms of the ARI, convergence, and the distribution of the temperature weighting function, ICS is better than PCS.

(2) Statistical inversion comparison experiments show that the

retrieval temperature of ICS in this paper is consistent with that of NCS. In particular, from 10 hPa to 0.02 hPa (the stratosphere and mesosphere), the retrieval temperature of ICS is obviously better than that of NCS at about 1 K. In general, the accuracy of the retrieval temperature of ICS is improved. Especially, from 100 hPa to 0.01 hPa, the accuracy of ICS can be improved by more than 11%. The reason is that stratosphere and mesosphere are less affected by the ground surface, so the retrieval result of ICS is better than that of NCS. Additionally, due to the method selected in this paper there are more channels at 4.2 μm for the N_2O and at 4.3 μm for the CO_2 absorption bands; the channel combination of ICS is better than that of NCS for atmospheric temperature observation to the higher temperature.

(3) Statistical inversion comparison experiments in four typical regions indicate that ICS in this paper is significantly better than NCS and PCS in different regions and shows latitudinal variations, which shows potential for future applications.

Data availability. The data used in this paper are available from the corresponding author upon request.

Appendices

Appendix A

Table A1. Pressure levels adopted for RTTOV v12 54 pressure level coefficients and profile limits within which the transmittance calculations are valid. Note that the gas units here are ppmv. (From https://www.nwpsaf.eu/site/software/rttov/, RTTOV Users guide, 2019).

Level	Pressure	Tmax	Tmin	Qmax	Qmin	Q_2max	Q_2min	Q_2Ref
Number	hPa	K	K	ppmv*	ppmv*	ppmv*	ppmv*	ppmv*
1	0.01	245.95	143.66	5.24	0.91	1.404	0.014	0.296
2	0.01	252.13	154.19	6.03	1.08	1.410	0.069	0.321
3	0.03	263.71	168.42	7.42	1.35	1.496	0.108	0.361
4	0.03	280.12	180.18	8.10	1.58	1.670	0.171	0.527
5	0.13	299.05	194.48	8.44	1.80	2.064	0.228	0.769
6	0.23	318.64	206.21	8.59	1.99	2.365	0.355	1.074
7	0.41	336.24	205.66	8.58	2.49	2.718	0.553	1.471
8	0.67	342.08	197.17	8.34	3.01	3.565	0.731	1.991
9	1.08	340.84	189.50	8.07	3.30	5.333	0.716	2.787
10	1.67	334.68	179.27	7.89	3.20	7.314	0.643	3.756
11	2.50	322.5	17627	7.75	2.92	9.191	0.504	4.864
12	3.65	312.51	175.04	7.69	2.83	10.447	0.745	5.953
13	5.19	303.89	173.07	7.58	2.70	12.336	1.586	6.763
14	7.22	295.48	168.38	7.53	2.54	12.936	1.879	7.109
15	9.84	293.33	166.30	7.36	2.46	12.744	1.322	7.060
16	13.17	287.05	16347	7.20	2.42	11.960	0.719	6.574
17	17.33	283.36	161.49	6.96	2.20	11.105	0.428	5.687
18	22.46	280.93	161.47	6.75	1.71	9.796	0.278	4.705
19	28.69	282.67	162.09	6.46	1.52	8.736	0.164	3.870
20	36.17	27993	162.49	6.14	1.31	7.374	0.107	3.111

21	45.04	27315	164.66	5.90	1.36	6.799	0.055	2.478
22	55.44	265.93	166.19	6.21	1.30	5.710	0.048	1.907
23	67.51	264.7	167.42	9.17	1.16	4.786	0.043	1.440
24	81.37	261.95	159.98	17.89	0.36	4.390	0.038	1.020
25	97.15	262.43	163.95	20.30	0.01	3.619	0.016	0.733
26	114.94	259.57	168.59	33.56	0.01	2.977	0.016	0.604
27	134.83	259.26	169.71	102.24	0.01	2.665	0.016	0.489
28	156.88	260.13	169.42	285.00	0.01	2.351	0.013	0.388
29	181.14	262.27	17063	714.60	0.01	1.973	0.010	0.284
30	207.61	264.45	174.11	1464.00	0.01	1.481	0.013	0.196
31	236.28	270.09	177.12	2475.60	0.01	1.075	0.016	0.145
32	267.10	277.93	181.98	4381.20	0.01	0.774	0.015	0.110
33	300.00	285.18	184.76	6631.20	0.01	0.628	0.015	0.086
34	334.86	293.68	187.69	9450.00	1.29	0.550	0.016	0.073
35	371.55	300.12	190.34	12432.00	1.52	0.447	0.015	0.063
36	409.89	302.63	194.40	15468.00	2.12	0.361	0.015	0.057
37	449.67	304.43	198.46	18564.00	2.36	0.284	0.015	0.054
38	490.&5	307.2	201.53	21684.00	2.91	0.247	0.015	0.052
39	532.56	31217	202.74	24696.00	3.67	0.199	0.015	0.050
40	572.15	31556	201.61	27480.00	3.81	0.191	0.012	0.050
41	618.07	318.26	189.95	30288.00	6.82	0.171	0.010	0.049
42	661.00	321.71	189.95	32796.00	6.07	0.128	0.009	0.048
43	703.59	327.95	189.95	55328.00	6.73	0.124	0.009	0.047
44	745.48	333.77	189.95	37692.00	8.71	0.117	0.009	0.046
45	786.33	336.46	189.95	39984.00	8.26	0.115	0.008	0.045
46	825.75	338.54	189.95	42192.00	7.87	0.113	0.008	0.043
47	863.40	342.55	189.95	44220.00	7.53	0.111	0.007	0.041
48	898.93	346.23	189.95	46272.00	7.23	0.108	0.006	0.040
49	931.99	34924	189.95	47736.00	6.97	0.102	0.006	0.038
50	962.26	349.92	189.95	51264.00	6.75	0.099	0.006	0.034

51	989.45	350.09	189.95	49716.00	6.57	0.099	0.006	0.030
52	1013.29	360.09	189.95	47208.00	6.41	0.094	0.006	0.028
53	1033.54	350.09	189.95	47806.00	6.29	0.094	0.006	0.027
54	1050.00	350.09	189.95	47640.00	6.19	0.094	0.006	0.027

Table A2. Pressure levels adopted for IFS-137 137 pressure levels (in hPa).

Level number	pressure hPa	Level number	pressure hPa	Level number	pressure hPa	Level number	pressure hPa	Level number	pressure hPa
1	0.02	31	12.8561	61	106.4153	91	424.019	121	934.7666
2	0.031	32	14.2377	62	112.0681	92	441.5395	122	943.1399
3	0.0467	33	15.7162	63	117.9714	93	459.6321	123	950.9082
4	0.0683	34	17.2945	64	124.1337	94	478.3096	124	958.1037
5	0.0975	35	18.9752	65	130.5637	95	497.5845	125	964.7584
6	0.1361	36	20.761	66	137.2703	96	517.4198	126	970.9046
7	0.1861	37	22.6543	67	144.2624	97	537.7195	127	976.5737
8	0.2499	38	24.6577	68	151.5493	98	558.343	128	981.7968
9	0.3299	39	26.7735	69	159.1403	99	579.1926	129	986.6036
10	0.4288	40	29.0039	70	167.045	100	600.1668	130	991.023
11	0.5496	41	31.3512	71	175.2731	101	621.1624	131	995.0824
12	0.6952	42	33.8174	72	183.8344	102	642.0764	132	998.8081
13	0.869	43	36.4047	73	192.7389	103	662.8084	133	1002.225
14	1.0742	44	39.1149	74	201.9969	104	683.262	134	1005.356
15	1.3143	45	41.9493	75	211.6186	105	703.3467	135	1008.224
16	1.5928	46	44.9082	76	221.6146	106	722.9795	136	1010.849
17	1.9134	47	47.9915	77	231.9954	107	742.0855	137	1013.25
18	2.2797	48	51.199	78	242.7719	108	760.5996		
19	2.6954	49	54.5299	79	253.9549	109	778.4661		
20	3.1642	50	57.9834	80	265.5556	110	795.6396		
21	3.6898	51	61.5607	81	277.5852	111	812.0847		
22	4.2759	52	65.2695	82	290.0548	112	827.7756		
23	4.9262	53	69.1187	83	302.9762	113	842.6959		
24	5.6441	54	73.1187	84	316.3607	114	856.8376		
25	6.4334	55	77.281	85	330.2202	115	870.2004		
26	7.2974	56	81.6182	86	344.5663	116	882.791		
27	8.2397	57	86.145	87	359.4111	117	894.6222		
28	9.2634	58	90.8774	88	374.7666	118	905.7116		
29	10.372	59	95.828	89	390.645	119	916.0815		

30	11.5685	60	101.0047	90	407.0583	120	925.7571

Author contributions. ZS contributed the central idea. SC, ZS and HD conceived the method, developed the retrieval algorithm and discussed the results. SC analyzed the data, prepared the figures and wrote the paper. WG contributed to refining the ideas, carrying out additional analyses. All co-authors reviewed the paper.

Competing interests. The authors declare that they have no conflict of interest.

Acknowledgements. The study was supported by the National Key Research Program of China: Development of high-resolution data assimilation technology and atmospheric reanalysis data set in East Asia (Research on remote sensing telemetry data assimilation technology, Grant no. 2017YFC1501802). The study was also supported by the National Natural Science Foundation of China (Grant no. 41875045) and Hunan Provincial Innovation Foundation for Postgraduate (Grant no. CX2018B033 and no. CX2018B034).

References

Aires, F., Schmitt, M., Chedin, A., and Scott, N.: The "weighting smoothing" regularization of MLP for Jacobian stabilization, IEEE. T. Neural. Networks., 10, 1502-1510, https://doi.org/10.1109/72.809096, 1999.

Aires, F., Chédin, Alain., Scott, N. A., and Rossow, W. B.: A regularized neural net approach for retrieval of atmospheric and surface temperatures with the IASI instrument, J. Appl. Meteorol., 41,144-159, https://doi.org/10.1175/1520-0450(2002)041<0144:ARNNAF>2.0.CO;2, 2002.

Aumann, H. H.: Atmospheric infrared sounder on the earth observing system, Optl. Engr., 33, 776-784, https://doi.org/10.1117/12.159325, 1994.

Aumann, H. H., Chahine, M. T., Gautier, C., and Goldberg, M.: AIRS/AMSU/HSB on the Aqua mission: design, science objective, data products, and processing systems, IEEE. Trans. GRS., 41,253-264, http://dx.doi.org/10.1109/TGRS.2002.808356, 2003.

Brath, M., Fox, S., Eriksson, P., Harlow, R. C., Burgdorf, M., and Buehler, S. A.: Retrieval of an ice water path over the ocean from ISMAR and MARSS millimeter and submillimeter brightness temperatures, Atmos. Meas. Tech., 11, 611–632, https://doi.org/10.5194/amt-11-611-2018, 2018.

Chahine, M. I.: A general relaxation method for inverse solution of the full radiative transfer equation, J. Atmos. Sci., 29, 741-747, https://doi.org/10.1175/1520-0469(1972)029<0741:AGRMFI>2.0.CO;2, 1972.

Chang, K. W, L'Ecuyer, T. S., Kahn, B. H., and Natraj, V.: Information content of visible and midinfrared radiances for retrieving tropical ice cloud properties, J. Geophys. Res., 122, https://doi.org/10.1002/2016JD026357, 2017.

Chedin, A., Scott, N. A., Wahiche, C., and Moulinier, P.: The improved initialization inversion method: a high resolution physical method for temperature retrievals from satellites of the tiros-n series, J. Appl. Meteor., 24, 128-143, https://doi.org/10.1175/1520-0450(1985)024<0128:TIIIMA>2.0.CO;2, 1985.

Cyril, C., Alain, C., and Scott, N. A.: Airs channel selection for CO_2 and other trace-gas retrievals, Q. J. Roy. Meteor. Soc., 129, 2719-2740, https://doi.org/10.1256/qj.02.180, 2003.

Du, H. D., Huang, S. X., and Shi, H. Q.: Method and experiment of channel selection for high spectral resolution data, Acta. Physica. Sinica., 57, 7685-7692, 2008 .

Dudhia, A., Jay, V. L., and Rodgers, C. D.: Microwindow selection for high-spectral-resolution sounders, Appl. Opt. 41, 3665-3673, https://doi.org/10.1364/AO.41.003665, 2002.

Eresmaa, R. and McNally, A. P.: Diverse profile datasets from the

ECMWF 137-level short-range forecasts, Tech. rep., ECMWF, 2014.

Eyre, J. R., Andersson E., and McNally, A. P.: Direct use of satellite sounding radiances in numerical weather prediction, High Spectral Resolution Infrared Remote Sensing for Earth's Weather and Climate Studies, Springer, Berlin, Heidelberg, https://doi.org/10.1007/978-3-642-84599-4_25, 1993.

Fang, Z. Y.: The evolution of meteorological satellites and the insight from it, Adv. Meteorol. Sci. Technol., 4, 27-34, https://doi.org/ 10.3969/j.issn.2095-1973.2014.06.003, 2014.

Gong, J., Wu, D. L., and Eckermann, S. D.: Gravity wave variances and propagation derived from AIRS radiances, Atmos. Chem. Phys., 11, 11691-11738, https://doi.org/10.5194/acp-12-1701-2012, 2011.

He, M. Y., Du, H. D., Long, Z. Y., and Huang, S. X.: Selection of regularization parameters using an atmospheric retrievable index in a retrieval of atmospheric profile, Acta. Physica Sinica., 61, 024205-160, 2012.

Hoffmann, L. and Alexander, M. J.: Retrieval of stratospheric temperatures from atmospheric infrared sounder radiance measurements for gravity wave studies, J. Geophys. Res. Atm., 114, https://doi.org/10.1029/2008JD011241, 2009.

Huang, H. L., Li, J., Baggett, K., Smith, W. L., and Guan, L.: Evaluation of cloud-cleared radiances for numerical weather prediction and cloud-contaminated sounding applications, Atmospheric and Environmental Remote Sensing Data Processing and Utilization: Numerical Atmospheric Prediction and Environmental Monitoring, I. S. O. Photonics., https://doi.org/10.1117/12.613027, 2005.

Kuai, L., Natraj, V., Shia, R. L., Miller, C., and Yung, Y. L.: Channel selection using information content analysis: a case study of CO_2 retrieval from near infrared measurements. J. Q. S. Radiative. Transfer., 111, 1296-1304, https://doi.org/10.1016/j.jqsrt.2010.02.011, 2010.

Li, J., Wolf, W. W., Menzel, W. P., Paul, Menzel. W., Zhang, W. J., Huang, H. L., and Achtor, T. H.: Global soundings of the atmosphere from ATOVS measurements: the algorithm and validation, J. Appl. Meteor., 39, 1248-1268, https://doi.org/10.1175/1520-0450(2000)039<1248:GSOTAF>2.0.CO;2, 2000.

Li, J., Liu, C. Y., Huang, H. L., Schmit, T. J., Wu, X., Menzel, W. P., and Gurka, J. J.: Optimal cloud-clearing for AIRS radiances using MODIS, IEEE. Trans. GRS. , 43, 1266-1278, http://dx.doi.org/10.1109/tgrs.2005.847795, 2005.

Liu, Z. Q.: A regional ATOVS radiance-bias correction scheme for rediance assimilation, Acta. Meteorologica. Sinica., 65, 113-123, 2007.

Lupu, C., Gauthier, P., and Laroche, Stéphane.: Assessment of the impact of observations on analyses derived from observing system experiments, Mon. Weather. Rev., 140, 245-257, https://doi.org/10.1175/MWR-D-10-05010.1, 2012.

Menke, W.: Geophysical Data Analysis: Discrete Inverse Theory, Acad. Press., Columbia University, New York, https://doi.org/10.1016/B978-0-12-397160-9.00019-9, 1984.

Menzel, W. P., Schmit, T. J., Zhang, P. and Li, J.: Satellite-based atmospheric infrared sounder development and applications, Bull. Amer. Meteor. Soc., 99, 583–603, https://doi.org/10.1175/BAMS-D-16-0293.1, 2018.

Prunet, P., Thépaut J. N., and Cass, V.: The information content of clear sky IASI radiances and their potential for numerical weather prediction, Q. J. Roy. Meteor. Soc., 124, 211-241, https://doi.org/10.1002/qj.49712454510, 2010.

Xu, Q.: Measuring information content from observations for data assimilation: relative entropy versus shannon entropy difference, Tellus. A., 59, 198-209, https://doi.org/10.1111/j.1600-0870.2006.00222.x, 2007.

Rabier, F., Fourrié, N., and Chafäi, D.: Channel selection methods for infrared atmospheric sounding interferometer radiances, Q. J. Roy. Meteor. Soc., 128, 1011-1027, https://doi.org/10.1256/0035900021643638, 2010.

Richardson, M. and Stephens, G. L.: Information content of oco-2 oxygen a-band channels for retrieving marine liquid cloud properties, Atmospheric Measurement Techniques, 11, 1-19, https://doi.org/10.5194/amt-11-1515-2018, 2018.

Rodgers, C. D.: Information content and optimisation of high spectral resolution remote measurements, Adv. Spa. Research, 21, 136-147, https://doi.org/10.1016/S0273-1177(97)00915-0, 1996.

Rodgers, C. D.: Inverse Methods for Atmospheric Sounding, Inverse methods for atmospheric sounding, World Scientific, https://doi.org/10.1142/3171, 2000.

Saunders, R., Hocking, J., Turner, E., Rayer, P., Rundle, D., Brunel, P., Vidot, J., Roquet, P., Matricardi, M., Geer, A., Bormann, N., and Lupu, C.: An update on the RTTOV fast radiative transfer model (currently at version 12), Geosci. Model Dev., 11, 2717-2737, https://doi.org/10.5194/gmd-11-2717-2018, 2018.

Susskind, J., Barnet, C. D. and Blaisdell, J. M.: Retrieval of atmospheric and surface parameters from AIRS/AMSU/HSB data in the presence of clouds, IEEE Trans. Geosci. Remote Sensing, 41, 390-409, https://doi.org/10.1109/TGRS.2002.808236, 2003.

Smith, W. L., Woolf, H. M., and Revercomb, H. E.: Linear simultaneous solution for temperature and absorbing constituent profiles from radiance spectra, Appl. Optics., 30, 1117, https://doi.org/10.1364/AO.30.001117, 1991.

Wakita, H., Tokura, Y., Furukawa, F., and Takigawa, M.: Study of the information content contained in remote sensing data of atmosphere, Acta. Physica. Sinica., 59, 683-691, 2010.

Wang, G., Lu, Q. F., Zhang, J. W., and Wang, H. Y.,.: Study on method and experiment of hyper-spectral atmospheric infrared sounder channel selection, Remote Sensing Technology and Application., 29, 795-802 , 2014.

Zhang, J. W., Wang, G., Zhang, H., Huang J., Chen J., and Wu, L. L.: Experiment on hyper-spectral atmospheric infrared sounder channel selection based on the cumulative effect coefficient of principal component, Journal of Nanjing Institute of meteorology, 1, 36-42, http://dx.doi.org/10.3969/j.issn.1674-7097.2011.01.005, 2011.